INFORMATION TO USERS

This manuscript has been reproduced from the microfilm master. UMI films the text directly from the original or copy submitted. Thus, some thesis and dissertation copies are in typewriter face, while others may be from any type of computer printer.

The quality of this reproduction is dependent upon the quality of the copy submitted. Broken or indistinct print, colored or poor quality illustrations and photographs, print bleedthrough, substandard margins, and improper alignment can adversely affect reproduction.

In the unlikely event that the author did not send UMI a complete manuscript and there are missing pages, these will be noted. Also, if unauthorized copyright material had to be removed, a note will indicate the deletion.

Oversize materials (e.g., maps, drawings, charts) are reproduced by sectioning the original, beginning at the upper left-hand corner and continuing from left to right in equal sections with small overlaps.

Photographs included in the original manuscript have been reproduced xerographically in this copy. Higher quality 6" x 9" black and white photographic prints are available for any photographs or illustrations appearing in this copy for an additional charge. Contact UMI directly to order.

ProQuest Information and Learning
300 North Zeeb Road, Ann Arbor, MI 48106-1346 USA
800-521-0600

SYNTHESIS, CHARACTERIZATION AND NMR STUDIES OF SOME GOLD(I) AND SILVER(I) COMPLEXES WITH CYANIDE, THIONES AND SELENONES

BY

SAEED AHMAD

A Dissertation Presented to the

DEANSHIP OF GRADUATE STUDIES

KING FAHD UNIVERSITY OF PETROLEUM & MINERALS

DHAHRAN, SAUDI ARABIA

In Partial Fulfillment of the

Requirements for the Degree of

DOCTOR OF PHILOSOPHY

In

CHEMISTRY

JANUARY 2002

KING FAHD UNIVERSITY OF PETROLEUM & MINERALS

DHAHRAN 31261, SAUDI ARABIA

DEANSHIP OF GRADUATE STUDIES

This dissertation, written by Mr. SAEED AHMAD under the direction of his dissertation advisor and approved by his dissertation committee, has been presented to and accepted by the Dean of Graduate Studies, in partial fulfillment of the requirements for the degree of DOCTOR OF PHILOSOPHY IN CHEMISTRY.

Dissertation Committee:

Prof. Anvarhusein A. Isab
Dissertation Advisor

Prof. A. Rahman Al-Arfaj
Co-advisor

Prof. M. S. Hussain
Member

Prof. M. I. M. Wazeer
Member

Dr. Assad Ahmed Al-Thukair
Department Chairman

Dr. H. P. Perzanowski
Member

Dr. A. AbulKibash
Member

Dr. Osama Ahmed Jannadi
Dean of Graduate Studies

Dr. Akhtar A. Naqvi
Member

2/4/2002
Date

بِسْمِ اللَّهِ الرَّحْمَٰنِ الرَّحِيمِ

In the Name of Allah, the Most Compassionate & Merciful

Dedicated to the Allah's most beloved Prophet

Hazrat Muhammad (S.A.A.W)

ACKNOWLEDGEMENT

All the admirations are for Almighty **Allah**, who helped me in difficulties and gave me enough strength and ability to accomplish this research work. All devotions and salat and salaam are for Allah's Prophet, **Hazrat Muhammad** (salat and peace be upon him), who enabled us to recognize our Creator.

My acknowledgement and appreciation is due to King Fahd University of Petroleum & Minerals, for providing the assistantship and extending all facilities for this research.

With deep sense of gratitude and appreciation, I would like to express my sincere thanks to my dissertation advisor, Prof. Anvarhusein A, Isab for his inspiring guidance, help and excellent cooperation in supervising this research work.

I am also very grateful to my co-advisor, Prof. Abdul Rahman Al-Arfaj for his great help, continuous encouragement and several helpful discussions.

I would like to offer my sincere thanks to the other members of my dissertation committee, Dr. Herman Perzanowski, Prof. M.I.M. Wazeer, Prof. M. S. Hussain, Dr. A. Abulkibash and Dr. A. A. Naqvi for their great help and valuable suggestions in carrying out this research work.

My sincere thanks and appreciation are also due to Dr. Assad Ahmad Al-Thukair, chairman of the chemistry department, for his generous cooperation and providing all facilities in the department.

I am thankful to all faculty and staff members for their kind and cheerful cooperation.

Special thanks; for Dr. Herman Perzanowski and Mr. M. Arab, who trained me on the NMR instrument, and for Dr. A. Abulkibah, Dr. Imad and Mr. I. Kasumu for giving

me training on the elemental analyzer. I am also thankful to Mr. Sheikh Fayaz and Mr. Farooqi for their help in the lab.

My sincere thanks also go to my colleagues and friends, especially Shafique Ahmed, Abdul Hameed, Izzat W. Kazi and Abdul Karim and all those who contributed in one way or the other in completion of this work.

Thanks are also extended to my teachers at the previous institutions, who are responsible for making the base of this work, especially Mr. Karamat Hussain, Mr. M. Zafar Iqbal, Mr. Safdar Hussain, Mr. M. Ghose, Mr. M. Sharif Chaudary and Dr. Christy Munir, and all others.

My thanks and appreciation also go to my wife and daughter, who supported, helped and encouraged me through out this work.

Finally and humbly, I offer my sincere thanks to my parents and other family members for their encouragement, support and prayers.

(SAEED AHMAD)

Table of Contents

List of Figures

List of Tables

ABSTRACT

NAME: SAEED AHMAD

TITLE OF STUDY: SYNTHESIS, CHARACTERIZATION AND NMR STUDIES OF SOME GOLD(I) AND SILVER(I) COMPLEXES WITH CYANIDE, THIONES AND SELENONES

MAJOR FIELD: CHEMISTRY

DATE OF DEGREE: JANUARY 2002

A series of gold(I) and silver(I) complexes with various thiones and selenones have been prepared and characterized by elemental analysis, infra red (IR) spectroscopy and nuclear magnetic resonance (NMR) spectroscopy {^{1}H, ^{13}C, ^{15}N, ^{31}P and ^{107}Ag}. The general formulas of the complexes are; $[R_3PAuTu]Cl$, $[R_3PAuSeu]Cl$, [>C=S-AuCN], [>C=Se-AuCN], $[(>C=S)AgNO_3]$ and $[(>C=S)_2AgNO_3]$. The spectral data of all these complexes are consistent with the sulfur or selenium coordination of the ligands (thiones and selenones respectively) to metal ion.

The IR studies of cyanogold(I) complexes of thiones and selenones show that some of these complexes exist as nonionic complexes [LAuCN] while the others exist as ionic species, $[Au(L)_2]^+[Au(CN)_2]^-$ in the solid state. However, in solution all these complexes undergo scrambling reactions exhibiting the equilibrium, $2[LAuCN] \rightleftharpoons [Au(L)_2]^+ + [Au(CN)_2]^-$. Separate resonances, observed for $^{13}C^{15}N$ in [LAuCN] and $[Au(CN)_2]^-$ in both ^{13}C and ^{15}N NMR provide the evidence for this scrambling process. The equilibrium constants (K_{eq}) for these reactions were determined by the integration of $^{13}C^{15}N$ resonances in ^{13}C NMR.

Ligand exchange reactions of anti-rheumatic gold(I) complexes with some ligands of biological importance, have been studied using ^{13}C, ^{15}N and ^{31}P NMR. It has been observed that gold(I) thiomalate, $(AuStm)_n$ reacts with thiolated nucleosides (6-mercaptopurine {6-MP} and its derivatives) forming the complexes of the type, [>C=S-Au-Stm]. It is shown that two geometrical isomers are possible for the complex, [6-MP-Au-Stm]. The reaction of $(AuStm)_n$ with diselenides is a redox reaction resulting in the formation of $(Stm)_2$. Auranofin undergoes ligand exchange reactions with thiones forming the complexes of the type, $[Et_3P\text{-}Au\text{-}S{=}C<]^+$ and [>C=S-Au-SATg]. The displaced $SATg^-$ is oxidized to its disulfide, $(SATg)_2$. However, some of the displaced Et_3P is oxidized to Et_3PO while the remaining reacts with thiones to form $Et_3P\text{-}S{=}C<$ species, characterized by δ ^{31}P of 1.0 ppm. It is observed that thiourea (Tu) undergoes fastest exchange reactions with auranofin, while imidazolidine-2-thione (Imt) does the slowest among the thiones studied.

DOCTOR OF PHILOSOPHY DEGREE

KING FAHD UNIVERSITY OF PETROLEUM & MINERALS

DHARAN, SAUDI ARABIA

الخلاصة

الاسم : سعيداحمد

عنوان الدراسة : تركيب وتحليل ودراسة الطيف النووي المغناطيسي لمركبات الذهب(I) والفضة(I) مع السايانيد والثايونز والسيلينونز

المجال : الكيميا

لقد تم تحضير مجموعات من معقدات الذهب والفضة مع ثايونز وسيلينونز ولقد تم تصنيفها بالتحليل العنصري والأشعة تحت الحمراء والرنين النووي المغناطيسي (هيدروجين ١، كربون ١٣ ، نيتروجين ١٥ ، فوسفور ٣١ ،وفضه ١٠٧) الصيغة العامة لهذه المعقدات هي [R_3PAuTu] Cl,.. . البيانات الطيفية لكل هذه المعقدات تتفق في أن التساهم مع أيون المعدن من جانب الكبريت والسلينيوم (ثايونز وسيلينينوز)

الدراسات بالأشعة الحمراء لمعقدات الذهب والسيانيد مع الثايونز والسيلينينوز بينت أن بعض هذه المعقدات يوجد كمعقد غير أيوني [LAuCN] بينما البعض الآخر يوجد على الهيئة الايونية $[Au(L)_2]^+$ $[Au(CN)_2]^-$ في الحالة الصلبة ، بينما في الحالة السائلة فإن كل هذه المعقدات تتبادل المتصلات في تفاعلات تصل إلى حالة الاتزان [LAu] $[AuL_2]^+[Au(CN)_2]^-$ = [CN] ، ولقد لوحظ من دراسة للرنين ^{15}N ^{13}C وجود رنينين اثنين تمثل [LAuCN] و [$Au(CN)_2^-$] . وقد بين الرنين النووي المغناطيسي لكل من ^{13}C، ^{15}N هذا التبادل للمتصلات .

لقد تم قياس ثوابت الاتزان (Keq) في هذه التفاعلات وذلك بدراسة تكامل الرنين ^{13}C، ^{15}N في دراسات الرنين النووي المغناطيسي .

لقد تم دراسة تبادل المتصلات في معقدات الذهب الاحادي والمستخدمة في علاج الروماتيزم وذلك باستخدام الرنين النووي المغناطيسي بدراسة ^{13}C، ^{15}N ^{31}P وتم ملاحظة أن معقد ذهب (واحد) ثايومالية $(AuStm)_n$ يتفاعل مع نويات الثايوليت (٦ ميركابتو بيورين ومشتقاتها) مكونا معقدات من النوع [>C=S-Au-Stm] . وأظهرت الدراسة أن هناك متشاكلين لهذا المعقد .

أن تفاعل $(AuStm)_n$) مع داي سيلينايد يعتبر من نوع أكسدة واختزال ويكون نتيجة التفاعل $(Stm)_2$.

الاورانوفين يدخل في تفاعلات تبادل متصلات مع الثايونز مكونا معقد من نوع = S Au SATg [، C<] $^+$ >C = S Au SATg [والشق المزاح ($SATg^-$) يتم أكسدته إلى $_2$(SATG) وكذلك بعض Et_3P المزاح يتم أكسدته إلى Et_3PO بينما البقية تتفاعل مع الثايونز لتكون Et_3 P-S = C< وهذه تم تصنيفها باستخدام سيجما 31p. تم ملاحظة أن الثايو يوريا (Tu) تدخل في أسرع تفاعل تبادلي مع اورانوفين بينما اميدا زوليدين هو الأبطأ .

درجة الد كتوراة في الفلسفة

جامعة الملك فهد للبترول و المعا د ن

الظهران- المملكة العربية السعودية

CHAPTER 1

INTRODUCTION

Gold and silver have been known since the earliest records of human existence. Both elements belong to the group 1B of the periodic table and have the similar electronic structure, $(n-1)d^{10}\ ns^{1}$ [1]. Gold is a soft, yellow metal (m.p. 1063°C) with the highest ductility and malleability of any element. Silver is a white, lustrous, soft and malleable metal (m.p. 961°C) with the highest known electrical and thermal conductivities [2].

Gold is the most noble of the metals and as a result it can be found in nature as a pure element rather than combined with oxygen or other elements, which accounts for its early discovery [3,4]. Because of its softness, inertness and pleasing yellow luster, primitive man valued gold for ornamental purposes and still it is used in jewelry and as a monetary standard [5]. Gold compounds also have useful therapeutic applications. Current applications of gold in the area of medicine include; treatment of rheumatoid arthritis, dentistry, antitumor activity and treatment of pemphigus, a skin disorder [6,7]. Besides ornamental purposes and medicinal use, high thermal and electrical conductivity of gold along with its inertness make it ideal for employment in electronics and aerospace industry [8].

Silver is chemically more reactive than gold, however it is less reactive than copper [2,3]. Silver is used for making silver ware, ornaments and coins. It is also used in the development of devices such as photocells and in the studies of electrode and surface processes. Silver compounds are important in organic catalysis and in photographic

chemistry [9]. Silver ion also exhibits a rich biological chemistry, serving as a widely used antibacterial agent [10,11].

In spite of the similarity in electronic structure, the chemistry of silver and that of gold differ in several respects. The ionization potential of gold (9.23 ev) is more than that of silver (7.58 ev). Silver(I) forms a simple aqua ion in oxidation state +1, while gold(I) disproportionates in aqueous solution unless it is complexed. For silver, +1 oxidation state is typical while for gold, +1 and +3 are common. Gold is able to exist in -I and +V states but no such oxidation states are known for silver [2,3,12].

1.1 Compounds of Gold

Gold compounds with oxidation states -I, 0, I, II, III and V have been reported and characterized [3]. Among these gold(I) & gold(III) are the most common.

1.1.1 Gold(I)

Gold(I) is a $5d^{10}$ system with empty 6s and 6p orbitals, and considered as 'soft acid' or class 'b' metal. The softer character of Au^+ which results from the relatively small energy difference between the highest occupied and lowest unoccupied orbitals of the ion as illustrated by its affinity order with halogens, which is $I^- > Br^- > Cl^-$ [12].

Gold(I) can adopt a coordination number of 2, 3, or 4, but linear two coordinate complexes are the most common and the most stable [2,3,13]. The currently preferred explanation for the tendency towards linear coordination is the similarity in energy for the outer *ns*, *np* and (n-1)*d* orbitals which permits the formation of collinear *spd* hybrid orbitals. The actual comlex formation would involve the mixing of the metal *spd* hybrid

orbitals with the ligand orbitals to form five molecular orbitals, two bonding, one non bonding and two antibonding [14].

Depending upon the nature of ligands, gold(I) can also form π bonds with π acceptor or π donor ligands. The presence of CN^-, which is a π acceptor ligand, stabilizes the energy splitting between the highest occupied and lowest unoccupied orbitals [3].

Some gold(I) complexes with coordination number two are shown in the Figure 1.1.

Gold(I) forms complexes with a large variety of ligands. Gold(I) halides, $[AuX_2]^-$ have been known and their structures are characterized [15-17]. Among pseudohalides cyanide is the most important ligand for gold(I), which forms two types of complexes. One of these, AuCN possesses a chain structure while $[Au(CN)_2]^-$ is a monomeric complex with a linear geometry [18,19]. Examples of ligands containing sulfur bonded to gold(I) are thiolates [20-22], thiourea [23,24], thiones [25-27] and phosphine sulphides [28-30]. Phosphines are the common phosphorus containing ligands and several gold(I) complexes with different phosphines have been reported [31-34]. With phosphines, gold(I) compounds have general formula R_3P-Au-X and $[R_3P$-Au-$PR_3]^+$. Selenium also has a remarkable ability for bonding with gold(I). Some examples of selenium ligands are selenourea [35], phosphineselenides [36,37] and selenolates [38,39]. Oxygen and nitrogen donor ligands are not normally strongly bound to gold(I) and would be readily displaced in favor of softer sulfur or phosphorus containing ligands [40,41].

$(CH_3CH_2)_3P—Au—CN$

Cyano(triethylphosphine)gold(I)

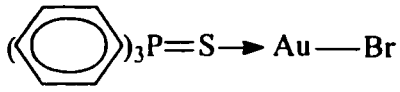

Bromo(triphenylphosphine sulphide)gold(I)

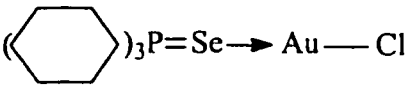

Chloro(tricyclohexylphosphine selenide)gold(I)

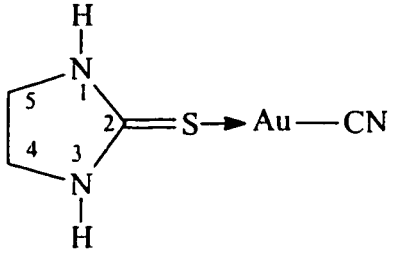

Cyano(imidazolidine-2-thione)gold(I)

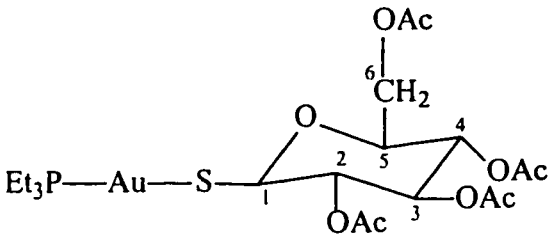

Auranofin

Figure 1.1 Structures of some linear gold(I) complexes.

The thermodynamic stability of AuL_2 complex depends on the type of ligand L, attached to the gold atom [6]. For anionic ligands the trend is as follows:

$CNO^- < CNS^- \sim Cl^- < Br^- < I^- < RS^- < RSe^- < CN^-$

For neutral ligands the trend is:

$PPh_3O < Me_2S < Py < AsPh_3 < NH_3 < C_6H_{11}NH_2 < >C=S < >C=Se < PPH_3$

The most stable being those containing π acceptor ligands i.e., cyanide [32] and phosphines [42].

Gold(I) complexes with three and four coordination are also known, most of which have one or more tertiary phosphine ligands. Examples of three coordinate complexes are chlorobis(triphenylphosphine) gold(I) and tris(triphenylphosphine) gold(I) cation [12,43], having regular trigonal planar geometry.

Four coordinate complexes include the complexes with tetrahedral geometry e.g., $[Au(PMePh_2)_4]^+$ and $[Au(SbPh_3)_4]^+$ [12,44].

1.1.2 Gold(III)

Gold(III) generally forms square planar four coordinate complexes, which are typical of d^8 model ions in the second and third row transition metal elements. Typical complexes, which have been characterized crystallographically include, $[AuCl_4]^-$, Ph_3PAuCl_3 [45,46], $[Au(NO_3)_4]^-$, [47] and $[Au(en)(SO_3)_2]^-$, [48]. All these complexes show square planar geometry.

The tendency to form four coordinate complexes with gold(III) is so strong that complexes of empirical formula AuL_3 such as $AuBr_3$ and $AuCl_3$ dimerize to complete the four coordination (with bridging L groups) about the gold and are correctly formulated as Au_2Br_6 [49] and Au_2Cl_6 [50], as shown in figure 1.2.

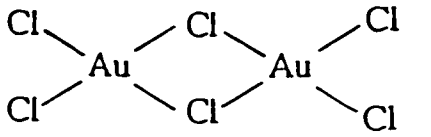

Au_2Cl_6

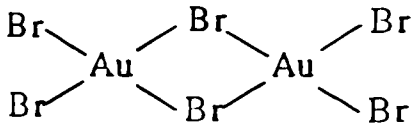

Au_2Br_6

Figure 1.2 Structures of gold(III) halides

The action of amine, phosphine or arsine ligands on Au_2Cl_6 readily gives a variety of the phosphine and arsine complexes. Auric complexes may also be prepared by oxidation of aurous species [51].

$$AuCl(PMe_3) + Br_2 \longrightarrow AuBr_2Cl(PMe_3)$$

Five and six coordinated complexes are also reported for example, trans diiodo bis(*o*-phenylene dimethyl arsine)gold(III) is six coordinated [52] and chloro (tetraphenyl porphyrinato)gold(III) [53] and trichloro(o-phenanthroline)gold(III) [54] are five coordinated.

Very few examples of Au(-I) are known. CsAu and RbAu are ionic crystals containing auride ions [55,56]. Au(II) is mostly stablised by organic ligands e.g., $[Au(CH_2.Et_2PCH_2Cl)]_2$ [57]. For Au(V) only flouro complexes e.g., $Cs[AuF_6]$ are known [3,44].

1.2 Compounds of Silver

Silver(I) is the most stable oxidation state of Silver [1,2]. Silver(I) forms numerous complexes with the donor atoms; N, S, P, Se and halogens [58-60]. In its complexes silver(I) ion shows a pronounced tendency to exhibit linear two fold coordination. However, the complexes with higher coordination numbers (3, 4, 5 and 6) are also known. Linear bonding involves *sp* hybridization, which can be enhanced by some mixing of d_Z^2 orbitals [1]. Structures of some silver(I) complexes are shown in Figure 1.3.

Ammonia is the most important of the nitrogen ligands. The linear $[H_3N\text{-}Ag\text{-}NH_3]^+$ has been observed crystallographically in several complexes. Aqueous pyridine and substituted pyridines form $[Ag(py)]^+$ and $[Ag(py)_2]^+$ ions, but in non-aqueous conditions tetrahedral complexes, such as $[Ag(py)_4]ClO_4$ may be obtained. The halides react with halide anions to give a series of anionic complexes with the relative stabilities, $I^- > Br^- > Cl^-$ [2]. Among the pseudohalides, AgCN and AgSCN are well known and possess a linear structure [2,17].

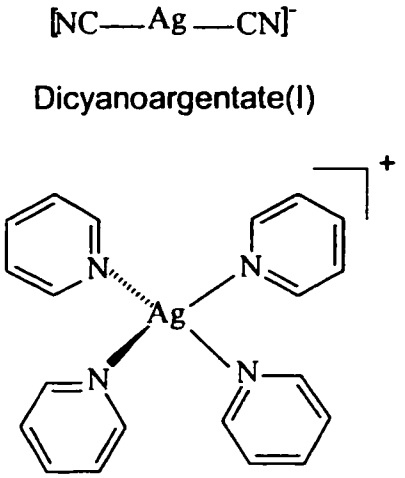

Dicyanoargentate(I)

Tetrapyridylsilver(I)

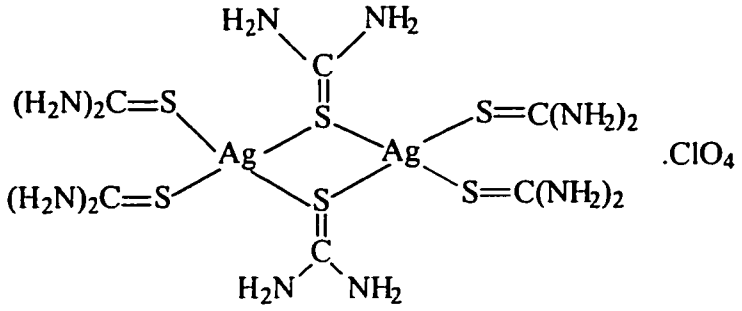

Tris(thiourea)silver(I) perchlorate

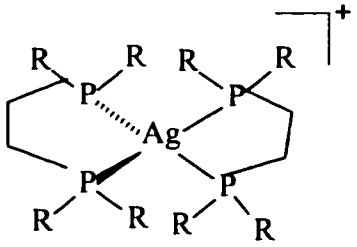

Where,

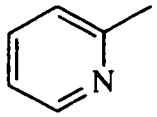

Bis(1,2-bis(di(2-pyridyl)phosphino)ethane)silver(I)

Figure 1.3 Structures of some silver(I) complexes

With sulfur, the thiosulfate complexes, $[Ag(S_2O_3)]^-$ and $[Ag(S_2O_3)_2]^{-3}$ are important and quite stable. Silver chloride and silver bromide will dissolve in aqueous thiosulfate solution to form silver thiosulfate complexes, which provide a means of fixing photographic images. Other important sulfur ligands for silver(I) are thiolate ions (which give oligomers, $(AgSR)_n$) [9,10], SCN^- [61,62], thioureas [62-65] and thioethers [65,66].

Numerous phosphine complexes and some arsine analogues are known. With mono phosphines they are mainly of the type $(R_3P)_nAgX$ with n = 1-4 [59,67]. The complexes $Ag(PR_3)_2X$ are generally dimeric with bridging X. PPh_3 forms 4-coordinate $[Ag(PPh_3)_4]^+$. Slightly larger phosphines such as $(CyPh_2)P$ and $(Cy_2Ph)P$ give three coordinate, $[AgL_3]^+$, while bulky phosphines such as $(^tBu)_3P$ and $(mesityl)_3P$ form linear cations, $[L\text{-}Ag\text{-}L]^+$ [2,68].

Silver(I) has a relatively low affinity for oxygen donors, although compounds and complexes containing carboxylate ions, DMSO, DMF and crown ethers are known [2].

Ag(II) and Ag(III) are the less common oxidation states of silver. Some examples of $[Ag(py)_4](NO_3)_2$ and $[Ag(bipy)_2]^+$. These complexes are presumably planar. AgF_4^- is the example of Ag(III) complexes [1,2].

In the present research work, some new gold(I) and silver(I) complexes have been synthesized. These complexes have the general formula [L-Au-R]X or $[L_n\text{-}M\text{-}X]$, where L is some sulfur or selenium containing ligand, X is an anion and R is a phosphine; M = Ag or Au. Some of these complexes could be useful models for gold drugs. Among the sulfur containing ligands, thiourea and several other thiones, and among the selenium containing ligands selenourea and other selenones were used for complexation.

1.3 Medicinal Use of Gold Compounds

Gold(I) cyanide was the first inorganic compound introduced as a drug for the treatment of tuberculosis [5]. The cyanide group was later replaced by thiols (or phosphine) and gold(I) thiolates such as gold(I) thiomalate (myocrisin) and gold(I) thioglucose (solganol), and a phosphine derivative of gold(I) acetylthioglucose, auranofin have been successfully used over many years for the treatment of rheumatoid arthritis [41,69-71]. Structures of some important gold drugs with their trade names are shown in Figure 1.4.

Auranofin [(2,3,4,6-tetra-*o*-acetyl-1-thio-β-D-glucopyranosato-S) (triethyl phosphine) gold(I)] is an orally active drug, while solganol and myocrisin are only active by injection [69-71]. Auranofin is a lipophilic and nonionic compound, where as gold(I) thiolates are hydrophilic. The hydrophobic phosphine complexes readily penetrate the cells and their exchange reactions with the cells are more rapid on NMR scale than those of aurothiolates. Auranofin possesses several potential advantages over other gold drugs. These are oral administration, less kidney retention, equal distribution between the cellular components and serum proteins of the blood and inhibition of release of lysosomal enzyme, which is responsible for tissue damages [5].

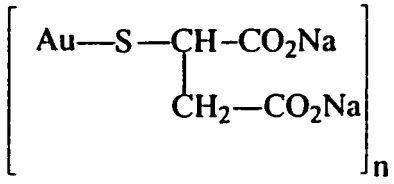

Myocrisin

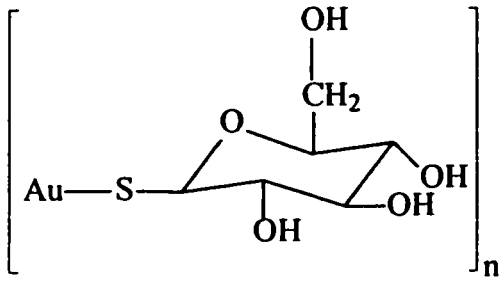

Solganol

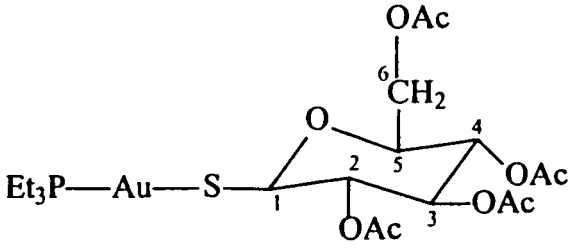

Auranofin

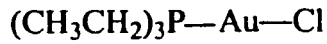

Chloro (triethylphosphine) gold(I)

Figure 1.4 Structures of some important gold drugs

The crystal structure of auranofin shows that gold is linearly coordinated by the sulfur atom of thioglucose and phosphorus of Et_3P to give a discrete monomeric molecular species [72]. The gold thiolates are polymeric in nature [73,74] (by sulfur bridging) with a gold-gold interaction (Figure 1.5).

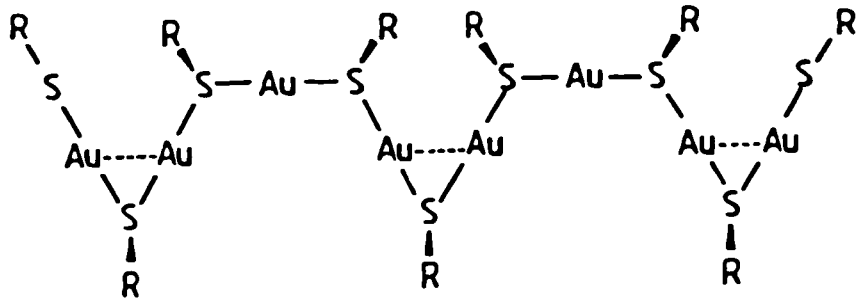

Where, R = Thiomalate or Thioglucose

Figure 1.5 Polymeric structure of gold(I) thiolates

Rheumatoid arthritis is the most common of the chronic and inflammatory diseases. It is a systematic disorder characterized primarily by inflammation of the synovium, in and around joints with secondary involvement of cartilage and bone. The major clinical manifestations are prolonged morning stiffness, pain on motion and swelling of multiple joints. The strikingly low levels of serum -SH (sulfhydral group) in patients with rheumatoid arthritis appear to be associated with the disturbance of the sulfhydral-disulfide equilibrium [75].

Gold(I) drugs inhibit the -SH reactivity and prevents sulfhydral-disulfide interchange reactions that can cross link proteins such as bovine serum albumin during their denaturation by either heat or urea [76]. In the body gold(I) binds to the SH and S-S units of proteins such as blood serum albumin which transport gold compounds throughout the body [77]. Gold has no known biological function in the body and hence there are no natural mechanisms for gold in the body [5]. Therefore toxic effects may arise by the use of gold drugs. Toxic effects generally appear in kidney, on mucous membrane and skin [78].

Gold compounds have also been shown to possess antitumor and antibacterial activity, analogous to that of cisplatin [79]. In the light of close chemical similarity between the compounds of Pt and Au, there is a possibility that both may use DNA as a target site. Au(I) and Au(III) complexes can bind to DNA in vitro and can cleave DNA in cell culture [80]. The chelate complex, $[Au(dppe)_2]Cl$ is active against certain types of cancer cell [81]. The gold complexes, $(C_2H_5)_3P\text{-}AuBr_3$, $[Au(PPh_3)L]$, (L= Imidazole) and $[AuCl_2(dmamp)]$, (dmamp= 2-(dimethylaminomethyl) phenyl) are also known to exhibit antibacterial and antitumor activity [79,82,83].

In the present research work, the exchange reactions of antirheumatic gold(I) complexes with several sulfur and selenium containing ligands of biological importance have been studied. We hope that these studies will contribute towards the understanding of several mechanistic steps involved in the biological action of gold drugs.

1.4 Objectives

The goals of this study are to enhance our knowledge of gold(I) and silver(I) chemistry and gain an insight into the mechanism of action of gold drugs. The primary objectives are:

1. Synthesis of gold(I) complexes with some sulfur and selenium containing ligands and their characterization by elemental analysis, IR and NMR methods.
2. Synthesis and characterization of silver(I) complexes with various thiones and selenones.
3. To synthesize and study the ligand scrambling reactions in cyanogold(I) complexes of various thiones and selenones using NMR spectroscopy.
4. Comparative study of interaction of gold(I) thiomalate, $(AuStm)_n$ with 6-mercaptopurine and its derivatives using carbon-13 NMR.
5. The ^{13}C NMR study of the redox and exchange reactions of $(AuStm)_n$ with diselenides (selenocystine and selenocystamine).
6. To study the ligand exchange reactions of $(AuStm)_n$, auranofin and Et_3P-Au-Cl with thiourea (^{13}C and ^{15}N labeled) by ^{13}C, ^{15}N and ^{31}P NMR spectroscopy.
7. Comparative ^{13}C and ^{31}P NMR study of the exchange reactions of auranofin with ergothionine and its analogous thiones.

CHAPTER 2

LITERATURE REVIEW AND AN OVERVIEW OF THE OBJECTIVES

2.1 Complexes of Gold(I)

Gold(I) being a soft Lewis acid forms very stable complexes with softer sulfur, phosphorus or selenium containing ligands [25,27,33,35]. Recent interest in gold(I) complexes with sulfur and phosphorus donor ligands was stimulated by the antiarthritic properties exhibited by gold compounds like mycrisin, solganol and auranofin [69,70].

Thioureas (Tu) are simple suitable substituents for the sulfur containing ligands and thus gold(I) complexes of thiourea are expected to form useful additional new compounds, which may serve as models for presently available therapeutic agents. The chemistry of these model systems may aid in understanding the chemical behavior of actual drugs. The ability of thiourea (Tu) to form stable adducts with a variety of transition metals (Cu, Ag, Au and Pt) is well established and the structures of several such complexes have been determined [23,62,84,85].

Although extensive research has been done on gold(I) complexes of sulfur donating ligands [25-27] but only limited reports are available about the coordination of selenium containing ligands [35]. Selenourea, $[SeC(NH_2)_2]$ (Seu) has a high nucleophilicity, caused by the strong electron donating effect of the amino groups, which is comparable to that of thiourea [86]. Some gold(I) complexes of Seu are already reported in the literature

[35,87,88], but there is no known report describing the complexation of $AgNO_3$ with selenourea. Characterization of gold(I) and silver(I) complexes of such small ambidentate ligands would provide a basis for understanding and predicting the interaction with more complex thiones and selenone ligands.

A relationship between the basicity of phosphines and NMR shifts of CN for various R_3PAuCN complexes has been established in the previous studies [32]. In the present work, this relationship was extended for phosphine-gold(I) complexes with ^{13}C and ^{15}N labeled thiourea and selenourea.

The 6-mercaptopurine (6-MP) and 2-amino-6-mercaptopurine (2-A-6MP), and their ribosides (6-MPR & 2-A-6MPR respectively) are known to form complexes in solution with several metals, for example Pt(II) [89], Co(III) [90], Hg(II) [91], Cu(II) [92], Au(I) [93,94], Mo(II) [95] , Rh(III), Ru(III) and Ir(I) [96] *etc.* Some gold(I) complexes of these ligands with the formula, $[R_3PAuL]Cl$ and [LAuX] (X = Cl, Br) have been prepared in this study.

2.2 Complexes of Silver(I)

Complexes of heterocyclic thiones such as imidazolidine-2-thione (Imt), diazinane-2-thione (Diaz) and their derivatives with transition metals are of interest in bioinorganic chemistry because of the search for simple model compounds for metal proteins. In view of this, Cu(I) [97], Ag(I) [98], Au(I) [25-27], Hg(II) [99] and Cd(II) [100] complexes with thiones have been widely studied in recent years. In the previous work on silver(I)-thione complexes, the synthesis of various $[LAgNO_3]$ complexes and their characterization by ^{13}C NMR has been reported [98]. The present study describes the synthesis of a number

of silver(I) complexes with thiourea ($[Ag(Tu)_xNO_3]$) and several other thiones ($[LAgNO_3]$ and $[AgL_2]NO_3$, where L is Imt or Diaz and their derivatives) and their characterization by ^1H, ^{13}C, ^{15}N and ^{107}Ag NMR spectroscopy. In order to obtain information about various coupling constants and to report ^{15}N chemical shifts, we use 5-10 % ^{13}C and ^{15}N labeled Tu and in two of the thiones, Imt and Diaz they are 2-3 % labeled.

The occurrence of two spin ½ isotopes for silver, ^{107}Ag and ^{109}Ag with high natural abundances (51 % and 49 % respectively) provides an additional useful tool for NMR studies of silver complexes. However, because of the low receptivities of its isotopes (3.4 x 10^{-5} and 4.9 x 10^{-5} respectively, relative to ^1H) only limited reports are available in the literature on silver NMR [101].

Recent research has shown that heavy metals like gold, silver and mercury are known to interact with selenium in the body resulting in reduction of the toxicity of both the metal ions and selenium [102,103]. Therefore, a systematic investigation of metal complexation with selenium containing ligands is also important from biological point of view. In spite of this importance there are only limited reports describing the metal complexation with the selenone ligands. The present report describes the synthesis of silver(I) complexes with the stoichiometries, $[LAgNO_3]$ and $[AgL_2]NO_3$ for a series of selenones and their characterization by ^1H, ^{13}C and ^{107}Ag NMR spectroscopy.

The combined use of ^{13}C and ^{107}Ag NMR would provide a powerful means of studying silver complexes in solution. These studies provide a useful data base of ^{13}C and ^{107}Ag NMR spectra for silver(I) complexes of thiones and selenones.

2.3 Ligand Scrambling Reactions of Gold(I) Complexes

It is well known that gold drugs (used for the treatment of rheumatoid arthritis [69,70]) and their metabolites react in vivo with cyanide to form the intermediates [RS-Au-CN]$^-$ and [Et_3P-Au-CN], which undergo disproportionation generating $[Au(CN)_2]^-$ that is readily taken up by red blood cells (RBCs) [104-109]. The cyanide is produced in the body by oxidation of SCN^- in polymorphonuclear leukocytes [104,105]. Although the concentration of cyanide in RBCs is very low (0.3-1 μM) [110], the very large formation constant of $[Au(CN)_2]^-$ ($\log\beta = 36$) [111] favors its formation. The level of $[Au(CN)_2]^-$ is higher for smokers than for nonsmokers because of inhalation of HCN from tobacco smoke [107,112]. The formation of $[Au(CN)_2]^-$ by the scrambling reactions of cyanogold(I) complexes of phosphine and sulfur containing ligands is therefore important from a biological point of view.

Disproportionation reactions have been reported for a variety of cyano(phosphine)gold(I) complexes [32,113,114]. These complexes are usually monomer and two coordinate in solid state [31,115]. But in solution they are known to undergo disproportionation to form the symmetrically substituted complexes according to the equilibrium (2.1):

$$2\,[R_3PAuCN] \rightleftharpoons [Au(CN)_2]^- + [(R_3P)_2Au]^+ \qquad (2.1)$$

However, cyano(2-cyanoethylphosphine)gold(I) exists as an ionic complex, $[AuL_2]^+[Au(CN)_2]^-$ both in solution as well as in the solid state [116]. Recently, it was

observed that [Cy_3P=S-AuCN] [30] and [Cy_3P=Se-AuCN] [31] type complexes (Cy = cyclohexyl) undergo similar disproportionation reactions. Disproportionation is also known for cyano-thiolatogold(I) complexes [108,117]. But there does not appear to be any study describing disproportionation in cyano(thione)gold(I) complexes, although the synthesis of various cyano(thione)gold(I) complexes has already been reported but without any evidence of disproportionation [27]. However, cyano(N,N′-dimethylthiourea)gold(I) is known to exist as an ionic complex $[AuL_2]^+[Au(CN)_2]^-$, in the solid state [118]. Cyano(thione)gold(I) complexes may be useful as models for the cyano intermediates of gold drugs, $[RS\text{-}Au\text{-}CN]^-$. Therefore, in the present study we carried out an investigation of scrambling reactions of various cyano(thione)gold(I) complexes. We were also able to measure the equilibrium constants (K_{eq}) for the scrambling reactions of the complexes by integration of the CN^- resonances in the ^{13}C NMR. Because of the possible biological implications of these reactions [104-107], the effects of several extrinsic factors on K_{eq} were systematically examined for one of the complexes, Imt-Au-CN. The external influences examined are the initial concentrations, ionic strength of the medium, temperature and polarity of the solvent. The dependence of K_{eq} on initial concentration was studied in DMSO-d_6, while the effects of temperature and ionic strength were examined in methanol-d_4.

The structures of the thiones used in this study are described in scheme 2.1.

The study of scrambling reactions given by eq. (2.1) was also extended [6,7,10,11] for a number of cyano(selenone)gold(I) complexes, [>C=Se-Au-CN]. The equilibrium constants (K_{eq}) for the scrambling reactions of these complexes were also determined by integration of $^{13}C^{15}N$ resonances in ^{13}C NMR. Although the complexes of thiones with

gold(I) have been studied extensively [25-27], there is no known report describing the synthesis of gold(I) complexes of selenones except selenourea [35].

The structures of the selenones used in this study are described in scheme 2.2

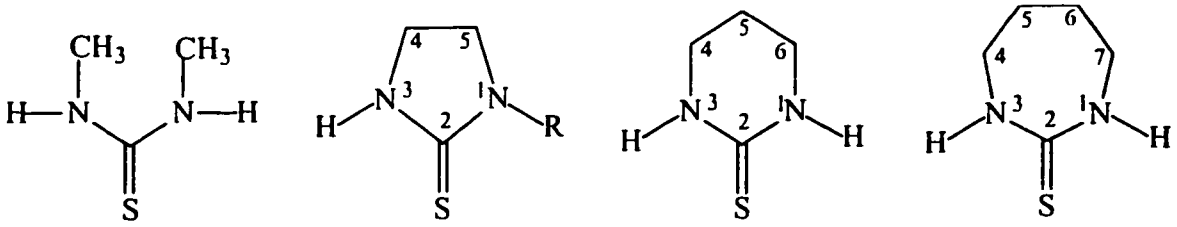

(a) (b-f) (g) (h)

(a) N,N′-dimethylthiourea (DmTu)

(b) R = H; Imidazolidine-2-thione (Imt)

(c) R = CH_3; N-methylimidazolidine-2-thione (MeImt)

(d) R = C_2H_5; N-ethylimidazolidine-2-thione (EtImt)

(e) R = C_3H_7; N-propylimidazolidine-2-thione (PrImt)

(f) R = *i*-C_3H_7; N-(*i*-propyl)imidazolidine-2-thione (*i*-PrImt)

(g) 1,3-Diazinane-2-thione (Diaz)

(h) 1,3-Diazipane-2-thione (Diap)

Scheme 2.1

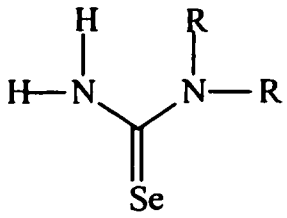

(a-b)

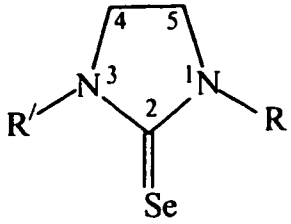

(c-h)

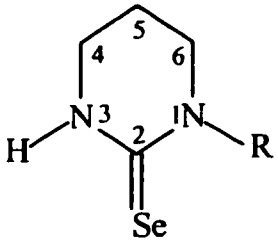

(i-j)

(a) R = H; Selenourea (Seu)

(b) R = CH_3; N,N-Dimethylselenourea (DmSeu)

(c) R = R′ = H; Imidazolidine-2-selenone (ImSe)

(d) R = H, R′ = CH_3; N-methylimidazolidine-2-selenone (MeImSe)

(e) R = H, R′ = C_2H_5; N-ethylimidazolidine-2-selenone (EtImSe)

(f) R = H, R′ = *i*-C_3H_7; N-(*i*-propyl)imidazolidine-2-selenone (*i*-PrImSe)

(g) R = H, R′ = C_6H_5; N-phenylimidazolidine-2-selenone (PhImSe)

(h) R = R′ = C_2H_5; N,N′-diethylimidazolidine-2-selenone (Et_2ImSe)

(i) R = H; 1,3-Diazinane-2-selenone (DiazSe)

(j) R = CH_3; N-methyl-1,3-Diazinane-2-selenone (MeDiazSe)

Scheme 2.2

2.4 Ligand Exchange Reactions of Anti-rheumatic Gold(I) Complexes

Gold-based drugs after their administration undergo ligand exchange reactions in the body with biofluids, cells and proteins [5,110,119-121]. The exchange reactions of gold drugs have been studied with various biologically available S-containing ligands, *e.g.*, bovine serum albumin, red blood cells at physiological concentration of the drug and biomolecules [5,110,120,121]. These ligand exchange reactions have been studied extensively using ^{13}C, ^{15}N, and ^{31}P NMR spectroscopy [5,120,121].

2.4.1 Exhange Reactions of Gold(I) Thiomalate $(AuStm)_n$

Gold(I) thiolates, such as myocrisin, $(AuStm)_n$ and solganol exist as polymers in the solid state as well as in solution [73,74]. However, in the presence of other thiols RSH, they undergo exchange reactions forming $[Au(SR)_2]^-$ type complexes [122,123], while, with thiones $(AuStm)_n$ was suggested to form [>=S-Au-Stm] type complexes [124,125]. In the present work, the interactions of $(AuStm)_n$ with 6-mercaptopurine (6-MP), 6-mercaptopurine-9-β-D-riboside (6-MPR) and 2-amino-6-mercaptopurine- 9-β-D-riboside (2-A-6-MPR) are investigated using ^1H and ^{13}C NMR spectroscopy. The structures of these ligands and $(AuStm)_n$ are shown in Figure 2.1.

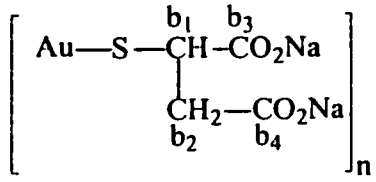

Myocrisin ([AuStm]$_n$)

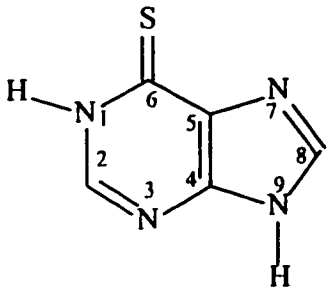

6-Mercaptopurine (6-MP)

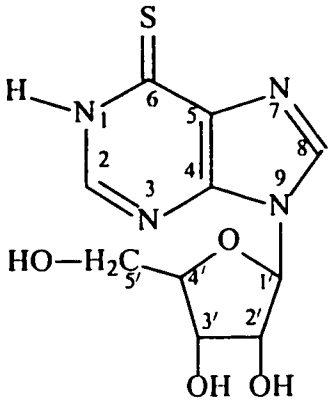

6-Mercaptopurine riboside (6-MPR)

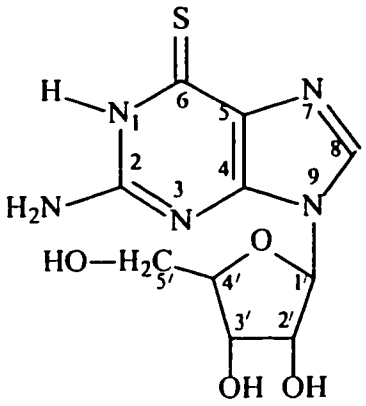

2-Amino-6-Mercaptopurine riboside (2-A-6-MPR)

Figure 2.1 Structures of $(AuStm)_n$ and 6-mercaptopurines

2.4.1.1 Exchange Reactions with 6-Mercaptopurine and Its Derivatives

The thio analogues of the purine bases, 6-mercaptopurine and 2-amino-6-mercaptopurine are among the most active anti-metabolites and their ribosides are known to exhibit antitumor activity [89, 126]. Mercaptopurine and its riboside are anticancer metabolites, clinically effective against human leukemias [96]. These thiolated compounds have seen only limited use in therapy as single agents. However, some metal complexes of purine thiones especially those of Pt and Pd show antitumor activity [127]. Some gold(I) purine-6-thiolate complexes are also known to possess the antiarthritic activity [20]. The Cu^{+2} complexes of 6-mercaptopurine are also reported to possess anti-inflammatory activity, a property that is common with gold(I) thiolate drugs [92].

The mercaptopurines and their ribosides are known to exist as thiones in the solid state as well as in the aqueous solution at room temperature, while heating favors the thiol form [96]. It would be of interest to investigate, whether these mercaptopurines act as anions, thiolates or as thiones. For the first time it is shown that two geometrical isomers are possible for the complex 6-MP-Au-Stm, formed by 6-MP after interacting with $(AuStm)_n$.

2.4.1.2 Exchange Reactions with Diselenides

The complexation of gold(I) thiomalate (Myocrisin), $(AuStm)_n$ with selenium containing amino acids is also important since selenocysteine is present at the active binding site of Se-glutathione peroxidase, the only mammalian selenoprotein with a

known catalytic activity [128-130]. The binding of $(AuStm)_n$ with some selenolate ligands, selenopropionate, selenocysteine, selenocystamine and selenoethanoic acid in aqueous solutions has already been reported and it was observed that these ligands replaced all thiomalate from gold(I) forming bis complexes, $[Au(SeR)_2]^-$ [131,132].

Redox reactions of $(AuStm)_n$ with $SeCN^-$ in aqueous solution (where Stm^-, is thiomalate) have also been reported [133]. These reactions resulted in the generation of $[(Stm)Au(SeCN)]^-$ which underwent disproportionation to give $[Au(SR)_2]^-$(where RS^- is Stm), $[Au(CN)_2]^-$ and metallic selenium. The free ligand, released from $[Au(SR)_2]^-$ was oxidised to disulfide, $(RS)_2$, reducing gold(I) to metallic gold.

$(AuStm)_n$ exists as a polymer (Figure 1.5) in the solid state as well as in solution [73,74]. With its chain structure it may have a capacity, to react with disufides and diselenides in addition to do with thiols and selenols. Since on binding to $(AuStm)_n$, the disulfide (S-S) and diselenide (Se-Se) linkages should be reduced to the thiolate and selenolate forms respectively, therefore redox, instead of simple exchange reactions are expected to occur in these interactions. The opening of S-S linkage by $(AuStm)_n$ has already been reported [134]. The present study describes the exchange kinetics of $(AuStm)_n$ with two diselenides, selenocystine and selenosyctamine in D_2O using ^{13}C NMR spectroscopy. Structures of gold(I) thiomalate (Myocrisin), thiomalic disulfide, selenocystine and selenocystamine and their resonance assignments are shown in Figure 2.2.

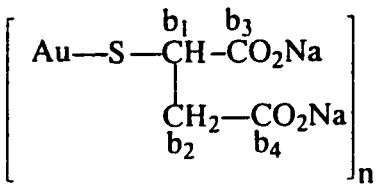

Myocrisin $(AuStm)_n$

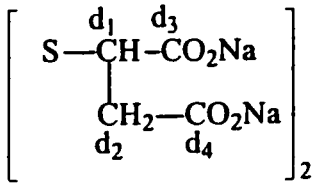

Thiomalic disulfide $[(Stm)_2]$

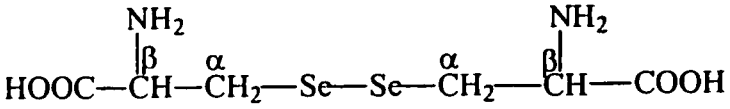

Selenocystine

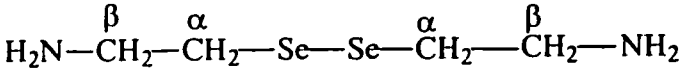

Selenocystamine

Figure 2.2 Structures of gold(I) thiomalate (Myocrisin), thiomalic disulfide, selenocystine and selenocystamine

2.4.2 Exchange Reactions of Auranofin

Despite the strong binding of both triethylphosphine and thioglucose ligand to gold(I), auranofin undergoes facile thiol exchange reactions [120,121]. Exchange reactions of auranofin have been studied with various biologically available sulfur containing ligands, *e.g.*, bovine serum and red blood cells at physiological concentrations of drugs and biomolocules [110,120,121]. Auranofin ($Et_3PAuSATg$) reacts rapidly with mercaptalbumin (AlbSH) via a ligand exchange reaction to form AlbS-Au-PEt_3 with gold binding to cystein-34. The albumin gold phosphine complex is stable if isolated from displaced thiol. If $ATgS^-$ remains in solution or is replaced with other thiols, the Et_3P is displaced and is oxidized to Et_3PO [120,121,135,136]. When Cl^-, a low affinity ligand for gold(I) is substituted for $SATg^-$, no Et_3PO is formed [120,121,135]. The preferred ligands for R_3PAu^+ would be; $R_3P \sim CN^- > RS^- > >C{=}S > R_2S$ [137].

Gold(I) thiolates, (Gold(I), thiomalate and thioglcose) being polymers can not enter red blood cells (RBCs) [138,139], while auranofin being monomeric does enter into RBCs immediately after its absorption and binds to glutathione (GSH) and hemoglobin (Hb) [140,141]. The RBCs, which contain thiol and thione ligands, *e.g.*, Hb, GSH and ergothionine (ErS), can form stable complexes with gold drugs [116,142,143]. The concentrations of Hb and GSH in RBCs are 4 mM and 2.5 mM respectively, while that of ErS is 0.15-0.60 mM [142]. GSH and Hb have SH group as their binding site and are more reactive than ErS, which exists in thione (ErS), I - thiol (ErSH), II equilibrium as given by eq. (2.2). The thione form, I is predominant in the solid state and at physiological pH [142,144]. In order to gain an insight into the mechanism of action of

gold drugs with intracellular ligands, it is important to assess independently the chemical reactivities of these ligands towards gold(I) complexes.

Most studies of the exchange reactions of auranofin deal with thiols and cyanide [106,107,120,135]. To learn about the role of thiones like thiourea on the reactions of gold drugs, we undertook an investigation of the interaction of thiourea (Tu) (5 % ^{13}C and ^{15}N labeled) with auranofin and Et_3PAuCl in methanol using ^{13}C, ^{31}P and ^{15}N NMR spectroscopy. The study of exchange reactions of auranofin was extended to other thiones including ergothionine (ErS).

The structures of auranofin and the thiones under study are shown in Figure 2.3.

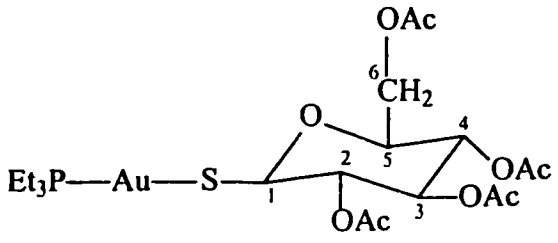

Auranofin

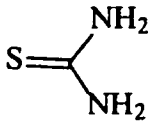

Thiourea (Tu)

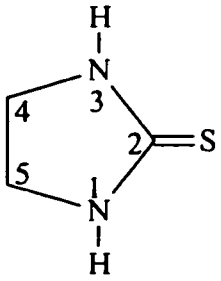

Imidazolidine-2-thione (Imt)

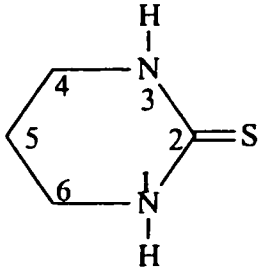

Diazinane-2-thione (Diaz)

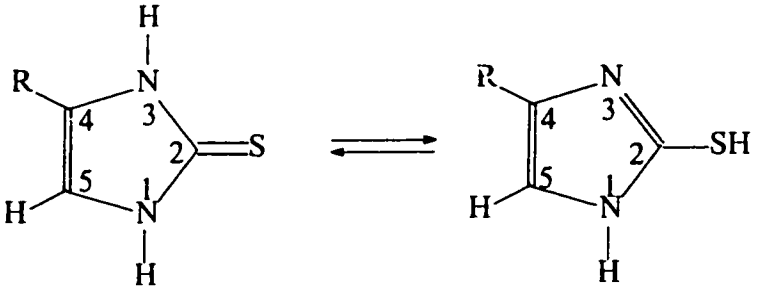

(2.2)

I II

Ergothionine (ErS)

Where,

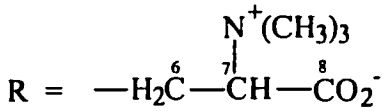

Figure 2.3 Structures of auranofin and various thiones

CHAPTER 3

EXPERIMENTAL SECTION

3.1 Chemicals

Thiourea, selenourea, N,N′-dimethylthiourea, N,N-dimethylselenourea, CD_3OD, CH_3OD, DMSO-d_6, Acetone-d_6, D_2O, NaOD, DCl, ergothionine, 6-MP, 6-MPR, 2-A-6-MPR, tetraacetylthioglucose, KCN, $(CH_3)_2S$, $AuBr.2H_2O$, $AgNO_3$, NH_4NO_3, carbon disulfide, diamines and all solvents were obtained from Fluka-Aldrich Chemical Co., Germany. Carbon-13 and ^{15}N labeled thiourea selenourea and KCN were obtained from Isotec Co, USA. $HAuCl_4.3H_2O$ and all phosphines were obtained from Strem Chemical Co. Gold(I) thiomalate $[(AuStm)_n]$ and Et_3PAuCl were obtained from ICN K & K Labs Plainview, New York. Selenocystine and selenocystamine dihydrochloride were obtained from Sigma Chemical Co. Auranofin was a generous gift from Smith Kline and French Laboratories, Philadelphia.

3.2 Instrumentation

3.2.1 IR Measurements

The solid state IR spectra of the ligands and their cyanogold(I) complexes were recorded on a Perkin Elmer FTIR 180 spectrophotometer using KBr pellets in the 4000-400 cm^{-1} range.

3.2.2 ^{1}H NMR Measurements

The ^{1}H NMR spectra were obtained on Jeol JNM-LA 500 NMR spectrometer operating at a frequency of 500.00 MHz. The conditions were 32 K data points, 1.50 s pulse delay, and 45° pulse angle.

3.2.3 ^{13}C NMR Measurements

The ^{13}C NMR spectra were obtained at the frequency of 125.65 MHz with ^{1}H broadband decoupling at 298 K. The spectral conditions were: 32 K data points, 0.967 s acquisition time, 1.00 s pulse delay and 45° pulse angle. The ^{13}C chemical shifts were measured relative the internal reference TMS or dioxane, which is 67.4 ppm from TMS.

T_1 values for ^{13}C nuclei were measured for the complexes, Imt-Au-CN and ImSe-Au-CN using inversion recovery method. The average values obtained are; 5.5 seconds for $[Au(CN)_2]^-$, 3.9 seconds for CN carbon of Imt-Au-CN, 4.0 seconds for CN of ImSe-Au-CN and 5.0 seconds for >C=S carbon of Imt-Au-CN. Based on these T_1 values, a

delay time of 30.0 seconds was used to record the ^{13}C NMR spectra of the cyanogold(I) complexes so that the spectra could be integrated quantitatively.

3.2.4 ^{31}P NMR Measurements

The ^{31}P NMR spectra were recorded at a frequency of 202.35 MHz, using 0.269 s acquisition time, 5.00 s pulse delay and 6.20 μs pulse width (45°). The ^{31}P NMR chemical shifts were measured relative to the internal reference 85 % H_3PO_4. A delay time of 20.0 seconds was used where quantitative integration was required.

3.2.5 ^{15}N NMR Measurements

The ^{15}N NMR spectrum was recorded at 50.55 MHz using 2.1 M $^{15}NH_4{}^{15}NO_3$ in D_2O as an external reference, which lies at 375.11 ppm relative to pure CH_3NO_2, 380.2 ppm [33]. The spectral conditions for ^{15}N were: 32 K data points, 0.721 s acquisition time 2.50 s delay time, 60° pulse angle and approx. 5000-10000 scans.

3.2.6 ^{107}Ag NMR Measurements

The ^{107}Ag NMR was obtained at the frequency of 20.13 MHz using 10 mm low frequency probe with 9.1 M $AgNO_3$ in D_2O as an external reference. The spectral conditions were: 32 K data points, 1.02 s acquisition time, 6.0 s delay time, 45° pulse angle and approx. 2000-4000 scans.

3.2.7 pH measurements

All pH measurements were made at 296 K with a Fischer Accumet pH meter, model 630. The pH indicates the actual meter reading for D_2O solutions with no correction for deuterium isotope effects. The pH was adjusted using DCl and NaOD. The pH higher than the physiological pH was selected, because thionucleosides and diselenides were insoluble at that pH.

3.2.8 Conductance measurements

The conductance measurements were made for silver(I) complexes of thiones and selenones in DMSO at 297 K on PHYWE conductivity meter, model 18151.93. The cell constant of the electrode was 0.91 cm^{-1}. The conductance values were obtained in terms of μ siemens (μ mho). The observed conductance was multiplied by cell constant to calculate the specific conduntance (k). The molar conductance (λ) was obtained by using the following relation [145];

$$\lambda = \frac{k \times 1000}{C} \quad (mho.cm^2/mole) \qquad (3.1)$$

Where C is the concentration of solution in moles per liter.

3.3 Synthesis of Ligands

3.3.1 Thiones

Thiones were synthesized according to the procedure described in the literature (by the addition of CS_2 to diamines in ether and then heating the resulting adduct at 100°C for 2-3 hrs, followed by its crystallization in methanol) [146,147]. In all ligands except DmTu and Diap, C-2 contains 5 % labeled carbon-13. The ligands were analysed by ^{1}H and ^{13}C NMR spectroscopy.

The selenones were provided generously by Prof. Alan P. Arnold, University of New South Wales, Australia. They were synthesized according to the procedure described in the literature [148,149].

3.4 Synthesis of Gold(I) and Silver(I) Complexes

The synthetic procedures of the complexes prepared in this study are explained below.

3.4.1 Synthesis of Gold(I) Complexes

3.4.1.1 Chloro(dimethylsulfide)gold(I), $(CH_3)_2SAuCl$

2.1418 g of $HAuCl_4 \cdot 3H_2O$ (5.44×10^{-3}moles) was dissolved in 50 ml of ethanol. Dimethyl sulfide, $(CH_3)_2S$ was added in excess with continuous stirring and under nitrogen. The flask was wrapped in an aluminum foil, and also lights were turned off.

The solution was stirred for few minutes and cooled in ice. The white precipitates formed, were filtered and washed with cold ethanol and cold anhydrous ether.

$2(CH_3)_2S + HAuCl_4 \cdot H_2O \rightarrow (CH_3)_2S\text{-}AuCl + 3HCl + 3H_2O + (CH_3)_2SO$

The elemental analysis is; C = 8.20 % (calcd 8.15 %), H = 2.21 % (calcd 2.04%).

3.4.1.2 Synthesis of AuCN

Me_2S-AuCl, 1.4911 g (5.06×10^{-3} moles) was slurried in 150 ml acetone. To it was added 0.6602 g (0.0101 moles) KCN (or $K^{13}C^{15}N$ for the synthesis of $Au^{13}C^{15}N$). The reaction mixture turned colorless. Then 50 ml concentrated H_2SO_4, was added carefully and slowly by stirring continuously. Evolution of HCN and heat occurred from the mixture. A bright yellow ppt was formed and the mixture was left in fume hood overnight. The precipitate was decanted and washed twice with water, twice with ethanol and thrice with anhydrous ether. A lemon yellow product was obtained. Yield = 79.24 %.

$Me_2S\text{-}AuCl + 2KCN \rightarrow Me_2S + K[Au(CN)]_2 + KCl$

$K[Au(CN)_2] + H_2SO_4 \rightarrow KHSO_4 + AuCN + HCN$

The elemental analysis is; C = 5.30 % (calcd 5.38 %), N = 5.90 % (calcd 6.27 %).

Note: *HCN is a very poisonous gas, therefore addition of H_2SO_4 should be carried out carefully in the fume hood.*

3.4.1.3 R_3PAuCl Complexes

These complexes were prepared by adding phosphines to the slurry of $(CH_3)_2S$-AuCl in acetone under N_2 and stirring for half an hour. After keeping the resulting

colorless solution in refrigerator, white products were obtained. Their formation was confirmed by recording their ^{31}P NMR spectra. These complexes were used as precursors for the preparation of mixed ligand gold(I) complexes of thiourea and selenourea.

The phosphines used in the study are; Me_3P, Et_3P, Ph_3P, Cy_3P, $CyPh_2P$, $(o\text{-Tol})_3P$, $(m\text{-Tol})_3P$, $(p\text{-Tol})_3P$ (where, Me = methyl, Et = ethyl, Ph = phenyl, Cy = cyclohexyl, Tol = tolyl).

3.4.1.4 [R_3PAuTu]Cl Complexes

They were prepared by addition of thiourea as solid to R_3PAuCl solutions in methanol or acetone and stirring the mixture for 15-20 minutes. The resulting colorless solution was filtered and kept in refrigerator for crystallization. As a result, white crystalline products were obtained with a yield of 60-70 %. The complex [$(m\text{-Tol})_3$PAuTu]Cl was prepared in acetonitrile and [$(CyPh_2)$PAuTu]Cl was isolated from a mixture of acetone and hexane.

The elemental analysis of these complexes is given in Table 3.1.

3.4.1.5 [R_3PAuSeu]Cl Complexes

Selenourea (Seu), dissolved in acetonitrile was added to R_3PAuCl solution in acetone (or in acetonitrile if it is soluble). After stirring for 15-20 minutes the resulting colorless solution was filtered and kept in the refrigerator. As a result, white crystalline products were obtained with 50-60 % yield. After preparation, the complexes were stored in refrigerator.

The elemental analysis of these complexes is given in Table 3.2.

3.4.1.6 Gold(I) Complexes of 6-Mercaptopurine and Its Derivatives

Complexes of the type $[R_3PAuL]Cl$, (where L = 6-MP, 6-MPR and 2-A-6-MPR) were prepared by adding the ligands to R_3PAuCl solutions in methanol and stirring for half an hour, resulting in a colorless solution. After evaporation of the solvent, the product was either washed with acetone or crystallized from a mixture of acetone and methanol (yield 30-40 %).

Complexes of the type [LAuX] were prepared by the addition of the ligands to either $(CH_3)_2S$-AuCl or $AuBr.2H_2O$ in methanol. In the cases of [6-MPAuCl] and [6-MPRAuBr] the resulting solutions were of light yellow color while, in the case of [2-A-6-MPRAuCl] it was orange red colored with the same color of the product.

The elemental analyses of the complexes are given in Table 3.3.

3.4.1.7 Cyano(thione)gold(I) Complexes

All [>C=S-Au-CN] complexes were prepared according to the published procedure [27], by refluxing an equimolar amount of thione and AuCN in methanol and then crystallizing in methanol. The complexes of DmTu, Diaz and Diap ligands could not be crystallized in methanol, instead sticky materials were obtained which were separated by addition of diethyl ether. For ErS-AuCN (ErS = ergothionine, Figure 2.3) the ligand was dissolved in water. After evaporation of solvent, the resulting colorless substance was redissolved in 2-3 ml methanol and precipitated by the addition of 20 ml chloroform. The

precipitates were filtered, washed with acetone and dried as an off white product. The complex is sensitive to moisture. The structures of thiones are shown in scheme 2.1.

The elemental analyses of the complexes are given in Table 3.4.

3.4.1.8 Cyano(selenone)gold(I) Complexes

AuCN was suspended in acetone and an equimolar amount of the selenone in acetonitrile was added. The mixture was stirred for almost half an hour (in the case of Et_2ImSe, it was stirred for one day), after which a colorless solution was obtained. The solution was filtered and kept in refrigerator for crystallization. As a result, white crystalline products were obtained with 50-60 % yield.

The cyanogold(I) complexes of Seu and 4-MeImSe could not be isolated in the solid state. They were prepared in solution by mixing an equimolar amount of the selenone and AuCN (corresponding to 0.025 M) in DMSO-d_6 and stirring for about half an hour (AuCN was added in slight excess). The NMR spectra were recorded for the resulting almost colorless solution. The structures of selenones are shown in scheme 2.2.

The elemental analyses of the complexes are given in Table 3.5.

3.4.2 Synthesis of Silver(I) Complexes

3.4.2.1 $[Ag(Tu)_xNO_3]$ Complexes

The series of complexes was prepared by adding Tu in MeOH to $AgNO_3$ in MeCN in the required molar ratios. In the case of $[Ag(Tu)_1NO_3]$ white precipitate were formed

on mixing the two solutions, while for other complexes the mixing resulted in a colorless solution, which after keeping in refrigerator yielded white crystalline products. Mixing of Tu with $AgNO_3$ at the ratio of 5:1 did not result in the complex $[Ag(Tu)_5]NO_3$, instead $[Ag(Tu)_4]NO_3$ was obtained.

The elemental analysis of the complexes is given in Table 3.6.

3.4.2.2 $[Ag(Seu)_xNO_3]$ Complexes

Selenourea solution in actonitrile was added to $AgNO_3$ dissolved in acetonitrile in a required molar ratio. Immmediately white precipitates were formed. The solution was stirred for about 15 minutes. White precipitates were filtered and washed with acetone. Yield = 85 %.

The elemental analysis of the complexes is given in Table 3.6.

3.4.2.3 Silver(I) Complexes of Thiones

The complexes were prepared by adding thiones in methanol (20-25 ml) to $AgNO_3$ in 15 ml acetonitrile in the required molar ratios and stirring for 15 minutes. For the complexes of DmTu, Imt and Diaz ligands, white or yellow precipitates were formed on mixing the two solutions (dark brown for $[ImtAgNO_3]$), which were filtered and washed with methanol. The $[Ag(Diaz)_2]NO_3$ complex was crystallized from water-methanol mixture. For the complexes of MeImt, EtImt, PrImt, *i*-PrImt and EtDiaz mixing resulted in a colorless or yellow solution. White or yellow solids were obtained on evaporation of the solvent. In the case of EtImt and *i*-PrImt the products were washed with water and

acetone. $[Ag(EtDiaz)_2]NO_3$ was isolated from acetone. The experimental yield of the products was around 60 to 70 % (40 % for $[Ag(EtDiaz)_2]NO_3$). The structures of thiones are explained in scheme 2.1.

The elemental analyses of these complexes are given in Tables 3.7 and 3.8.

3.4.2.4 Silver(I) Complexes of Selenones

The silver(I) complexes of selenones were prepared by mixing the solutions of selenones and $AgNO_3$ in acetonitrile in the required molar ratios and stirring for about 15 minutes. The resulting white precipitates were filtered and washed with acetonitrile or acetone. For the complexes, mixing resulted in a colorless solution, which after refrigeration yielded the white crystalline product. After preparation the complexes were stored in refrigerator.

The experimental yield of the products was around 60-70 %. The elemental analyses and melting points (m.p.) of the complexes are given in Tables 3.9 and 3.10.

The structures of selenones are explained in scheme 2.2.

Table 3.1 Elemental analysis of $[R_3PAuTu]Cl$ complexes

Complex	Found (Calcd) %				m.p. (°c)
	C	H	N	S	
$[Me_3PAuTu]Cl$	12.67	3.52	7.36	7.93	199-200
	(12.49)	(3.41)	(7.28)	(8.33)	
$[Et_3PAuTu]Cl$	19.83	4.61	6.64	7.21	135-136
	(19.70)	(4.50)	(6.57)	(7.51)	
$[Cy_3PAuTu]Cl$	38.74	6.42	5.42	4.76	204-206
	(39.97)	(6.34)	(4.76)	(5.44)	
$[Ph_3PAuTu]Cl$	40.67	3.35	5.38	5.73	146-148
	(39.97)	(3.36)	(4.91)	(5.62)	
$[(CyPh_2)PAuTu]Cl$	40.38	4.76	5.36	5.95	112-114
	(39.55)	(4.38)	(4.86)	(5.56)	
$[(o\text{-Tol})_3PAuTu]Cl$	43.32	4.46	4.74	4.60	199-201
	(43.11)	(4.12)	(4.57)	(5.22)	
$[(m\text{-Tol})_3PAuTu]Cl$	41.85	4.10	4.46	4.35	124-125
	(43.11)	(4.12)	(4.57)	(5.22)	

Table 3.2 Elemental analyses of $[R_3PAuSeu]Cl$ complexes

Complex	Found (Calcd)			m.p. (°c)
	C	H	N	
$[Me_3PAuSeu]Cl$	11.26	3.06	7.14	178-179
	(11.13)	(3.04)	(6.49)	
$[Et_3PAuSeu]Cl$	17.76	4.24	6.14	145-146
	(17.75)	(4.05)	(5.92)	
$[Cy_3PAuSeu]Cl$	36.51	6.15	4.96	155-157
	(36.58)	(5.88)	(4.41)	
$[Ph_3PAuSeu]Cl$	37.69	3.42	5.03	137-138
	(36.94)	(3.12)	(4.54)	
$[CyPh_2)PAuSeu]Cl$	37.38	4.36	4.70	140-143
	(36.58)	(4.05)	(4.49)	
$[(m\text{-}Tol)_3PAuSeu]Cl$	39.49	3.83	5.14	135-136
	(40.04)	(3.83)	(4.25)	

Table 3.3 Elemental analyses of gold(I) complexes of 6-MP and its derivatives

Complex	Found (Calcd) %			
	C	H	N	S
$[Ph_3PAu\text{-}6MP]Cl$	41.68	3.20	8.69	4.80
	(42.70)	(2.97)	(8.66)	(4.95)
$[Cy_3PAu\text{-}6MP]Cl$	39.94	5.44	11.88	6.59
	(41.53)	(5.62)	(8.43)	(4.81)
$[(CyPh_2)PAu\text{-}6MP]Cl$	39.45	3.78	11.82	6.47
	(42.30)	(3.87)	(8.58)	(4.90)
$[Me_3PAu\text{-}6MPR]Cl$	26.19	3.50	9.31	5.06
	(26.34)	(3.58)	(9.45)	(5.40)
$[Ph_3PAu\text{-}6MPR]Cl$	42.82	3.48	8.09	4.26
	(43.17)	(3.50)	(7.19)	(4.11)
$[Me_3PAu\text{-}2A6MPR]Cl$	25.44	3.56	11.14	5.40
	(25.69)	(3.65)	(11.52)	(5.27)
$[Ph_3PAu\text{-}2AMPR]Cl$	40.35	3.56	10.54	4.70
	(42.35)	(3.50)	(8.82)	(4.03)
6MP-AuCl	16.33	1.20	14.46	8.12
	(15.61)	(1.05)	(14.57)	(8.34)
6MPR-AuBr	21.74	2.28	10.39	6.14
	(21.40)	(2.15)	(9.99)	(5.71)
2A6MPR-AuCl	21.31	2.42	11.79	5.73
	(22.59)	(2.47)	(13.18)	(6.03)

Table 3.4 Elemental analyses of the [>C=S-Au-CN] complexes

Complex	Found (Calcd) %			
	C	H	N	S
DmTuAuCN	15.18	2.44	11.85	8.00
	(14.68)	(2.46)	(12.85)	(9.80)
MeImtAuCN	17.37	2.31	11.38	11.97
	(17.70)	(2.38)	(12.39)	(9.45)
DiapAuCN	19.58	2.73	11.19	8.42
	(20.40)	(2.85)	(11.90)	(9.08)
ErSAuCN	25.84	3.52	11.56	6.60
	(26.56)	(3.35)	(12.39)	(7.09)

Table 3.5 Elemental analyses of the [>C=Se-Au-CN] complexes

Complex	Found (Calcd) %			m.p.(°C)
	C	H	N	
DmSeuAuCN	12.27	2.06	10.74	145 (decomp)
	(12.84)	(2.16)	(11.24)	
ImSeAuCN	13.36	1.70	11.12	168 (decomp)
	(12.91)	(1.63)	(11.30)	
MeImSeAuCN	15.75	2.19	10.69	172 (decomp)
	(15.55)	(2.09)	(10.89)	
EtImSeAuCN	18.05	2.65	10.12	140 (decomp)
	(18.01)	(2.52)	(10.50)	
i-PrImSeAuCN	20.58	2.99	10.46	160 (decomp)
	(20.30)	(2.92)	(10.15)	
PhImSeAuCN	26.63	2.37	9.85	165 (decomp)
	(26.74)	(2.40)	(9.36)	
Et_2ImSeAuCN	22.62	3.31	9.89	110-111
	(22.44)	(3.29)	(9.82)	
DiazSeAuCN	16.17	2.22	10.90	119-121
	(15.55)	(2.09)	(10.89)	
MeDiazSeAuCN	17.95	2.65	10.40	153-155
	(18.01)	(2.52)	(10.50)	

Table 3.6 Elemental analyses of the $[Ag(Tu)_x]NO_3$ and $[Ag(Seu)_x]NO_3$ complexes

Complex	Found (Calcd) %				m.p (°C)
	C	H	N	S	
$[TuAgNO_3]$	5.52	1.74	17.98	14.27	170 (decomp)
	(4.88)	(1.64)	(17.08)	(13.03)	
$[Ag(Tu)_2]NO_3$	7.90	2.59	22.47	20.71	102-104
	(7.45)	(2.50)	(21.74)	(19.89)	
$[Ag(Tu)_3]NO_3$	9.60	3.19	24.75	24.03	122-124
	(9.04)	(3.03)	(24.61)	(24.13)	
$[Ag(Tu)_4]NO_3$	10.43	3.55	26.72	26.12	97-99
	(10.13)	(3.40)	(26.73)	(27.01)	
$[SeuAgNO_3]$	4.46	1.43	14.82	-	108 (decomp)
	(4.10)	(1.38)	(14.35)		
$[Ag(Seu)_2]NO_3$	5.99	1.99	16.97	-	157-158
	(5.77)	(1.94)	(16.84)		

Table 3.7 Elemental Analyses of silver(I)-thione complexes, [$LAgNO_3$]

Complex	Found (Calcd) %			
	C	H	N	S
[$DmTuAgNO_3$]	14.97	3.71	15.56	13.47
	(13.14)	(2.94)	(15.34)	(11.70)
[$ImtAgNO_3$]	13.17	2.38	15.93	11.93
	(13.24)	(2.22)	(15.45)	(11.79)
[$MeImtAgNO_3$]	19.55	3.08	14.81	13.52
	(16.79)	(2.82)	(14.69)	(11.21)
[$EtImtAgNO_3$]	20.09	3.43	13.58	10.72
	(20.01)	(3.36)	(14.01)	(10.68)
[*n*-$PrImtAgNO_3$]	23.38	3.98	13.63	9.94
	(22.94)	(3.85)	(13.38)	(10.21)
[*i*-$PrImtAgNO_3$]	23.46	3.96	13.65	10.59
	(22.94)	(3.85)	(13.38)	(10.21)
[$DiazAgNO_3$]	18.53	3.18	15.07	10.34
	(16.79)	(2.82)	(14.69)	(11.21)
[$EtDiazAgNO_3$]	20.85	4.37	12.58	9.56
	(22.94)	(3.85)	(13.38)	(10.21)
[$DiapAgNO_3$]	19.82	3.39	13.50	11.27
	(20.01)	(3.36)	(14.01)	(10.68)
[6-$MPAgNO_3$]	18.06	1.19	21.05	11.10
	(18.65)	(1.24)	(21.75)	(9.95)

Table 3.8 Analysis of silver(I)-thione complexes, $[AgL_2]NO_3$

Complex	Found (Calcd) %				m.p.
	C	H	N	S	(°C)
$[Ag(DmTu)_2]NO_3$	18.70	3.91	17.06	15.42	169-170
	(19.05)	(4.26)	(18.52)	(16.95)	
$[Ag(Imt)_2]NO_3$	17.98	3.12	17.61	15.23	217-219
	(19.26)	(3.23)	(18.72)	(17.14)	
$[Ag(MeImt)_2]NO_3$	23.77	3.90	17.04	17.53	154-155
	(23.89)	(4.01)	(17.41)	(15.94)	
$[Ag(EtImt)_2]NO_3$	27.82	5.10	16.07	16.56	118-120
	(27.91)	(4.68)	(16.28)	(14.90)	
$[Ag(i\text{-}PrImt)_2]NO_3$	31.10	5.76	15.72	15.04	126-128
	(31.44)	(5.28)	(15.28)	(13.99)	
$[Ag(Diaz)_2]NO_3$	21.84	3.79	16.62	14.46	204-206
	(23.89)	(4.01)	(17.41)	(15.94)	
$[Ag(EtDiaz)_2]NO_3$	31.10	5.76	15.72	15.04	118-120
	(31.44)	(5.28)	(15.28)	(13.99)	

Table 3.9 Elemental analyses of the [>C=Se-$AgNO_3$] complexes

Complex	Found (Calcd) %			m.p.(°C)
	C	H	N	
[DmSeuAgNO_3]	11.13	2.47	12.79	79-80
	(11.23)	(2.51)	(13.10)	(decomp)
[ImSeAgNO_3]	11.43	1.85	13.06	128-129
	(11.30)	(1.90)	(13.18)	(decomp)
[MeImSeAgNO_3]	14.62	2.44	12.45	107
	(14.43)	(2.42)	(12.62)	(decomp)
[EtImSeAgNO_3]	16.74	2.78	11.46	106
	(17.31)	(2.90)	(12.11)	(decomp)
[*i*-PrImSeAgNO_3]	19.18	3.20	11.01	86-88
	(19.96)	(3.35)	(11.64)	
[PhImSeAgNO_3]	27.27	2.60	10.54	116
	(27.36)	(2.55)	(10.64)	(decomp)
[DiazSeAgNO_3]	13.77	2.40	11.71	133-134
	(14.43)	(2.42)	(12.62)	
[MeDiazSeAgNO_3]	17.19	2.88	11.86	100-102
	(17.31)	(2.90)	(12.11)	

Table 3.10 Elemental analyses of the $[Ag(>C=Se)_2]NO_3$ complexes

Complex	Found (Calcd) %			m.p.(°C)
	C	H	N	
$[Ag(DmSeu)_2]NO_3$	15.23	3.41	14.53	165-166
	(15.27)	(3.42)	(14.84)	
$[Ag(ImSe)_2]NO_3$	15.56	2.58	14.87	138-140
	(15.40)	(2.58)	(14.97)	
$[Ag(MeImSe)_2]NO_3$	19.52	3.48	14.10	164-165
	(19.37)	(3.25)	(14.12)	
$[Ag(EtImSe)_2]NO_3$	22.87	4.01	13.06	107-109
	(22.92)	(3.85)	(13.37)	
$[Ag(i\text{-}PrImSe)_2]NO_3$	25.61	4.11	12.32	186-188
	(26.10)	(4.38)	(12.69)	
$[Ag(PhImSe)_2]NO_3$	34.70	3.42	11.27	186-188
	(34.86)	(3.25)	(11.30)	
$[Ag(DiazSe)_2]NO_3$	20.52	3.53	14.19	193-195
	(19.37)	(3.25)	(14.12)	

CHAPTER 4

RESULTS

4.1 Characterization of Gold(I) Complexes of Thiourea and Selenourea

A number of mixed ligand gold(I) complexes of thiourea and selenourea, $[R_3PAuL]Cl$ (L = Tu or Seu) for a series of phosphines were prepared and characterized by IR, ^{13}C, ^{31}P and ^{15}N NMR.

4.1.1 IR Studies

A shift in ν(C=S) mode of Tu towards lower frequency is observed on its complexation with R_3PAu^+ moiety and a similar observation was found for Seu complexes. There are also strong absorptions around 1500 cm^{-1} and 3200 cm^{-1} corresponding to ν(CN) and $\nu(NH_2)$ modes respectively for Tu or Seu in all complexes. IR frequencies for the complexes are given in Table 4.1.

4.1.2 ^{31}P NMR Studies

The ^{31}P NMR spectra of the complexes were recorded in methanol-d_1. In each case, a sharp singlet was observed for R_3P moiety in $[R_3PAuL]Cl$ complexes. No coupling

with ^{13}C of labeled thiourea was observed in any complex. The ^{31}P NMR chemical shifts of several gold(I) complexes are given in Table 4.2. The ^{31}P resonance in both the thiourea and selenourea complexes appear downfield compared to the R_3PAuCl complexes. The signal is more downfield in selenourea complexes than for their thiourea analogues showing that Seu is more basic compared to Tu towards gold(I). The trend for an increase in ^{31}P NMR chemical shifts is similar for both the Tu and Seu complexes.

4.1.3 ^{13}C NMR Studies

The ^{13}C chemical shifts for >C=S and >C=Se carbons of Tu and Seu complexes respectively, are given in Table 4.3 alongwith the values of electronic parameter, ν(CO) for the phosphines [150]. An upfield shift is observed in the >C=S and >C=Se resonances of thiourea and selenourea respectively, on their complexation with gold(I). The >C=S resonance of Tu appeared as a triplet in ^{13}C NMR, due to coupling with ^{15}N with a $^{1}J(^{13}C\text{-}^{15}N)$ value of 15.7 Hz. Only small changes were observed in coupling constant on complexation with gold(I). A typical ^{13}C NMR spectrum for $[Cy_3PAuTu]Cl$ complex is given in Figure 4.1a. For selenourea complexes, a doublet was observed for the >C=Se resonance in all complexes as well as in the free ligand, since only one of the two nitrogens is ^{15}N labeled. A typical ^{13}C spectrum for $[Cy_3PAuSeu]Cl$ complex is given in Figure 4.1b. The coupling constants due to the coupling of carbon with phosphorus, $^{1}J(^{13}C\text{-}^{31}P)$ were also observed in ^{13}C NMR of all the complexes. The values of coupling constants are given in Table 4.4. The C_1 carbon of the phosphines in all complexes appears downfield compared to other carbons except those of PPh_3 and $(m\text{-}Tol)_3P$.

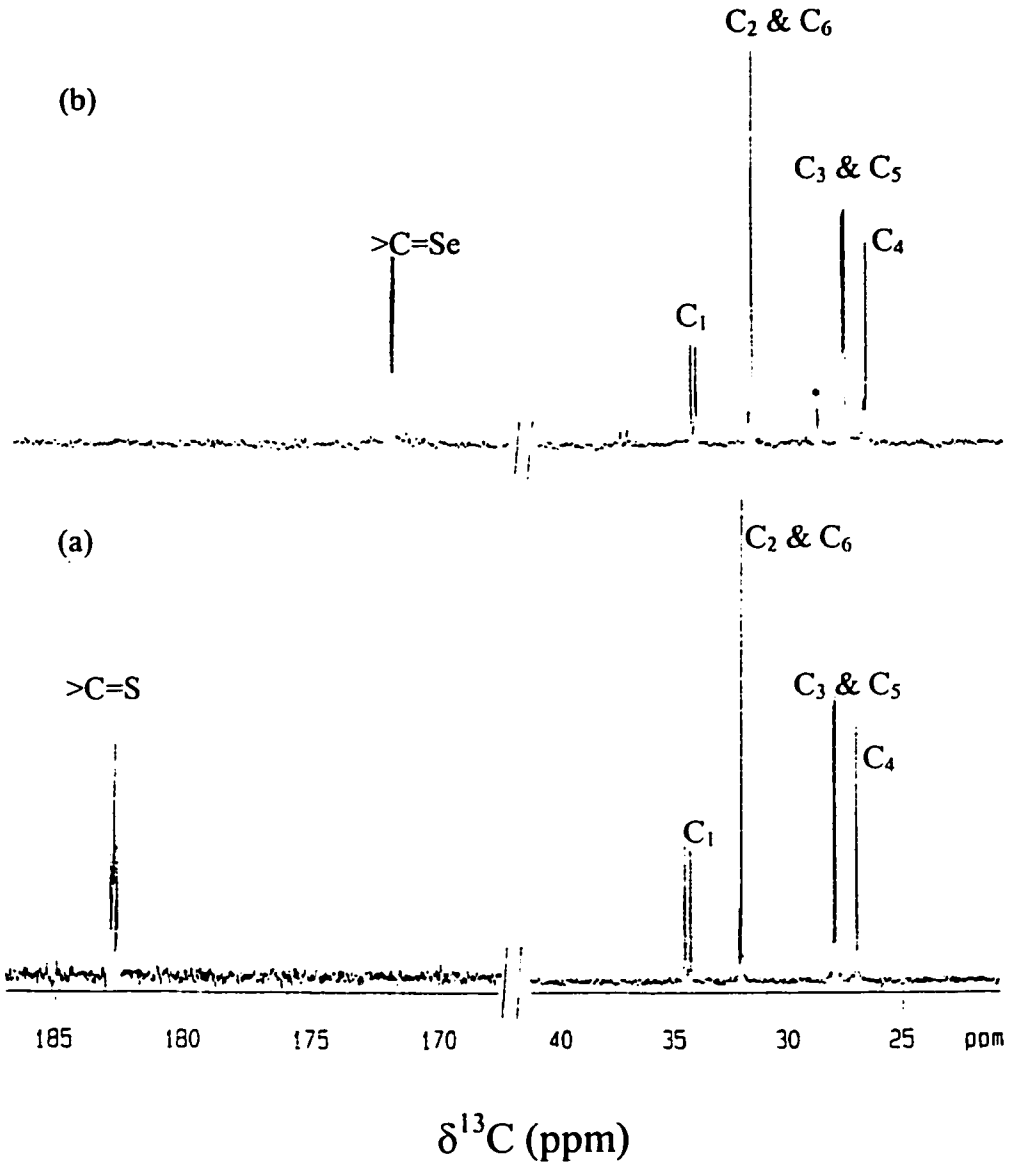

Figure 4.1 125.65 MHz ^{13}C NMR spectrum of (a) $[Cy_3PAuTu]Cl$ (b) $[Cy_3PAuSeu]Cl$

(*resonance due to some impurity)

4.1.4 ^{15}N NMR Studies

The ^{15}N chemical shifts in all complexes were observed at downfield position compared to that for free ligand. The ^{15}N chemical shifts for $[R_3PAuTu]Cl$ complexes are given in Table 4.3. The coupling constant, $^1J(^{13}C\text{-}^{15}N)$ could not be resolved by ^{15}N NMR.

Table 4.1 IR frequencies (cm^{-1}) of $[R_3PAuTu]Cl$ and $[R_3PAuSeu]Cl$ complexes

R_3P/Tu/Seu	ν(C=S) for $[R_3PAuTu]Cl$	ν(C=Se) for $[R_3PAuSeu]Cl$
Tu	730	-
Seu	-	736
Cy_3P	690	-
Et_3P	718	700
Me_3P	716	682
$(CyPh_2)P$	694	694
$(o\text{-Tol})_3P$	712	-
$(m\text{-Tol})_3P$	692	692
Ph_3P	710	710

Table 4.2 ^{31}P NMR chemical shifts (ppm) of $[R_3PAuL]$ complexes (L = Cl, Tu or Seu)

R_3P	δ $[R_3PAuCl]$ (I)	δ $[R_3PAuTu]^+$ (II)	Δδ (II-I)	δ $[R_3PAuSeu]^+$ (III)	Δδ(III-I)
Cy_3P	54.37	58.01	3.64	58.99	4.62
Et_3P	32.81	37.90	5.09	38.88	6.06
Me_3P	-9.56	-1.86	7.70	0.12	9.78
$(CyPh_2)P$	43.67	46.89	3.22	47.63	3.96
$(o\text{-Tol})_3P$	6.29	13.75	7.46	-	-
$(m\text{-Tol})_3P$	32.28	37.05	4.77	37.56	5.28
Ph_3P	32.22	37.01	4.79	37.72	5.50

Table 4.3 ^{13}C (>C=S & >C=Se) and ^{15}N NMR chemical shifts (ppm) for thiourea and selenourea (^{13}C & ^{15}N labeled) complexes

R_3P/Tu/Seu	ν (CO) of R_3P[a]	δ ^{13}C (>C=S)	δ ^{15}N (Tu)	δ ^{13}C (>C=Se)
Tu	-	185.54	103.65	-
Seu	-	-	-	178.64
Cy_3P	2056.4	182.76	104.74	172.59
Et_3P	2061.7	180.40	106.77	170.69
Me_3P	2064.1	179.34	106.47	170.75
(Cydiph)P	2064.8	177.26	-	171.13
(*o*-Tol)$_3$P	2066.6	178.58	107.64	-
(*m*-Tol)$_3$P	2067.9	177.33	107.92	170.62
Ph_3P	2068.9	177.21	107.32	169.45

[a] Values in cm^{-1} from ref. 150

Table 4.4 Coupling constants, $^{1}J(^{13}C-^{31}P)$ for various $[R_3PAuL]Cl$ complexes

R_3P	$[R_3PAuTu]Cl$	$[R_3PAuSeu]Cl$
Cy_3P	28.9	28.9
Et_3P	35.2	34.2
Me_3P	39.2	37.2
$(CyPh_2)P$	36.2	35.2
$(o\text{-Tol})_3P$	4.15	-
$(m\text{-Tol})_3P$	59.9	58.8
Ph_3P	59.9	63.1

4.1.a Gold(I) Complexes of 6-Mercaptopurine and Its Derivatives

These complexes were studied by ^{1}H, ^{13}C and ^{31}P NMR spectroscopy in DMSO-d_6. In ^{31}P NMR of the R_3PAuL type complexes (where, L = 6-MP, 6-MPR and 2-A-6-MPR; for the structures refer Figure 2.1), a slight downfield shift of 0.2-0.3 ppm was observed on the complexation of thione ligands R_3PAu^+ moiety. In the ^{13}C NMR, the shifts are too small to describe the complexation effect of the thiones. These observations indicate either their weak binding to R_3PAu^+ moiety or that they are existing as independent species.

On the other hand, in the complex 2-A-6-MPRAuCl, a significant shift of 11.0 ppm was observed in the C-6 resonance in the ^{13}C NMR. This clearly indicates that the ligand (2-A-6-MPR) has coordinated to gold(I). Compared to C-6, the shift difference for other resonances is very small. The very large shift in C-6 resonance clearly indicates that the ligand is binding through sulfur atom only. The resonances of the ribose were almost unshifted showing that the hydoxyl group do not participate in binding to gold(I). The ^{13}C chemical shifts of the ligand and the complex in DMSO-d_6 are given below;

Species	C-2	C-4	C-5	C-6	C-8
2-A-6-MPR	138.37	153.02	128.33	175.08	147.89
2-A-6-MPR-AuCl	142.16	153.60	126.01	163.92	151.33

4.2 Characterization of Cyano(thione)gold(I) Complexes

The ^{1}H NMR chemical shifts of N-H protons and ^{13}C NMR chemical shifts of all the ligands and their gold(I) complexes are given in Table 4.5. The N-H signal in the ^{1}H NMR was broadened upon coordination and a downfield shift of almost 1.0 ppm was observed in the N-H proton of all the ligands. The appearance of N-H signal in ^{1}H NMR of all ligands after complexation shows that the ligands are coordinating in the thione form in solution.

In ^{13}C NMR, no significant change in the chemical shifts of the ligands upon complexation was observed except in the C-2 resonance (Table 4.5). A shift of 8-10 ppm in C-2 resonance indicates that in all the complexes, gold(I) is bonded to thione ligands through sulfur atom only.

4.2.1 Characterization of ErS-Au-CN*

In IR, ergothionine (ErS)* shows ν(C=S) absorption at 502 cm^{-1} while ν(C=S) of ErS-Au-CN comes at 480 cm^{-1}. A shift of 22 cm^{-1} in the ν(C=S) band is indicative of gold(I) bonded via a thione group. A significant shift of ν(CN) from 2220 cm^{-1} to 2066 cm^{-1} also indicates thione binding to gold(I) cyanide. The lowering of frequency for CN^- group indicates an increase in the ionic nature of the CN^- ligand [27].

*For structure of ErS refer Figure 2.3 (page 29).

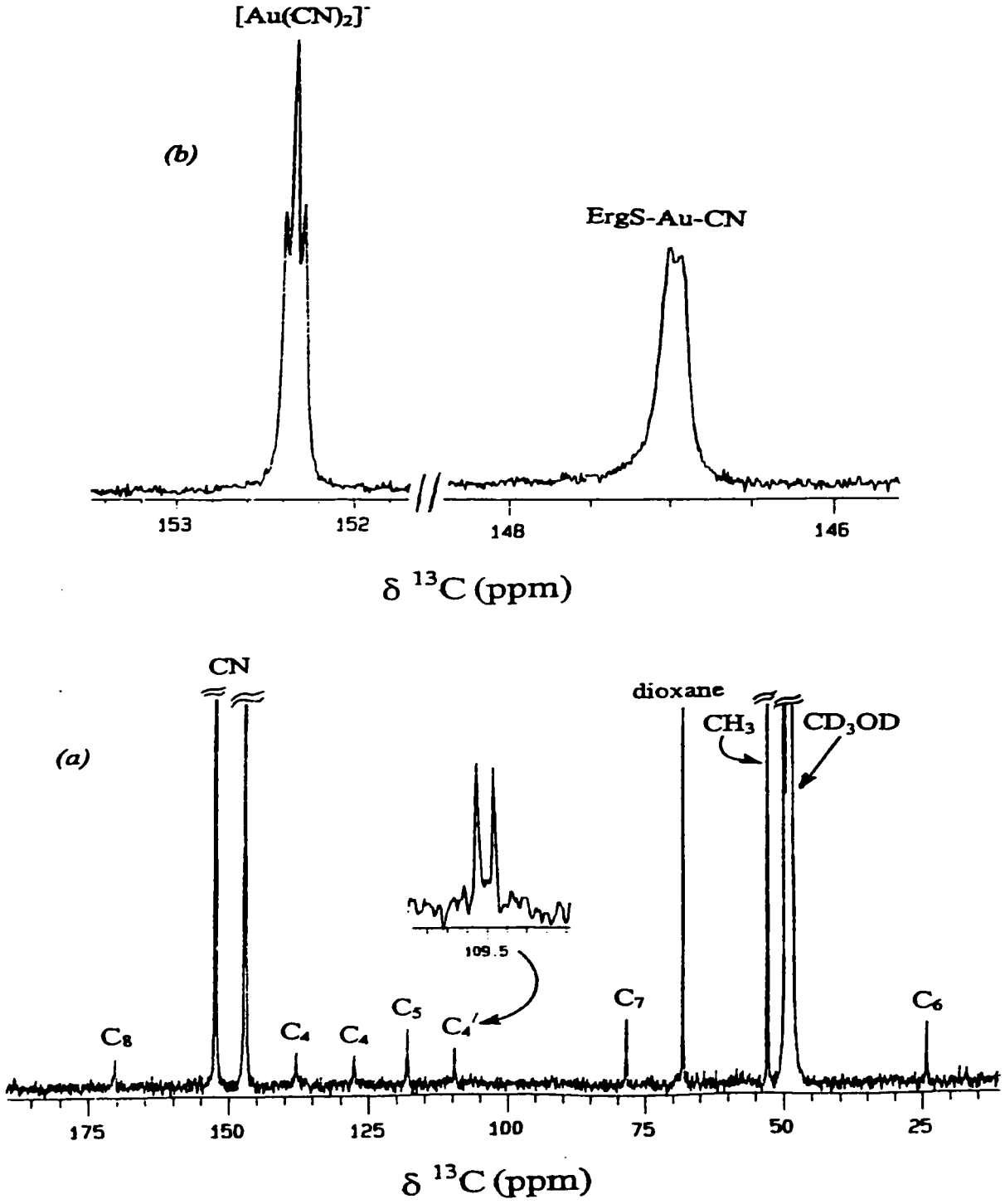

Figure 4.2 (a) 125.65 MHz $^{13}C\{^{1}H\}$ NMR of 0.025 M ErS-AuCN in methanol

(b) An expansion of CN^- region of $^{13}C\{^{1}H\}$ spectrum

The ^{13}C NMR chemical shifts of ErS and its corresponding gold(I) complex are: ErS in CD_3OD-D_2O (75:25 V/V); C_2 158.93, C_4 125.18, C_5 116.20, C_6 24.08, C_7 78.27, C_8 170.34, N-CH_3 53.11. ErS-AuCN in CD_3OD; C_2 not observed, C_4 (127.56, 137.91) C_4' (109.46, 109.54) C_5 118.00, C_6 24.28, C_7 78.39, C_8 170.17, N-CH_3 52.94 (C_4' is for $(ErS)_2Au^+$). In ^{13}C NMR, no significant change in chemical shifts of ErS on its coordination was observed except in the region, 100-155 ppm (Figure 4.2a). The two very intense resonances at 147 ppm and 152 ppm represent the CN^- region. One resonance at 152.35 ppm is characteristic of $[Au(^{13}C^{15}N)_2]^-$ [32,37], while the other at 146.98 ppm is assigned to '^{13}C' of [ErS-Au$^{13}C^{15}$N]. This is explained by the equilibrium (4.1):

$$2[\text{ErS-Au-CN}] \rightleftharpoons [Au(CN)_2]^- + [Au(ErS)_2]^+ \qquad (4.1)$$

In an expansion of the CN^- region of ^{13}C NMR (Figure 4.2b), it is observed that the resonance due to '^{13}C' of [ErS-Au$^{13}C^{15}$N] is a doublet with $^1J(^{13}C\text{-}^{15}N) = 8.3$ Hz, while the $[Au(CN)_2]^-$ resonance appeared as a triplet with an average coupling constant of 6.5 Hz.

The four signals in the region 105-140 ppm are due to C_4 and C_5 of the imidazole ring (Figure 2.3). In order to distinguish between these four signals, ^{13}C NMR using DEPT 135° pulse sequence was run for the same solution. The DEPT experiment showed only one signal for C_5 carbon, which explains that δ ^{13}C of C_5 for ErS-Au-CN and $[Au(ErS)_2]^+$ is the same. The other three signals are due to quartenary carbons (C_4) and among these, one at 109.5 is a doublet. These four signals (C_4 & C_4' in Figure 4.2a)

explain the D and L forms of ergothionine (being a type of amino acid) [144]. The two downfield C_4 signals are expected to be due to ErS-Au-CN, since cyanide is a π acceptor ligand [151] that will cause a downfield shift and also because each line of cyanide shows a small further splitting. The other two resonances at 109.5 ppm, since they are very close, are assumed to be due to C_4 of $[Au(ErS)_2]^+$.

The ^{15}N NMR also showed two resonances corresponding to equilibrium (4.1). One resonance at 261.98 ppm appeared as a doublet due to '^{13}C-^{15}N' coupling in the complex with $^1J(^{13}C\text{-}^{15}N)$ of 9.6 Hz. The other resonance at 264.40 ppm is a triplet of $[Au(CN)_2]^-$ [32,37] with an average coupling constant of 6.5 Hz. The ^{13}C and ^{15}N parts are identical in appearance as expected from $AA'XX'$ system.

Table 4.5 ^{1}H and ^{13}C chemical shifts of thiones and their cyanogold(I) complexes in DMSO-d_6

Species	N-H	C-2	C-4	C-5	C-6	N-C1	N-C2
DmTu	7.38	182.64	-	-	-	30.66	-
DmTuAuCN	8.63	172.70	-	-	-	32.12	-
	8.46					29.96	
Imt	7.98	183.44	43.97	43.97	-	-	-
		185.14	45.71	45.71[a]			
ImtAuCN	9.30	174.64	45.05	45.05	-	-	-
		178.08	46.30	46.30[a]			
$[Au(Imt)_2]^+$	-	177.32	46.39	46.39[a]	-	-	-
MeImt	8.02	182.90	40.60	50.18	-	33.39	-
MeImtAuCN	9.12	174.08	41.88	51.61	-	33.91	-
EtImt	7.99	182.05	40.68	47.03	-	40.41	11.80
EtImtAuCN	9.18	173.22	41.92	48.61	-	41.63	11.96
PrImt	7.99	182.55	40.79	47.70	-	47.38	19.86, 11.00[b]
PrImtAuCN	9.17	173.68	41.93	49.12	-	48.28	19.84, 10.88[b]
i-PrImt	7.96	181.44	40.85	42.02	-	45.64	18.92
i-PrImtAuCN	9.10	172.90	41.84	43.63	-	47.96	19.24
Diaz	7.81	175.62	39.76	19.19	39.76	-	-
DiazAuCN	8.98	166.67	[c]	18.16	[c]	-	-
Diap	7.76	187.91	44.76	27.12	27.12	-	-
DiapAuCN	8.84	[d]	44.62	25.83	25.83	-	-

[a] Resonances in methanol, [b] N-C3, [c] overlapped with DMSO, [d] not observed.

4.3 Characterization of Cyano(selenone)gold(I) Complexes

4.3.1 IR Studies

Table 4.6 lists the significant IR bands of free selenones and their gold(I) complexes. In IR spectra, the ν(C=Se) vibration, which occurs around 600 cm^{-1} for the free ligands [152] shifts towards lower frequency upon complexation, in accordance with the data observed for the analogous thione complexes [27]. Another important vibrational band observed in IR spectra of the selenones is the ν(NH), which appears around 3200 cm^{-1}. Upon coordination to AuCN this band shifts to higher wave numbers with some exceptions. One or two bands around 2100 cm^{-1} corresponding to CN stretch are observed in IR spectra of all the complexes. For the complexes of DmSeu, ImSe, DiazSe and MeDiazSe, only one ν(CN) mode was observed which appears at lower frequency compared to AuCN. For the rest of the complexes, two stretching bands are observed for CN (asymmetric & symmetric), which are the characteristic of $[Au(CN)_2]^-$ (since the NC-Au-CN bond angle in $[Au(CN)_2]^-$ is found to be less than 180°) [116,118].

Table 4.6 IR frequencies, $\nu(cm^{-1})$ of the selenones and their cyanogold(I) complexes

Species	ν(C=Se) of ligands	ν(C=Se) of complexes	ν(NH) of ligands	ν(NH) of complexes	ν(CN) of complexes
DmSeu	594	562	3260	3290	2064
ImSe	558	520	3254	3310	2048
MeImSe	580	550	3184	3230	2136, 2096
EtImSe	588	582	3198	3200	2144, 2096
i-PrImSe	600	582	3200	3192	2146, 2106
PhImSe	596	584	3190	3186	2146, 2098
Et_2ImSe	628	624	-	-	2132, 2090
DiazSe	602	586	3198	3260	2060
MeDiazSe	596	590	3214	3222	2068
AuCN	-	-	-	-	2220
$K[Au(CN)_2]$	-	-	-	-	2140, 2068

4.3.2 NMR Studies

In solution, the complexes were characterized by ^{1}H, ^{13}C and ^{15}N NMR in DMSO-d_6. In ^{1}H NMR, the N-H signal was broadened upon coordination and a downfield shift of 0.7 to 1.0 ppm was observed in the N-H proton for all the ligands. The appearance of N-H signal in ^{1}H NMR of all ligands after complexation shows that the ligands are coordinating in the selenone form in solution. The ^{1}H NMR chemical shifts of N-H protons and ^{13}C NMR chemical shifts of all the ligands and their gold(I) complexes are given in Table 4.7. In ^{13}C NMR, no significant change in the chemical shifts of the ligands upon complexation was observed except in the C-2 resonance (Table 4.7). A shift of 9 to 13 ppm in C-2 resonance indicates that in all the complexes, gold(I) is bonded to the selenone ligands through selenium atom only. In the case of bonding through nitrogen, a considerable shift of the C-4 resonance would have been observed, but there is only a slight shift in C-4. The N-CH_3 carbons in free DmSeu give two signals showing that they are nonequivalent. However, after complexation they are found to be equivalent since only one signal is observed. The resonances due to CN^-, both in ^{13}C and ^{15}N NMR were observed to split in to two due the scrambling reactions of the cyanogold(I) complexes.

Table 4.7 ^{1}H and ^{13}C chemical shifts of the ligands and their cyanogold(I) complexes in DMSO-d_6

Species	N-H	C-2	C-4	C-5	N-C1	N-C2
Seu*	7.45/7.75	178.92	-	-	-	
SeuAuCN	8.12/8.48	168.75	-	-	-	
DmSeu*	7.53	177.81	-	-	45.32[a]	
DmSeuAuCN	8.35/8.64	166.30	-	-	45.41	
ImSe	8.48	177.09	44.94	44.94	-	-
ImSeAuCN	9.51	166.72	45.39	45.39	-	-
MeImSe	8.47	178.67	42.07	50.35	35.06	-
MeImSeAuCN	9.31	167.65	43.10	51.55	35.35	-
4-MeImSe	8.41/8.62	175.90	52.96	51.90	20.51[b]	
4-MeImSeAuCN	9.68/9.50	165.33	54.03	52.19	20.46[b]	
EtImSe	8.44	177.72	42.17	47.21	42.14	11.93
EtImSeAuCN	9.34	166.64	43.12	48.47	43.08	12.21
i-PrImSe	8.43	177.18	42.28	47.72	42.26	19.10
i-PrImSeAuCN	9.34	165.94	43.56	49.71	42.96	19.41

Table 4.7 (Continued)

Species	N-H	C-2	C-4	C-5	C-6	N-C1	N-C2
PhImSe	9.02	177.22	42.61	51.74	-	140.81	128.20[c]
							125.61[d], 124.67[e]
PhImSeAuCN	9.92	168.54	43.93	53.63	-	138.67	129.43[c]
							128.47[d], 126.29[e]
Et_2ImSe	-	178.57	45.81	45.81	-	43.07	11.77
Et_2ImSeAuCN	-	165.68	46.96	46.96	-	44.06	12.24
DiazSe	8.23	169.14	40.10	18.76	40.10	-	-
DiazSeAuCN	9.15	158.48	40.50	18.01	40.50	-	-
MeDiazSe	8.38	172.65	39.95	20.39	44.02	47.39	-
MeDiazSeAuCN	8.98	161.42	40.29	19.50	44.06	48.95	-

* δ (^{77}Se) = 1854.5 ppm for Seu and 1872.1 ppm for DmSeu (relative to SeO_2 in D_2O at 1301.4 ppm [153]), [a] Another resonance at 38.07 ppm, [b] The resonance for CH_3 at C-4, [c] N-C2/6, [d] N-C4, [e] N-C3/5

4.4 Spectroscopic Studies of the Silver(I) Complexes of Thiourea and Selenourea (^{13}C,^{15}N labeled)

4.4.1 IR Studies

In IR spectra of all the complexes, the ν(C=S) mode of Tu was observed at a lower frequency compared to that for free Tu at 730 cm^{-1}. In the IR of $Ag(Tu)_1NO_3$, ν(C=S) was observed at 698 cm^{-1} with a shoulder at 726 cm^{-1}. For the remaining complexes two bands were observed for the ν(C=S) mode, one intense band at 714 cm^{-1} with a shoulder at 724 cm^{-1} and the other at 698 cm^{-1}. This observation is contrary to a reported one, showing an intense band at 724 with a shoulder at 715 cm^{-1} but no peak at 698 cm^{-1} [65]. The ν(C=Se) mode of Seu occurs at 736 cm^{-1}, while for Seu complexes the ν(C=Se) was observed at 714 cm^{-1} and 724 cm^{-1} in $Ag(Seu)_1NO_3$ and $Ag(Seu)_2NO_3$ respectively. Three ν(NH_2) bands around 3200 cm^{-1} are observed at comparatively higher frequency for complexes compared to those for the free ligands. A sharp band for NO_3^- bending was observed at 824 cm^{-1} for all the complexes (at 826 cm^{-1} for $Ag(Tu)_1NO_3$).

4.4.2 ^1H NMR Studies

In ^1H NMR of all the complexes, the N-H proton of Tu or Seu shifts downfield by approx. 1.0 ppm with respect to that of uncoordinated ligands [65,154]. As shown in Figure 4.3a, the signal appears as a doublet showing coupling with nitrogen (which is ^{15}N labeled). The doublet in free Tu was not clear; therefore the coupling constant $^1J_{N\text{-}H}$ was

resolved by ^{15}N NMR. There is a significant change in the $^{1}J_{N-H}$ coupling constant as the number of Tu ligands change (Table 4.8).

4.4.3 ^{13}C NMR Studies

The ^{13}C NMR chemical shifts are listed in Table 4.8. The ^{13}C NMR of free Tu shows a triplet due to ^{13}C-^{15}N coupling (Figure 4.3b). Upon complexation with $AgNO_3$, the >C=S carbon of Tu in the complexes is shifted upfield compared to the free ligand (Figure 4.3b). No significant change in the coupling constant ($^{1}J_{C-N}$) was observed. For Seu and its complexes, the coupling constant, $^{1}J_{C-N}$ could not be obtained by ^{13}C NMR since the expected triplet could not be resolved properly in ^{13}C NMR. However, we were able to observe the $^{1}J_{C-N}$ coupling constant by ^{15}N NMR.

4.4.4 ^{15}N NMR Studies

The ^{15}N chemical shifts of the complexes are given in Table 4.8. The NH_2 resonances for Tu and Seu in ^{15}N NMR appear as doublets by coupling with ^{13}C. When the spectrum was run without decoupling, the doublet changed to a triplet of doublets and thus the $^{1}J_{N-H}$ coupling constant was also resolved (Figure 4.3c). We are also able to resolve the ^{1}H-^{13}C coupling constant in Tu, which is 3.0 Hz.

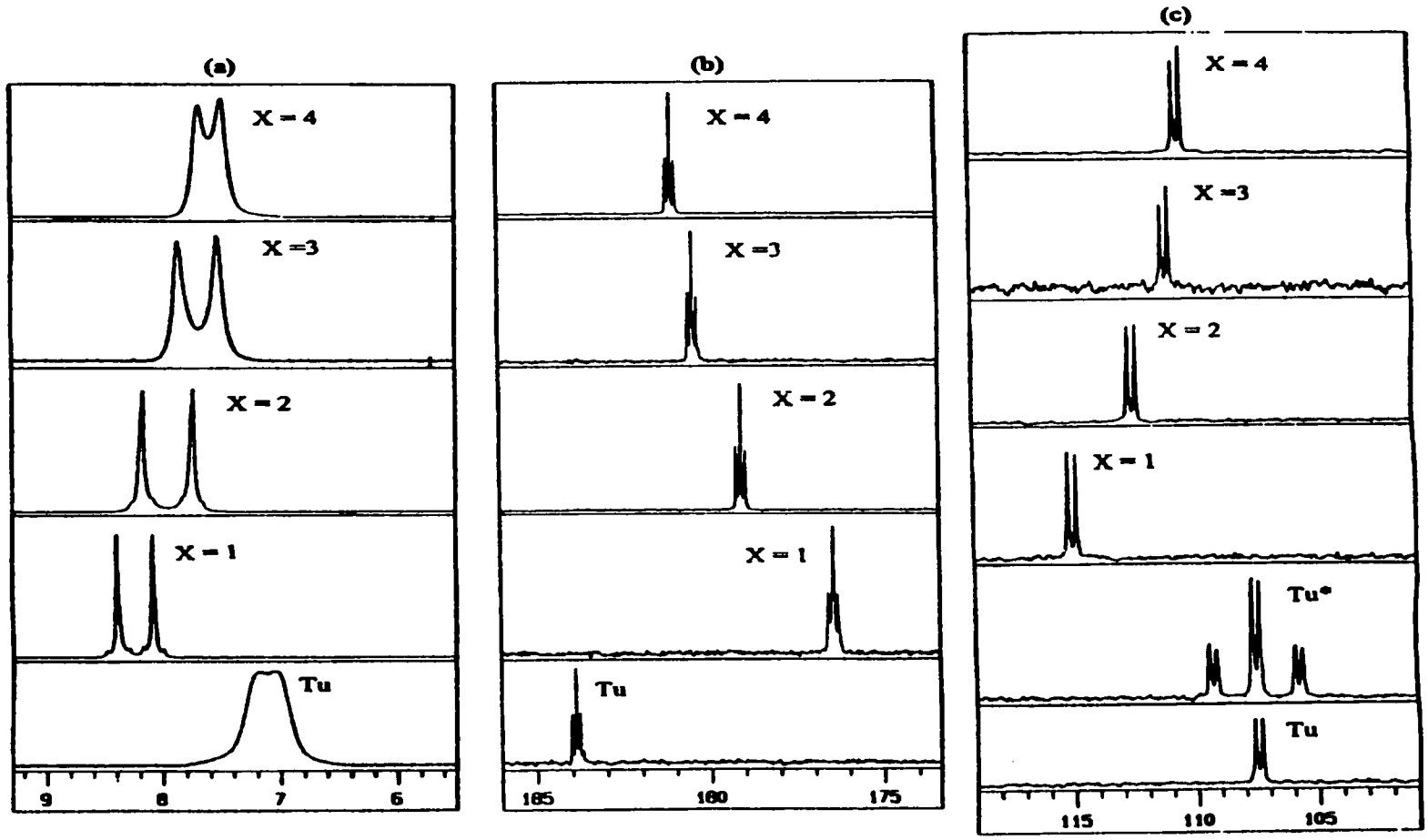

Figure 4.3 NMR spectra of Tu and $Ag(Tu)_xNO_3$ complexes in DMSO (a) ^{1}H (b) $^{13}C\{^{1}H\}$ (c) $^{15}N\{^{1}H\}$

* ^{15}N spectrum of Tu without decoupling (showing coupling with ^{1}H and ^{13}C)

4.4.5 ^{107}Ag NMR Studies

The ^{107}Ag chemical shifts of the complexes are listed in Table 4.8. It is observed that when ^{107}Ag NMR of $AgNO_3$ is recorded in DMSO instead of D_2O, the signal is shifted by 166 ppm showing that the ^{107}Ag chemical shift is not only sensitive to the nature of ligands but is also affected by changing the solvent. One possible reason for this change is that the solvent could also act as a ligand for the metal ion. On complexation with Tu, ^{107}Ag NMR silver resonances are deshielded by as much as 700 ppm depending upon the number of Tu ligands. The ^{107}Ag chemical shifts for Seu complexes were observed at approx. 100 ppm downfield position compared to Tu complexes. Since the Seu complexes give black deposits in solution after some time therefore, spectra were measured within 30-40 minutes using more concentrated samples (0.25 M) compared to Tu complexes (0.1 M).

Table 4.8 ^{1}H, ^{13}C, ^{15}N and ^{107}Ag NMR chemical shifts (ppm) of various species in DMSO-d_6 in complexation of Tu and Seu with $AgNO_3$

Species	δ (^{1}H)	$^{1}J_{N-H}$ (Hz)	δ (^{13}C)	δ (^{15}N)	$^{1}J_{C-N}$ (Hz)	δ (^{107}Ag)
Tu	7.05	91.5	183.81	107.52	14.0	-
$AgNO_3$	-	-	-	-	-	165.96
$[TuAgNO_3]$	8.18	151.3	176.53	115.00	17.1	685.93
$[Ag(Tu)_2]NO_3$	7.88	217.2	179.10	112.52	16.5	671.77
$[Ag(Tu)_3]NO_3$	7.64	171.2	180.44	111.12	15.0	797.38
$[Ag(Tu)_4]NO_3$	7.59	98.5	181.05	110.54	16.0	835.51
Seu	7.60	144.9	179.99	116.48	13.6	-
$[SeuAgNO_3]$	8.64	37.8	167.16	124.12	16.7	810.46
$[Ag(Seu)_2]NO_3$	8.25	112.2	172.07	120.63	15.2	784.34

4.5 Spectroscopic Characterization of the Silver(I) Complexes of Various Thiones

4.5.1 IR Studies

Selected IR vibrations for the ligands and their silver(I) complexes, $[AgL_2]NO_3$ are listed in Table 4.9. The IR data for $[LAgNO_3]$ complexes has already been reported [98]. In the IR of thione complexes the ν(C=S) mode of thiones is observed at lower frequency, while the ν(N-H) band is observed at higher frequency compared to the free thiones. A band, between 830-820 cm^{-1} is observed for all complexes due to the bending vibrations of NO_3^-.

4.5.2 Conductance Studies

The molar conductivity measurements in DMSO show that for $[LAgNO_3]$ complexes, NO_3^- ion is weakly coordinated except in the complexes of Diaz, EtDiaz and Diap. For $[AgL_2]NO_3$ complexes, the conductance values lie in the range acceptable for 1:1 electrolyte except the DmTu complex, which indicates that this complex exist in the polymeric form. The polymeric structure of $[Ag(DmTu)_2]ClO_4$ is already known [64]. The conductance values are listed in Table 4.10.

4.5.3 ^{1}H, ^{13}C, ^{15}N and ^{107}Ag NMR Studies

The ^{1}H and ^{13}C NMR chemical shifts of 0.10 M solutions of the complexes in DMSO-d_6 are summarized in Table 4.11. In the ^{1}H NMR spectra of the complexes, N-H signal of thiones became less intense upon coordination and shifted downfield by 0.7-1.0 ppm from their positions in the free ligand. The deshielding of N-H proton is related to an increase of the π electron density in the C-N bond [155].

In all complexes, C-2 resonance appears upfield by 4-7 ppm compared to the free ligands in accordance with the data observed for other complexes of Cu(I), Ag(I) and Au(I) with heterocyclic thiones. A small shift of 1-2 ppm is observed in other carbon atoms, which shows that nitrogen atoms are not involved in coordination. In the complexes of Imt and its derivatives a deshielding effect is observed at C-4/5 while in Diaz and EtDiaz complexes, a deshielding effect is observed at C-4 and C-6, but C-5 bears a shielding effect. The deshielding at C-4/6 is due to an increase in π character of the C-N bond [85,155].

As expected, the ^{15}N NMR for four of the complexes shows an opposite trend compared to that observed in ^{13}C NMR. A greater shift is observed for Diaz complexes in ^{15}N NMR in a way similar to that observed in ^{13}C NMR. The ^{15}N chemical shifts of Imt, Diaz and their complexes are given in Table 4.12.

In ^{107}Ag NMR the signal for $AgNO_3$ is deshielded by 166 ppm when taken in DMSO compared to that in aqueous solution. The complexation with thiones shifts the signal further downfield by approx. 300-500 ppm. The ^{107}Ag chemical shifts of all the complexes are listed in Table 4.13.

Table 4.9 Selected IR absorption (cm^{-1}) for free ligands and their silver(I) complexes

Species	ν(C=S)	$\nu(NH_2)$	$\delta(NO_3)$
DmTu	722	3204	-
$[DmTuAgNO_3]$	718	3282	826
$[Ag(DmTu)_2]NO_3$	718	3288	833, 822
Imt	510	3200	-
$[Ag(Imt)_2]NO_3$	496	3214	834, 820
MeImt	520	3200	-
$[Ag(MeImt)_2]O_3$	506	3232	822
EtImt	515	3200	-
$[Ag(EtImt)_2]NO_3$	504	3210	824
i-PrImt	525	3210	-
$[Ag(i\text{-}PrImt)_2]NO_3$	522	3208	826
Diaz	510	3200	-
$[Ag(Diaz)_2]NO_3$	522	3230	820
EtDiaz	505	3210	-
$[Ag(EtDiaz)_2]NO_3$	487	3220	825
Diap	527	3224	-
$[DiapAgNO_3]$	524	3224	812

Table 4.10 Observed and molar conductances of the silver(I) complexes of selenones in DMSO

Complex	Concentration (M)	Observed Conductance (μ mho)	Molar* Conductance (λ, mho.cm^2/mol)
$AgNO_3$	1.63×10^{-2}	683	38.1
[$DmTuAgNO_3$]	1.72×10^{-2}	422	22.3
[$Ag(DmTu)_2$]NO_3	1.13×10^{-2}	372	29.8
[$ImtAgNO_3$]	6.30×10^{-3}	167	24.1
[$Ag(Imt)_2$]NO_3	2.14×10^{-3}	88	37.5
[$MeImtAgNO_3$]	3.20×10^{-2}	813	23.1
[$Ag(MeImt)_2$]NO_3	4.07×10^{-3}	144	32.2
[$EtImtAgNO_3$]	8.10×10^{-3}	224	25.2
[$Ag(EtImt)_2$]NO_3	6.98×10^{-3}	257	33.5
[$PrImtAgNO_3$]	4.91×10^{-3}	193	35.8
[*i*-$PrImtAgNO_3$]	8.64×10^{-3}	238	25.2
[$Ag($*i*-$PrImt)_2$]NO_3	8.73×10^{-3}	294	30.6
[$DiazAgNO_3$]	8.99×10^{-3}	332	33.6
[$Ag(Diaz)_2$]NO_3	6.44×10^{-3}	230	32.5
[$EtDiazAgNO_3$]	1.09×10^{-2}	403	33.6
[$Ag(EtDiaz)_2$]NO_3	6.04×10^{-3}	176	26.5
[$DiapAgNO_3$]	2.95×10^{-3}	105	32.5

*For calculation of λ, refer section 3.2.8.

Table 4.11 ^{1}H and ^{13}C chemical shifts of thiones and their Ag(I)-thione complexes in DMSO-d_6

Species	N-H	C-2	C-4	C-5	N-C1	N-C2
DmTu	7.38	182.64	-	-	30.66	-
[$DmTuAgNO_3$]	8.32, 8.53	174.69			29.74[a]	32.29[a]
[$Ag(DmTu)_2$]NO_3	8.27, 8.53	175.18	-	-	29.65[a]	32.16[a]
Imt	7.98	183.44	43.97	43.97	-	-
[$ImtAgNO_3$]	9.04	176.96				
[$Ag(Imt)_2$]NO_3	8.95	177.81	44.85			
MeImt	8.02	182.90	40.60	50.18	33.39	-
[$MeImtAgNO_3$]	8.75	177.50	51.30	41.32	33.79	-
[$Ag(MeImt)_2$]NO_3	8.76	178.27	51.25	33.82	33.82	-
EtImt	7.99	182.05	40.68	47.03	40.41	11.80
[$EtImtAgNO_3$]	8.74	176.83	48.33	41.42	41.33	12.02
[$Ag(EtImt)_2$]NO_3	8.78	177.26	41.28	48.22	41.42	12.04
PrImt	7.99	182.55	40.79	47.70	47.38	19.86, 11.00[b]
[$PrImtAgNO_3$]	8.7	173.68	41.93	49.12	48.28	19.84, 10.88[b]

[a] Resonances due to nonequivalent Me groups, [b] Resonances for N-C3

Table 4.11 (Continued)

Species	N-H	C-2	C-4	C-5	C-6	N-C1	N-C2
i-PrImt	7.96	181.44	40.85	42.02	-	45.64	18.92
[*i*-PrImtAgNO$_3$]	8.65	176.26	41.47	43.40	-	47.30	19.25
[Ag(*i*-PrImt)$_2$]NO$_3$	8.73	176.47	41.38	43.19	-	47.09	19.15
Diaz	7.81	175.62	39.76	19.19	39.76	-	-
[DiazAgNO$_3$]	8.96	167.83					
[Ag(Diaz)$_2$]NO$_3$	8.82	168.91	40.04	18.24	40.04	-	-
EtDiaz	7.89	176.05	40.12	12.05	45.03	47.54	20.84
[EtDiazAgNO$_3$]	8.71	168.07	46.29	19.66	48.91	40.48	12.36
[Ag(EtDiaz)$_2$]NO$_3$	8.40	171.18	45.79	20.01	48.41	40.12	12.18
Diap	7.76	187.91	44.76	27.12	27.12	-	-
[DiapAgNO$_3$]	8.87	174.92	44.58	25.85	25.85	44.58	-

Table 4.12 ^{15}N NMR chemical shifts of Imt, Diaz and their Ag(I) complexes in DMSO-d_6

Species	δ (^{15}N)
Imt	112.24
[$ImtAgNO_3$]	119.09
[$Ag(Imt)_2$]NO_3	117.88
Diaz	108.47
[$DiazAgNO_3$]	115.66
[$Ag(Diaz)_2$]NO_3	114.62

Table 4.13 ^{107}Ag NMR chemical shifts of various silver(I)-thione complexes in DMSO-d_6

Thione (L)	δ (^{107}Ag) for [$LAgNO_3$]	δ (^{107}Ag) for [$Ag\ L_2$]NO_3
DmTu	657.9	656.1
Imt	571.0	608.29
MeImt	493.7	645.4
EtImt	480.2	645.2
PrImt	507.0	-
i-PrImt	489.6	650.3
Diaz	708.7	678.0
EtDiaz	612.0	731.0
Diap	664.0	-

δ (^{107}Ag) for $AgNO_3$ in DMSO-d_6 = 166.0 ppm

4.6 Spectroscopic Characterization of the Silver(I) Complexes of Various Selenones

4.6.1 IR Studies

Table 4.14 lists the significant IR bands of free selenones and their silver(I) complexes. In IR spectra, the ν(C=Se) vibration, which occurs around 600 cm^{-1} for the free ligands [152] shifts towards lower frequency upon complexation, similar to those found for the analogous thione complexes [27]. Another important vibrational band observed in IR spectra of the selenones is the ν(NH), which appears around 3200 cm^{-1}. Upon coordination to $AgNO_3$ this band shifts to higher wave numbers with some exceptions. A sharp band around 825 cm^{-1} for NO_3^{-1} bending was observed for all the complexes.

4.6.2 Conductance Studies

The molar conductivity measurements in DMSO show that for all complexes, the conductance values lie in the range acceptable for 1:1 electrolyte, showing that NO_3^- ion is either weakly coordinated or uncoordinated to silver(I). The complex $[Ag(ImSe)_2]NO_3$ has the lowest value, indicating that the complex may be polymeric. The conductance values are given in Table 4.15.

4.6.3 NMR Studies

The ^{1}H and ^{13}C NMR chemical shifts of the silver(I) complexes of selenones are given in Table 4.16. In ^{1}H NMR of all the complexes, the N-H signal of selenones shifted downfield by approx. 1.0 ppm compared to the free ligands. In the ^{13}C NMR of the complexes, the C-2 resonance exhibited upfield shifts ranging from 6-12 ppm as it was observed for silver-thiones complexes. The shift is greater for bis complexes (10-12 ppm) than for mono complexes (5-8 ppm). A small shift of 1-2 ppm was observed in other carbon atoms showing that nitrogen atoms of the selenones are not involved in coordination.

In ^{107}Ag NMR the silver signal in the complexes was observed at 450-650 ppm downfield position compared to free $AgNO_3$ in DMSO. This very large reduction in shielding seems to be due to silver(I) binding to selenium of the selenones [156]. In the case bonding through nitrogen a smaller shift of around 100 ppm would have been observed in ^{107}Ag NMR [156]. This provides a clear evidence that selenones bind to silver(I) through selenium only. The ^{107}Ag chemical shifts of the complexes are listed in Table 4.17.

Table 4.14 IR frequencies, $\nu(cm^{-1})$ of the selenones and their complexes

Species	ν(C=Se)	ν(NH)	$\delta(NO_3^-)$
DmSeu	594	3260	-
$[DmSeuAgNO_3]$	548	3304	824
$[Ag(DmSeu)_2]NO_3$	562	3270	828
ImSe	558	3254	-
$[ImSeAgNO_3]$	566	3222	834
$[Ag(ImSe)_2]NO_3$	572	3212	826
MeImSe	580	3184	-
$[MeImSeAgNO_3]$	572	3210	834
$[Ag(MeImSe)_2]NO_3$	562	3222	822
EtImSe	588	3198	-
$[EtImSeAgNO_3]$	-	3234	834
$[Ag(EtImSe)_2]NO_3$	580	3216	824
i-PrImSe	600	3200	-
$[i\text{-}PrImSeAgNO_3]$	598	3262	824
$[Ag(i\text{-}PrImSe)_2]NO_3$	600	3204	832
PhImSe	596	3190	-
$[PhImSeAgNO_3]$	542	3176	822
$[Ag(PhImSe)_2]NO_3$	548	3176	822
DiazSe	602	3198	-
$[DiazSeAgNO_3]$	588	3214	828
$[Ag(DiazSe)_2]NO_3$	586	3260	828
MeDiazSe	596	3214	-
$[MeDiazSeAgNO_3]$	584	3244	826

Table 4.15 Observed and molar conductances of the silver(I) complexes of selenones in DMSO

Complex	Concentration (M)	Observed Conductance (μ mho)	Molar Conductance (λ, mho.cm^2/mol)
$AgNO_3$	1.63×10^{-2}	683	38.1
[$DmSeuAgNO_3$]	5.07×10^{-3}	185	33.2.
[$Ag(DmSeu)_2$]NO_3	3.27×10^{-3}	120	33.4
[$ImSeAgNO_3$]	1.21×10^{-2}	221	16.6
[$Ag(ImSe)_2$]NO_3	8.24×10^{-3}	408	45.0
[$MeImSeAgNO_3$]	9.01×10^{-3}	412	41.6
[$Ag(MeImSe)_2$]NO_3	6.60×10^{-3}	360	49.5
[$EtImSeAgNO_3$]	3.29×10^{-3}	166	45.9
[$Ag(EtImSe)_2$]NO_3	4.63×10^{-3}	178	34.9
[*i*-$PrImSeAgNO_3$]	8.71×10^{-3}	281	29.4
[Ag(*i*-$PrImSe)_2$]NO_3	3.36×10^{-3}	168	45.5
[$PhImSeAgNO_3$]	5.06×10^{-3}	190	34.2
[$Ag(PhImSe)_2$]NO_3	3.69×10^{-3}	149	36.8
[$DiazSeAgNO_3$]	6.00×10^{-3}	147	22.3
[$MeDiazAgNO_3$]	7.41×10^{-3}	273	33.4

*For calculation of λ, refer section 3.2.8.

Table 4.16 ^{1}H and ^{13}C NMR chemical shifts of selenones and their silver(I) complexes in DMSO-d_6

Species	N-H	C-2	C-4	C-5	N-C1	N-C2
DmSeu	7.53	177.81	-	-	45.44*	-
[DmSeuAgNO$_3$]	8.57	165.63	-	-	45.83	-
[Ag(DmSeu)$_2$]NO$_3$	8.26	169.91	-	-	45.68	
ImSe	8.48	177.09	44.94	44.94	-	-
[ImSeAgNO$_3$]	9.56	166.12	45.60	45.60	-	-
[Ag(ImSe)$_2$]NO$_3$	9.29	170.48	45.31	45.31	-	-
MeImSe	8.47	178.67	42.07	50.35	35.06	-
[MeImSeAgNO$_3$]	9.29	167.29	43.05	51.59	35.58	-
[Ag(MeImSe)$_2$]NO$_3$	9.09	171.45	42.72	51.25	35.43	-
EtImSe	8.44	177.72	42.17	47.21	42.14	11.93
[EtImSeAgNO$_3$]	9.21	167.79	42.96	48.43	43.14	12.28
[Ag(EtImSe)$_2$]NO$_3$	9.08	171.04	42.70	48.14	42.88	12.21

* another resonance at 38.08 ppm

Table 4.16 (Continued)

Species	N-H	C-2	C-4	C-5	C-6	N-C1	N-C2
i-PrImSe	8.43	177.18	42.28	47.72	-	42.26	19.10
[*i*-PrImSeAgNO$_3$]	9.24	166.22	42.98	49.66	-	43.67	19.50
[Ag(*i*-PrImSe)$_2$]NO$_3$	9.00	170.39	42.61	48.98	-	43.17	19.30
PhImSe	9.02	177.22	42.61	51.74	-	140.81	128.20[a]
							125.61[b], 124.67[c]
[PhImSeAgNO$_3$]	9.89	168.66	43.76	53.41	-	138.79	129.36[a]
							128.20[b], 125.99[c]
[Ag(PhImSe)$_2$]NO$_3$	9.83	177.72	43.35	53.20	-	139.19	129.33[a]
							127.92[b], 126.07[c]
DiazSe	8.23	169.14	40.10	18.76	40.10	-	-
[DiazSeAgNO$_3$]	9.31	157.22	40.61	17.73	40.61	-	-
[Ag(DiazSe)$_2$]NO$_3$	8.87	163.24	40.22	18.15	40.22	-	-
MeDiazSe	8.38	172.65	39.95	20.39	44.02	47.39	-
[MeDiazSeAgNO$_3$]	9.06	160.61	40.46	19.36	44.68	49.10	-

[a] N-C2/6, [b] N-C4, [c] N-C3/5

Table 4.17 ^{107}Ag NMR chemical shifts of various silver(I)-selenone complexes in DMSO-d_6

Selenone (L)	δ (^{107}Ag) for [$LAgNO_3$]	δ (^{107}Ag) for [AgL_2]NO_3
DmSeu	748.64	839.81
ImSe	715.88	639.08
MeImSe	692.26	725.69
EtImSe	666.07	676.94
i-PrImse	661.91	677.67
PhImSe	615.58	625.39
MeDiaz	734.39	-

δ (^{107}Ag) for $AgNO_3$ in DMSO-d_6 = 166.0 ppm

4.7 Ligand Scrambling Reactions of Cyano(thione)gold(I) and Cyano(selenone)gold(I) Complexes

The ligand scrambling reactions of the cyano(thione)gold(I) and cyano(selenone)gold(I) complexes in DMSO-d_6 were investigated by ^{13}C and ^{15}N NMR spectroscopy. Some representative ^{13}C and ^{15}N spectra for the scrambling of cyano(thione)gold(I) complexes are shown in Figures 4.4-4.5 and for those of cyano(selenone)gold(I) complexes are shown in Figures 4.6-4.7. The ^{13}C and ^{15}N NMR shifts of CN^- and coupling constants ($^1J_{C\text{-}N}$) of the [>C=S-Au-CN] complexes are given in Table 4.18, while of the [>C=Se-Au-CN] are given in Table 4.19. In the CN region of the ^{13}C spectrum, two intense resonances were observed for all the complexes (Figures 4.4b, 4.5b). One resonance at 149.6 ppm is characteristic of $[Au(CN)_2]^-$ [32,114] while the other resonance corresponds to the CN of [>C=S/Se-Au-CN] complexes. These two resonances demonstrate that [>C=S-Au-CN] type complexes undergo following type of ligand scrambling reaction as given by eq. (4.2),

$$2\,[>C{=}S\text{-}Au\text{-}CN] \rightleftharpoons [Au(>C{=}S)_2]^+ + [Au(CN)_2]^- \qquad (4.2)$$

The same is the case for [>C=Se-Au-CN] type complexes (Figures 4.6b, 4.7b). The $[Au(CN)_2]^-$ resonance appeared as a triplet (or a broad singlet) with an average coupling constant of 5.9 Hz. The triplet appearance of $[Au(CN)_2]^-$ resonance is because the ^{13}C-^{15}N coupling in $[Au(CN)_2]^-$ follows the $AA'XX'$ spin system as described in the previous studies [32,37]. The triplet arises due to the fact that $^2J(^{13}C\text{-}^{13}C) >> {}^4J(^{15}N\text{-}^{15}N)$ and the inner lines of the AB spectrum are so close together that they cannot be resolved and the intensity of the outer lines lie below the detection limit. The resonance due to the $^{13}C^{15}N$

of [>C=S-Au-CN] complexes is a doublet with the $^{1}J_{C\text{-}N}$ values given in Table 4.18. In the ^{13}C NMR of Imt-Au-CN in methanol, $[Au(CN)_2]^-$ resonance was observed at 152.41 ppm.

For DmTu-Au-CN complex, separate resonances for methyl carbons of the DmTu were detected showing that the methyl groups are inequivalent. These two resonances for methyl carbons could not be due to [DmTu-Au-CN] and $[Au(DmTu)_2]^+$ species, since we also observed two resonances for methyl carbons in the reaction of DmTu with $AgNO_3$. Two resonances were also observed for N-H (and CH_3) protons in ^{1}H NMR (Table 4.5). Separate resonances for the thione/selenone ligands in [>C=S/Se-Au-CN] and $[Au(>C=S/Se)_2]^+$ species were not observed either due to their rapid exchange or the chemical shifts of the two species are overlapped so that they can not be resolved. However, we were able to resolve these resonances for one of the complex, Imt-Au-CN at 240 K in methanol (Figure 4.4c).

Dimethyl sufoxide is believed to interact weekly with AuCN, since in the ^{13}C NMR of a mixture of AuCN and DMSO, two CN resonances corresponding to $[Au(CN)_2]^-$ and DMSO-AuCN (135.03 ppm, $^{1}J_{C\text{-}N}$ = 10.1 Hz) species were observed. However, CN resonance due to DMSO-AuCN was not observed in any of the cyanogold(I) complexes, which suggests that solvent is not repacing any of the ligands from gold(I) complexes.

The results of the ^{15}N NMR studies are consistent with the ^{13}C NMR data. The ^{15}N NMR also showed two resonances for the CN^- nitrogen corresponding to equilibrium 2 for both types of the complexes (Figures 4.4d, 4.5c, 4.6c and 4.7c). The resonance at 284.1 ppm was a triplet (or a singlet) of $[Au(CN)_2]^-$ with an average coupling constant of 5.9 Hz. The other resonance is a doublet due to $^{13}C\text{-}^{15}N$ coupling in the [>C=S/Se-Au-$^{13}C^{15}N$] complexes (Tables 4.18 & 4.19). When ^{15}N NMR of Imt-Au-CN was taken in

methanol a significant shift in these resonances was observed. The $[Au(CN)_2]^-$ resonance was observed at 264.7 ppm and the Imt-Au-CN resonance at 262.2 ppm. This shows that ^{15}N chemical shift is highly dependent on the nature of the solvent. In methanol the chemical shifts of $[Au(CN)_2]^-$ and [LAuCN] species are very close, therefore for some R_3PAuCN complexes only average resonances were observed [32]. However, in the present study ^{15}N resonaces for the two species were separated in DMSO-d_6.

4.7.1 Measurement of Equilibrium Constant

Equilibrium constants (K_{eq}) were measured for the [>C=S/Se-Au-CN] complexes at 298 K using 0.025 M solution of each complex in DMSO-d_6. Equilibrium constants (K_{eq}) were calculated from relative intensities (I) of the $^{13}C^{15}N$ resonances of [>C=S/Se-Au$^{13}C^{15}N$] and $[Au(^{13}C^{15}N)_2]^-$ in the ^{13}C NMR, which gave relative concentrations of both species;

$$K_{eq} = (I[Au(^{13}C^{15}N)_2]^-)(I[Au(>C=S/Se)_2]^+)/(I[>C=S/Se\text{-}Au^{13}C^{15}N])^2 \qquad (4.3)$$

Where,

$I[Au(^{13}C^{15}N)_2]^- = I[Au >C=S/Se)_2]^+$

Each K_{eq} is the result of 5-7 measurements. The average K_{eq} values thus found for the complexes are listed in Tables 4.18 and 4.19 and for comparison K_{eq} values of some known cyanogold(I) complexes are given in Table 4.20. The intensity of the CN resonances was found unchanged when spectra were taken after a period of few days showing that the scrambling process was rapid for these complexes.

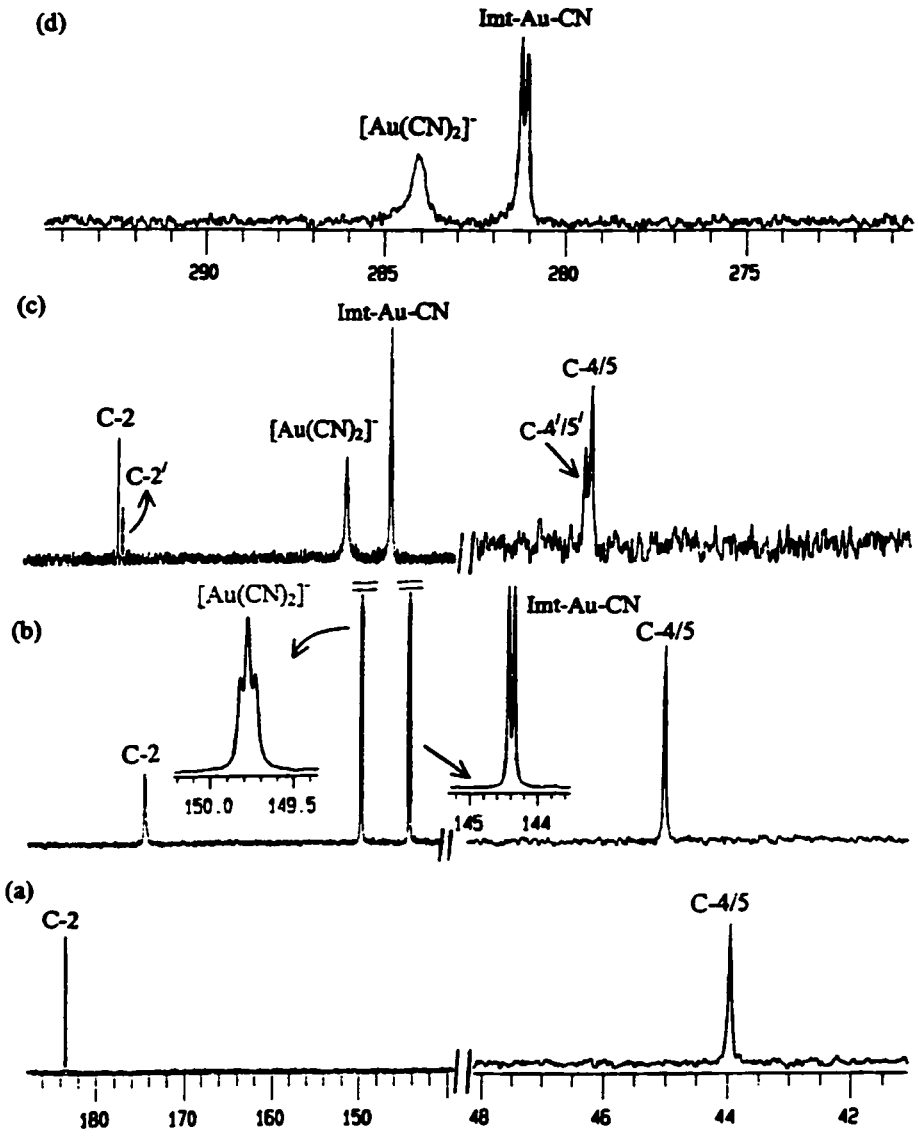

Figure 4.4 (a) 125.65 MHz ^{13}C NMR spectrum of Imt in DMSO (b) ^{13}C NMR spectrum of Imt-Au-CN at 298 K in DMSO (c) ^{13}C NMR spectrum of Imt-Au-CN at 240 K in methanol (C′ are the resonances for $[Au(Imt)_2]^+$) (d) 50.55 MHz ^{15}N NMR spectrum of Imt-Au-CN in DMSO

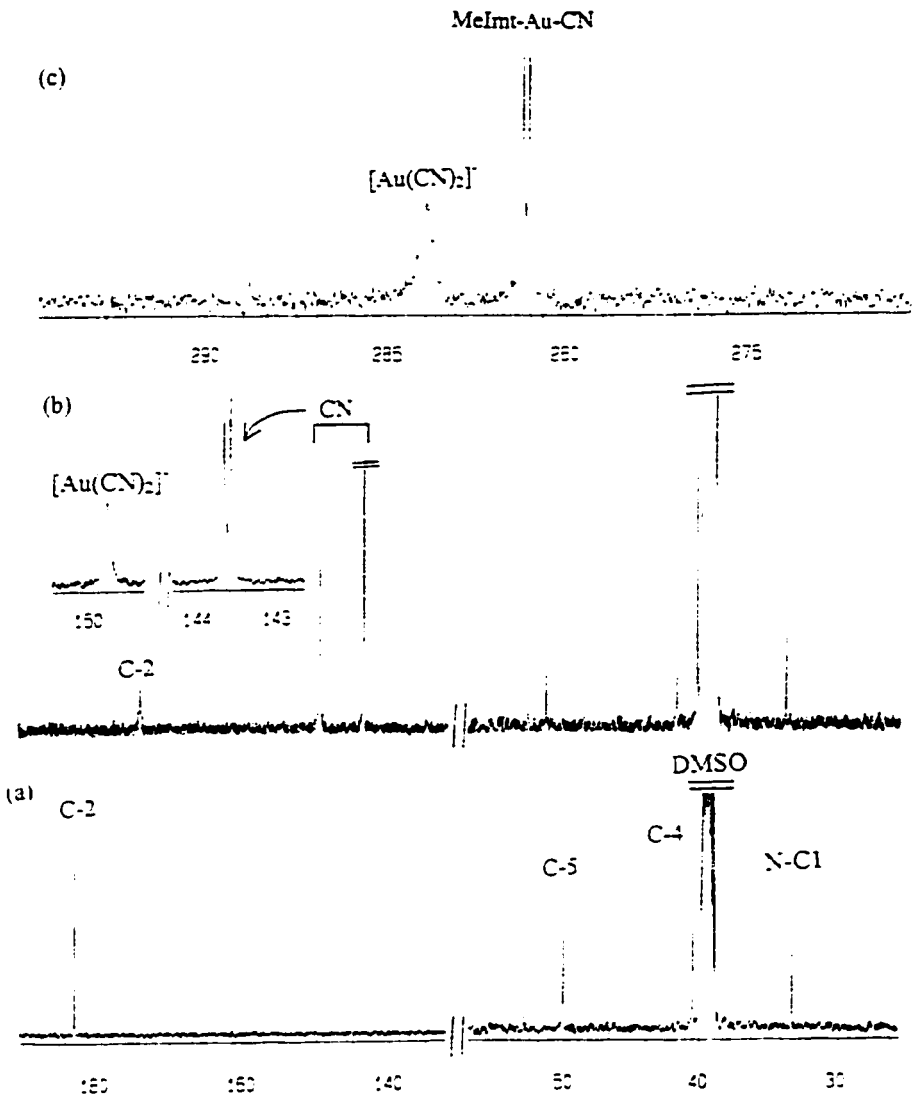

Figure 4.5 (a) 125.65 MHz ^{13}C NMR spectrum of MeImt in DMSO (b) ^{13}C NMR spectrum of MeImt-Au-CN (c) 50.55 MHz ^{15}N NMR spectrum of MeImt-AuCN

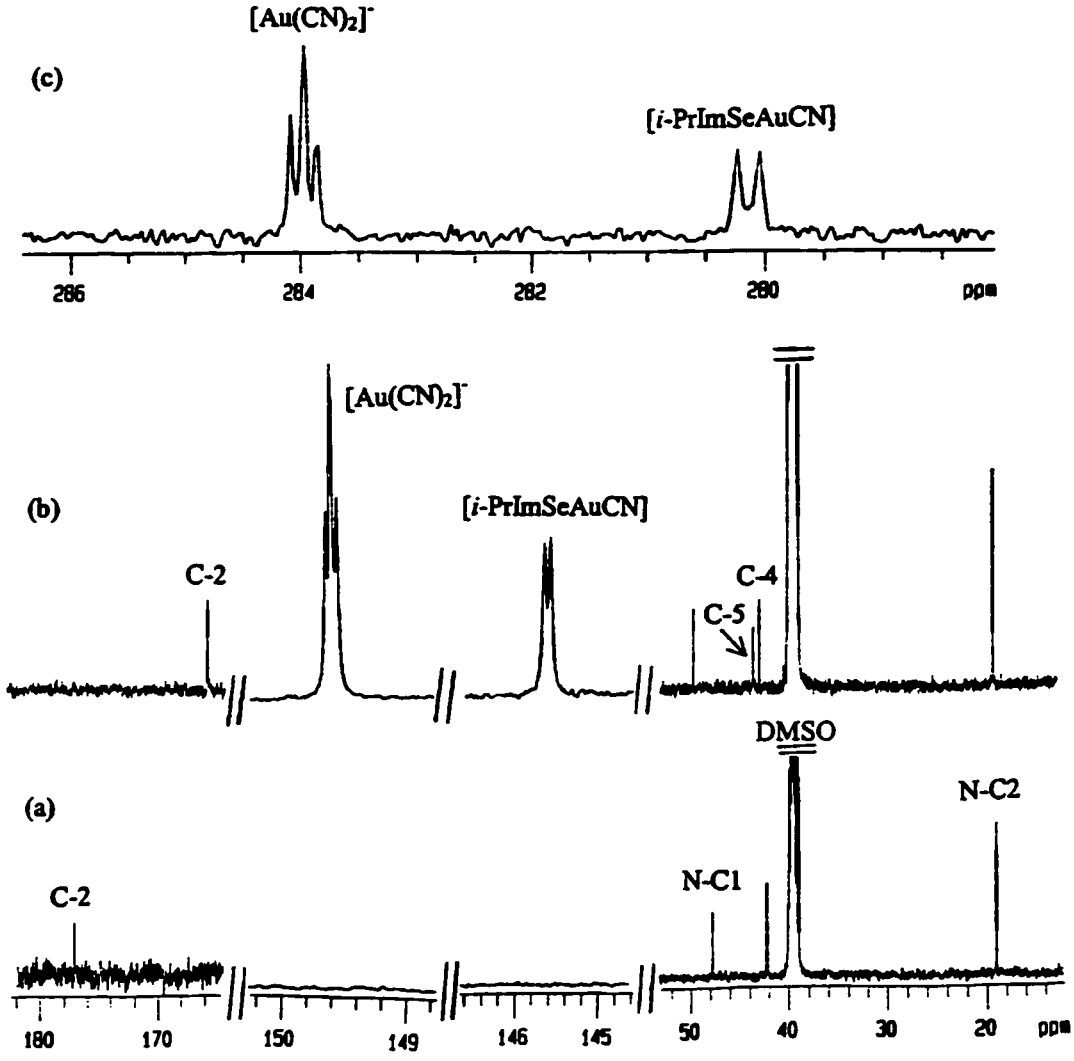

Figure 4.6 (a) 125.65 MHz ^{13}C NMR spectrum of *i*-PrImSe in DMSO (b) ^{13}C NMR spectrum of *i*-PrImSe-Au-CN (c) 50.55 MHz ^{15}N NMR spectrum of *i*-PrImSe-Au-CN

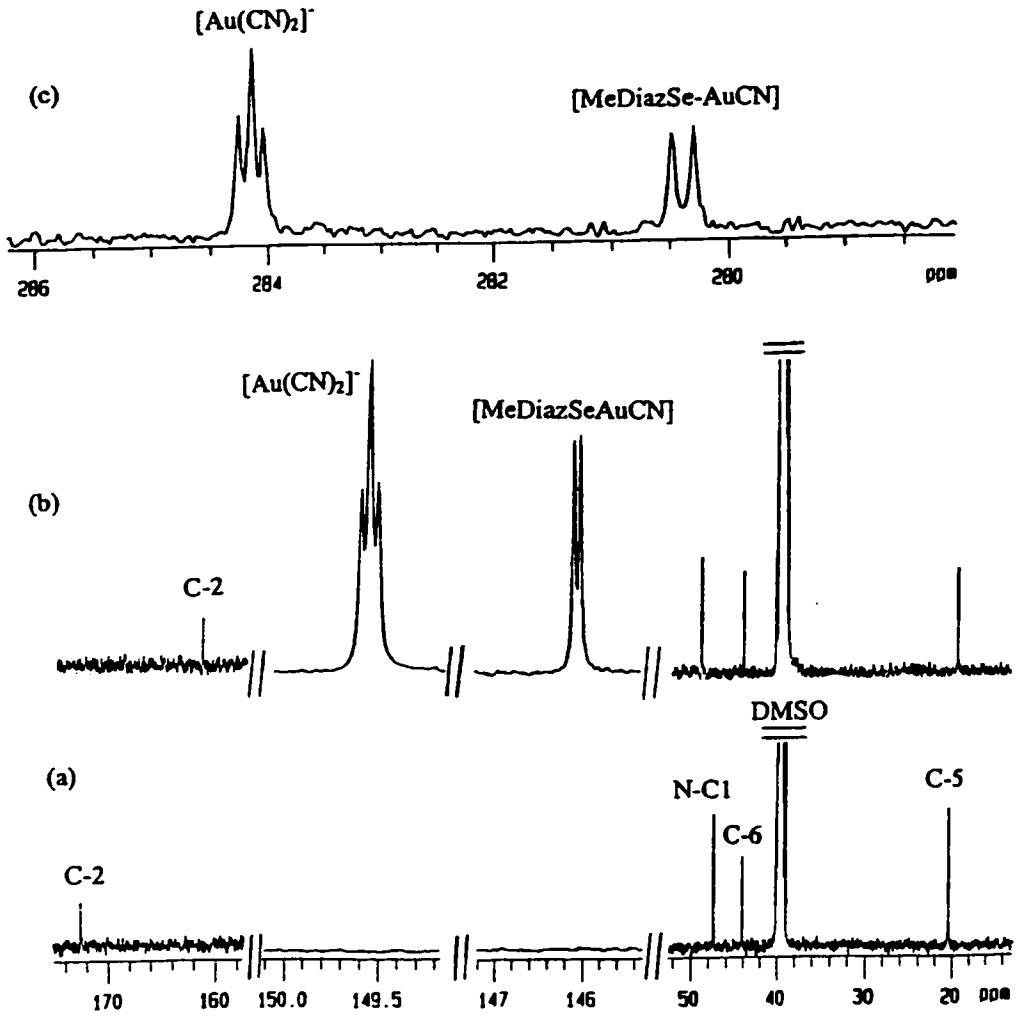

Figure 4.7 (a) 125.65 MHz ^{13}C NMR spectrum of MeDiazSe in DMSO (C_4 is overlapped with DMSO resonances) (b) ^{13}C NMR spectrum of MeDiazSe-Au-CN (c) 50.55 MHz ^{15}N NMR spectrum of MeDiazSe-Au-CN

Equilibrium constants (K_{eq}) values found for the complexes when prepared in solution are greater than the values, obtained after the isolation of complexes in the solid state (Table 4.19). For example, for the complex [DmSeu-Au-CN], the K_{eq} value is 5.28, when it is calculated from the data taken after its isolation in the solid state. But when the complex was prepared *in situ* in solution, the K_{eq} value was found to be 7.02. Similarly, the spectra were recorded for the two other complexes [ImSeAuCN] and [MeImSeAuCN], by preparing them in solution. The K_{eq} values for these two complexes after their isolation were also determined. Thus the percentage errors in K_{eq} values were calculated for these three complexes ([DmSeuAuCN], [ImSeAuCN] and [MeImSeAuCN]). The K_{eq} values of [SeuAuCN] and [4-MeImSeAuCN] were calculated after multiplying the observed values by the correction factor. The excess concentration of AuCN used in the preparation of these complexes could also be a factor for the larger values of K_{eq}, when prepared in solution.

4.7.1.1 Effect of Various Factors on Equilibrium Constant

The effect of several factors on the magnitude of K_{eq} was examined for a representative complex, Imt-Au-CN. The first extrinsic factor examined was the initial concentration of the complex, $[Imt\text{-}Au\text{-}CN]_o$. Initial concentrations ranging from 0.0125 M to 0.100 M in DMSO-d_6 were used. A plot of K_{eq} versus $[Imt\text{-}Au\text{-}CN]_o$ is linear with K_{eq} value steadily increasing with $[Imt\text{-}Au\text{-}CN]_o$ (Figure 4.8).

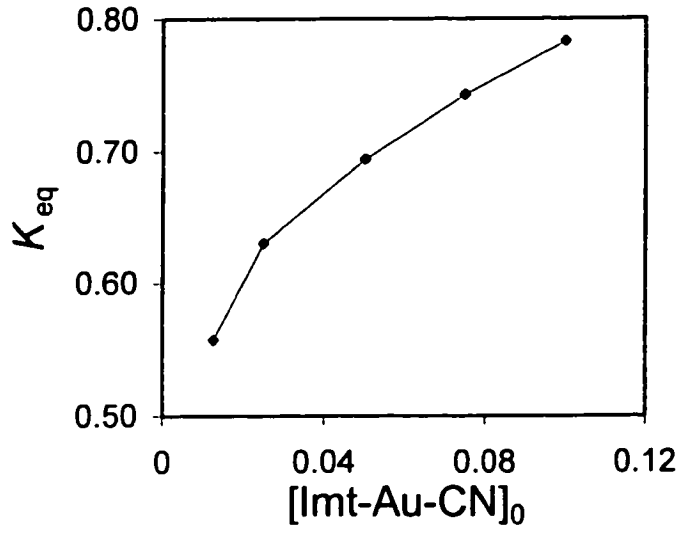

Figure 4.8 K_{eq} vs $[Imt\text{-}Au\text{-}CN]_0$ at 298 K and at the concentrations of 0.0125 M 0.10 M in DMSO

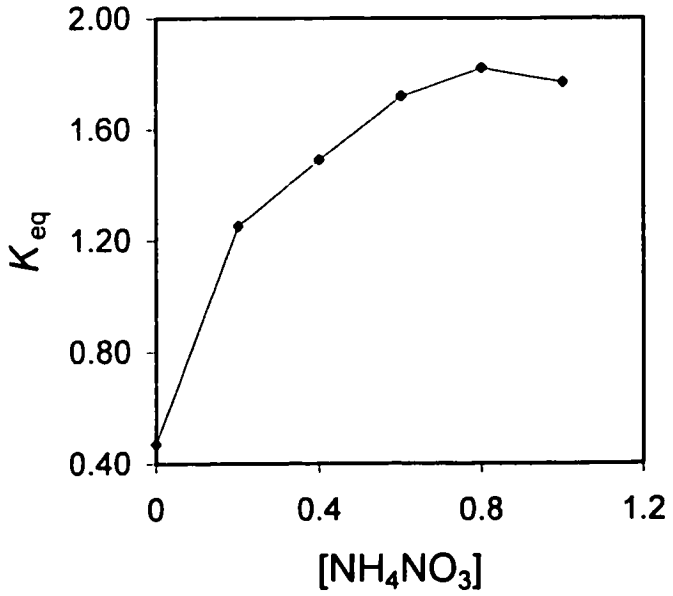

Figure 4.9 K_{eq} vs $[NH_4NO_3]$ for 0.05 M Imt-Au-CN at 298 K in methanol

The second external influence examined was the ionic strength of the solution. NH_4NO_3 (a salt having component ions with low affinity for gold(I) [114]) was used to control the ionic strength of the solution. The ^{13}C NMR spectra were acquired for 0.05 M [Imt-Au-CN] in CD_3OD with NH_4NO_3 at concentrations ranging from 0.20 M to 1.0 M. Figure 4.9 shows that a plot of K_{eq} versus the concentration of salt is linear up to 0.80 M concentration NH_4NO_3.

In order to examine the effect of temperature on K_{eq}, ^{13}C spectra were obtained at the temperatures of 240 K, 260 K, 280 K, 298 K and 320 K in CD_3OD. When K_{eq} values are plotted against temperature an inverse correlation was observed (Figure 4.10).

Polarity of the solvent should also have a significant effect on K_{eq} because the increased solvation of the ionic species generated as a result of the scrambling process should ultimately result in larger K_{eq}. The K_{eq} values obtained in different solvents using 0.025 M solution of the complex are shown in Table 4.21.

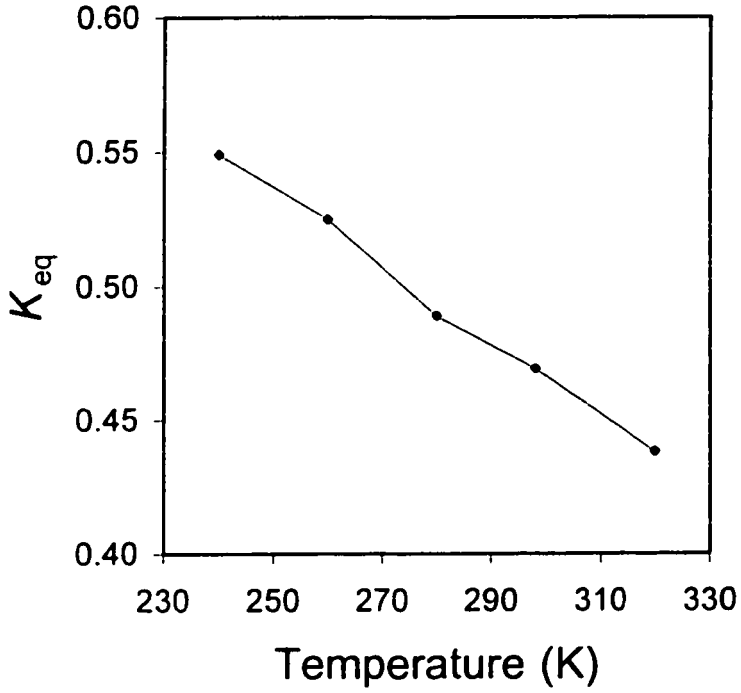

Figure 4.10 K_{eq} vs temperature for 0.05 M Imt-Au-CN in methanol

Table 4.18 ^{13}C and ^{15}N NMR chemical shifts of CN (ppm), coupling constants (Hz) and K_{eq} of cyano(thione)gold(I) complexes in DMSO-d_6

Species	$\delta^{13}C$	$\delta^{15}N$	$^{1}J_{C-N}$	K_{eq} (± esd)
DmTuAuCN	144.22	281.22	9.3	0.98 ± 0.03
ImtAuCN	144.40	281.18	9.3	0.630 ± 0.005
	147.02	262.23	10.3	0.47[a] ± 0.01
MeImtAuCN	143.64	281.18	9.0	0.56 ± 0.02
EtImtAuCN	143.62	281.36	10.4	0.62 ± 0.01
PrImtAuCN	143.60	281.38	9.3	0.59 ± 0.01
i-PrImtAuCN	143.81	280.99	[b]	0.55 ± 0.01
DiazAuCN	144.75	281.12	8.2	0.91 ± 0.01
DiapAuCN	144.69	281.10	[b]	0.96 ± 0.01
ErSAuCN	146.98	261.98	8.3	1.08

[a] values in methanol, [b] not observed

Table 4.19 ^{13}C and ^{15}N NMR chemical shifts of CN, coupling constants (Hz) and K_{eq} of cyanogold(I) complexes in DMSO-d_6

Species	$\delta^{13}C$	$\delta^{15}N$	$^{1}J_{C\text{-}N}$	K_{eq} ($\pm$ esd)
SeuAuCN	146.59	280.08	9.4	4.40 $\pm$ 0.07 (6.01)*
DmSeuAuCN	145.90	280.40	9.6	5.28 $\pm$ 0.08 (7.02)*
ImSeAuCN	146.03	280.26	8.2	2.95 $\pm$ 0.05[a] (3.62)*
MeImSeAuCN	145.58	280.32	10.0	2.90 $\pm$ 0.08[a] (4.09)*
4-MeImSeAuCN	146.24	279.02	9.4	2.75 $\pm$ 0.05 (3.74)*
EtImSeAuCN	145.54	280.32	9.0	2.76 $\pm$ 0.06
i-PrImSeAuCN	145.59	280.14	9.4	3.12 $\pm$ 0.02
PhImSeAuCN	145.66	279.84	9.4	4.28 $\pm$ 0.05
Et_2ImSeAuCN	143.93	280.36	8.9	2.84 $\pm$ 0.07
DiazSeAuCN	146.67	279.02	9.4	3.64 $\pm$ 0.06
MeDiazSeAuCN	146.11	280.40	9.4	3.33 $\pm$ 0.03

* K_{eq} values when complexes are prepared in solution

Table 4.20 ^{13}C and ^{15}N NMR chemical shifts of CN (ppm), coupling constants (Hz) and K_{eq} of some known cyanogold(I) complexes in methanol

Species	$\delta^{13}C$	$\delta^{15}N$	$^{1}J_{C-N}$	K_{eq}	Reference
Ph_3PAuCN	156.2	-	6.4	0.112	32,114
Me_3PAuCN	158.3	267.35	6.8	0.37	32,114
Et_3PAuCN	160.4	265.54	6.5	0.24	32,114
i-Pr_3PAuCN	160.9	264.61	6.2	0.29	32,114
Cy_3PAuCN	160.29	264.35	5.5	0.49	32,114
$Cy_3PSAuCN$	144.85	261.55	11.3	0.147	30
$Cy_3PSeAuCN$	146.44	260.65	8.9	1.81	30,37

Table 4.21 K_{eq} values for the scrambling of Imt-Au-CN in different solvents at 298 K

Solvent	μ(debye)[a]	K_{eq}
DMSO	3.9	0.630
Acetonitrile	3.44	0.338
Methanol	2.87	0.450
Acetone	2.69	0.189

[a] Values taken from reference 157.

4.8 ^{1}H and ^{13}C NMR Studies of the Interaction of Gold(I) Thiomalate with 6-Mercaptopurine and Its Derivatives

4.8.1 ^{1}H NMR Studies

The observed proton chemical shifts for thiolated bases with and without addition of $(AuStm)_n$ are given in Table 4.22. The ^{1}H NMR spectra were assigned according to the references given in literature [89,96,158].

In the ^{1}H NMR the signals near 8 ppm are due to the H-2 and H-8 protons of the free ligands and a doublet around 6 ppm is due to the anomeric proton of ribose [89,96]. It is observed that in 6-MP, H-2 appears downfield as compared to H-8 while the opposite trend is found in 6-MPR (Table 4.22). The H-2 signal also became less intense while the intensity of H-8 was not affected by addition to $(AuStm)_n$. Since the shift in H-8 is very small, so it can be concluded that N-7 is not involved in the binding. For 6-MP, the H-8 signal shifted upfield at pH 12, suggesting deprotonation at N-9. The N_1H-H-2 coupling has not been observed in the NMR spectra, which may be due to the rapid proton exchange. All the exchangeable protons (NH, SH and NH_2) have disappeared.

4.8.2 ^{13}C NMR Studies

The ^{13}C NMR were recorded after successive addition of ligands to $(AuStm)_n$. The observed chemical shifts of various resonances for the ligands and their complexes with gold(I) are summarized in Table 4.23. The changes in $(AuStm)_n$ resonances on addition of purine ligands are given in Table 4.24. It should be noted that $(AuStm)_n$

resonances are not affected by changing pH from 6 to 12 [122]. The ^{13}C chemical sifts were assigned according to the references reported earlier in the literature [90,91,159].

4.8.2.1 Interaction of $(AuStm)_n$ with 6-MP

The ^{13}C NMR spectrum of 0.05 M solution of $(AuStm)_n$ in D_2O at pH 6.93 is shown in Figure 4.11 (g_1 and g_2 are the CH and CH_2 resonances of glycerol respectively [124-125]). Figure 4.12, a and b shows the ^{13}C NMR spectrum of 0.05 M solution of 6-MP in D_2O at two different pHs. When 0.50 equivalent of 6-MP was added as a solid to 0.05 M $(AuStm)_n$ solution at pH 10, only C-2 resonance was observed. The C-4 and C-8 resonances were less intense compared to C-2. The C-5 and C-6 resonances did not appear. The b_1 resonance of $(AuStm)_n$ shifted from 47.66 ppm to 43.73 ppm, while b_3 and b_4 were broadened as shown in Figure 4.12c. The chemical shifts of 6-MP were observed to be pH dependent (Table 4.23). It was observed that at pH 12, the C-8, C-4 and C-5 were shifted downfield because of the removal of proton from N-9 position (Figure 4.12b). The chemical shift changes on further additions of 6-MP to $(AuStm)_n$ solutions are compared with the chemical shifts of the base at pH 12.

On addition of 1.0 equivalent of 6-MP to the above solution at pH 11.50, the C-6 resonance shifted upfield by 3.40 ppm. The C-2 remained unshifted and increased in intensity. The C-4 and C-8 shifted downfield but they were less intense. The C-5 resonance shifted upfield by about 2.36 ppm. The thiomalate resonances became more distinct (Figure 4.12d). At the ratio of 1:1 [illegible] to $(AuStm)_n$ the C-2, C-6, b_1, b_3 and b_4 resonances became more intense. The [illegible] resonance was suppressed due to the broadening of C-8 resonance. The C-5 resonance became more intense. At the 2:1 ratio

of base to $(AuStm)_n$, the C-6 resonance became more intense. The C-4 and C-8 were broadened due to an exchange between free and bound ligand. The resonances due to thiomalic disulfide, $(Stm)_2$ also appeared at 41, 54, 179 and 180 ppm (d_2, d_1, d_4 and d_3 respectively) [133] (Figure 4.13). The splitting of b_1, b_2 and b_3 resonances of thiomalate into two peaks showed that there was a possibility that 6-MP could form two geometrical isomers on its interaction with $(AuStm)_n$ (Figure 4.13).

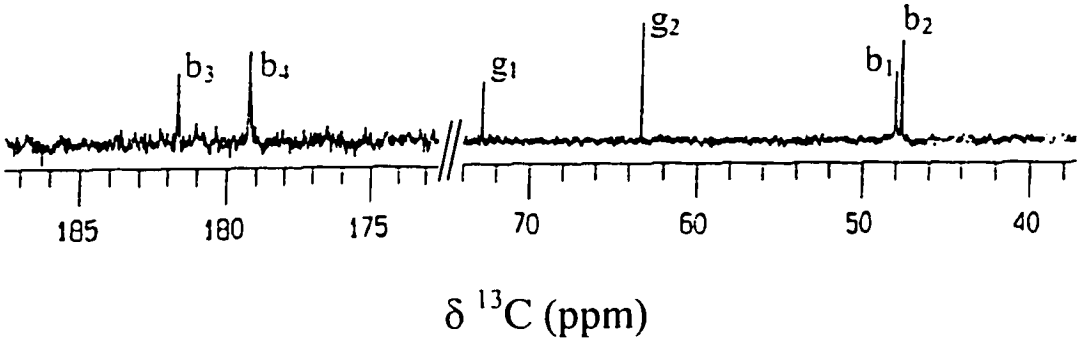

Figure 4.11 125.65 MHz $^{13}C\{^1H\}$ NMR spectrum of 0.05 M $(AuStm)_n$ in D_2O {g_1 and g_2 are resonance due to glycerol present as impurity in $(AuStm)_n$ }

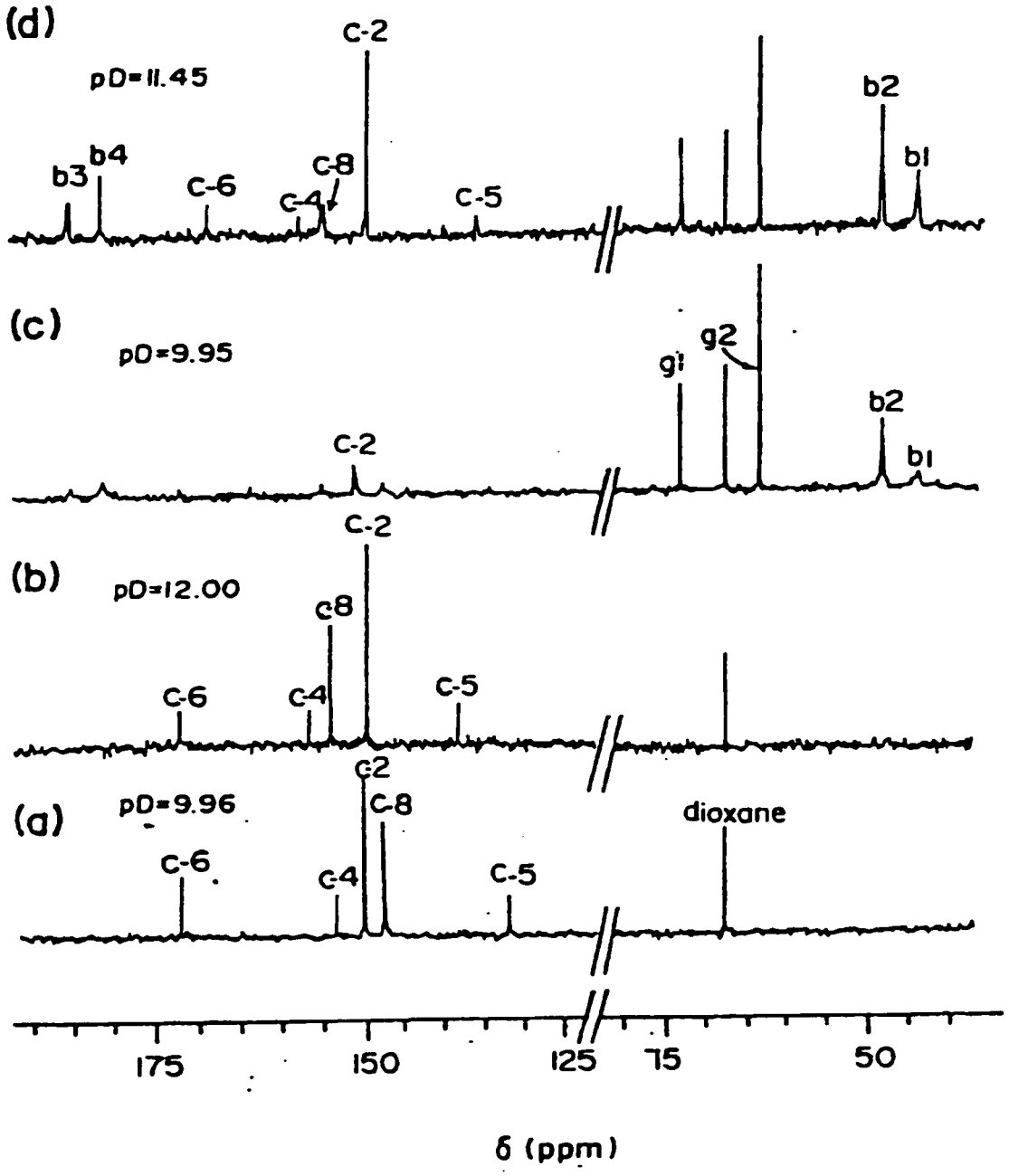

Figure 4.12 The 125.65 MHz $^{13}C\{^1H\}$ NMR spectrum of 6-MP:$(AuStm)_n$ at various molar ratios in D_2O: (a) and (b) 0.05:0 (c) 0.025:0.05, (d) 0.05:0.05.

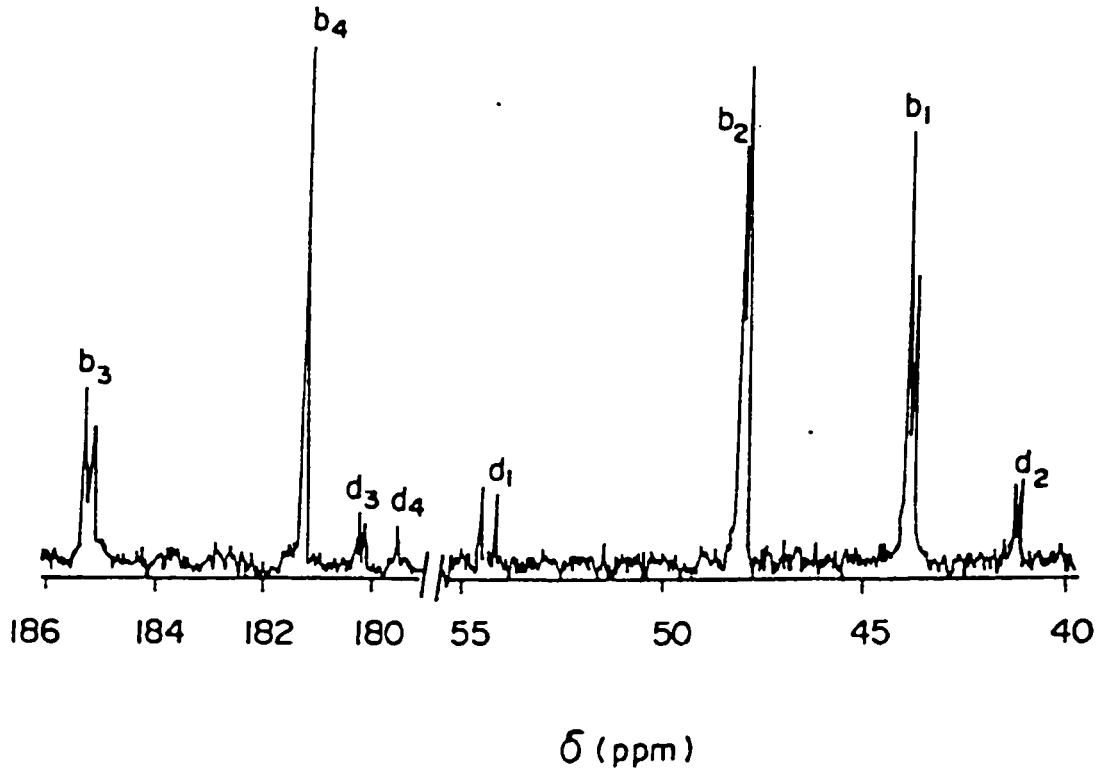

Figure 4.13 The 125.65 MHz $^{13}C\{^{1}H\}$ NMR spectrum of 6-MP:$(AuStm)_n$ of 2:1 at pH 10.96 (only $(AuStm)_n$ and $(Stm)_2$ resonances are shown).

4.8.2.2 Interaction of $(AuStm)_n$ with 6-MPR

Figure 4.14a shows the ^{13}C NMR spectrum of 0.05 M solution of 6-MPR in D_2O at pH 10.12. On addition of 0.50 equivalent of base to 0.05 M $(AuStm)_n$ solution, only C-6 and C-8 resonances appeared. The C-8 shifted upfield by 1.1 ppm while the C-6 by 7.1 ppm. The $(AuStm)_n$ resonances remained broad except b_2 (Figure 4.14b). When 1.0 equivalent of 6-MPR was added to the above solution, the C-6 shifted 10 ppm further upfield. The C-8 and C-4 shifted downfield by 1.2 ppm and C-5 shifted upfield by 2 ppm (Figure 4.14c). There was no significant change for C-2 resonance. As the ratio of base to $(AuStm)_n$ was increased to 1.5:1 and 2:1, all the resonances except C-2 remained broadened showing an exchange between free and bound ligand. The C-6 shifted downfield towards the free ligand at the higher concentrations of base. The b_1 and b_3 resonances of thiomalate appeared more clearly. The b_1 resonance split into two peaks attributed to the isomeric CH carbon of thiomalate (as explained in the Figure 4.13).

4.8.2.3 Interaction of $(AuStm)_n$ with 2-A-6-MPR

Figure 4.15a shows the ^{13}C NMR spectrum of 0.05 M solution of 2-A-6-MPR in D_2O at pH 11.30. Upon addition of 0.50 equivalent of 2-A-6-MPR as a solid to 0.05 M $(AuStm)_n$ solution, the C-6 and C-2 resonances were not observed. The C-5 resonance shifted upfield by 2.39 ppm and decreased in intensity. The other two resonances C-4 and C-8 appeared as sharp peaks. The b_2 resonance of thiomalate became sharp and b_1 shifted upfield from 47.66 ppm to 43.46 ppm. The b_3 resonance shifted downfield from 181.70 ppm to 185.15 ppm (Figure 4.15b).

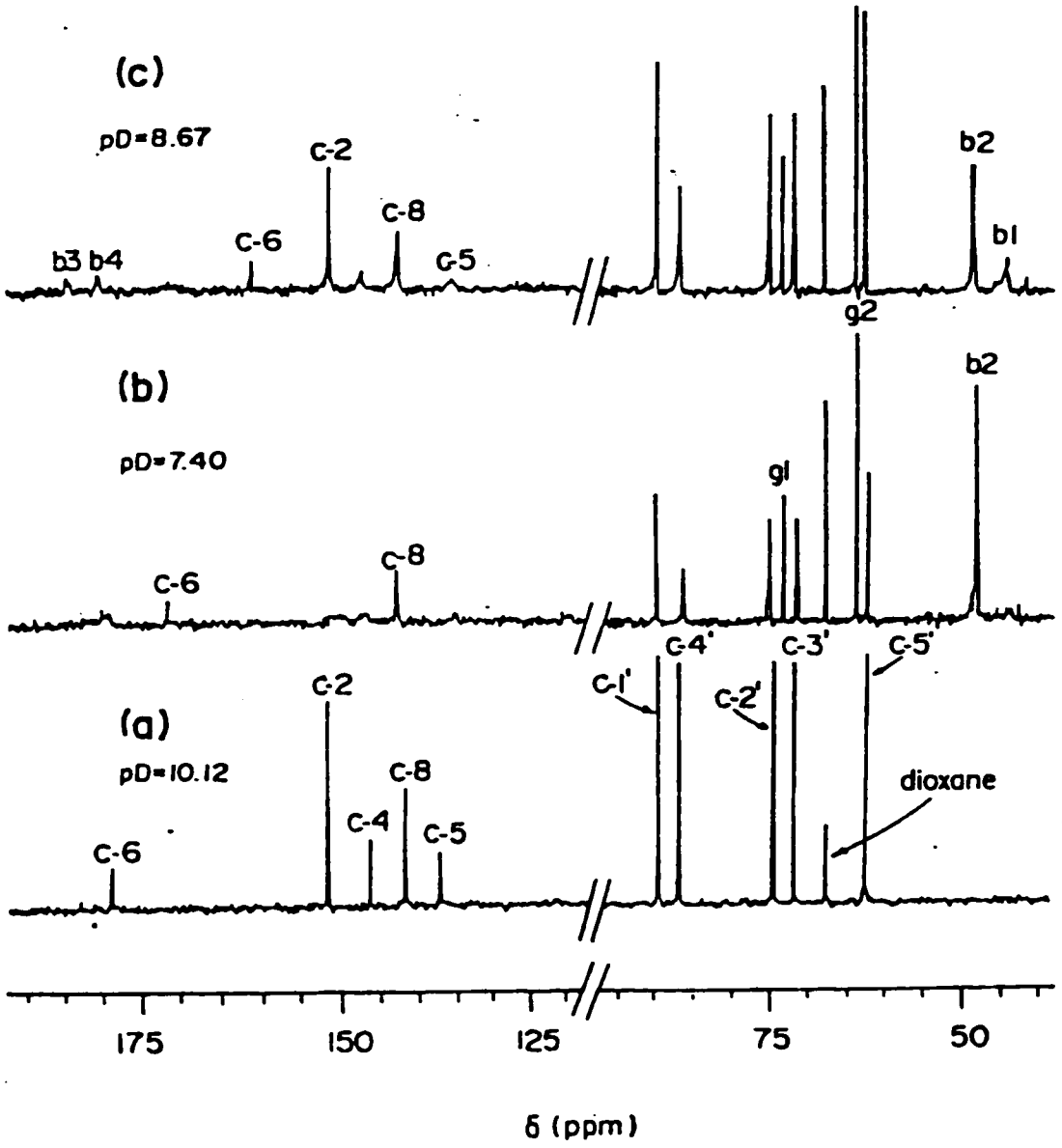

Figure 4.14 The 125.65 MHz $^{13}C\{^{1}H\}$ NMR spectrum of 6-MPR:$(AuStm)_n$ at various molar ratios in D_2O: (a) 0.05:0, (b) 0.025:0.05, (c) 0.05:0.05.

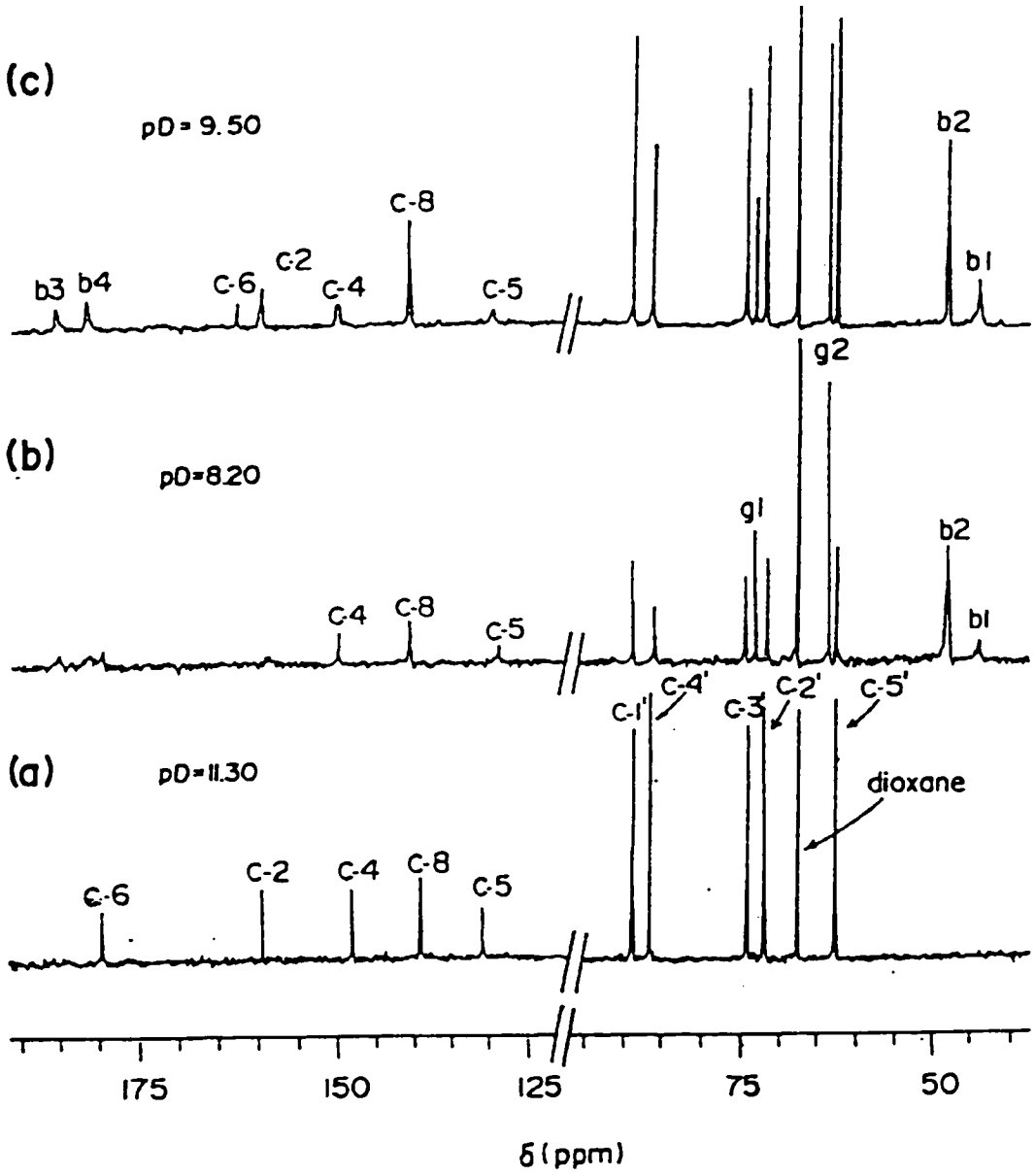

Figure 4.15 The 125.65 MHz $^{13}C\{^{1}H\}$ NMR spectrum of 2-A-6-MPR:$(AuStm)_n$ at various molar ratios in D_2O: (a) 0.05:0, (b) 0.025:0.05, (c) 0.05:0.05.

At the 1:1 ratio of base to $(AuStm)_n$ (Figure 4.15c) the C-2 resonance remained unchanged. The C-4 resonance is shifted downfield by 1.1 ppm. The C-5 resonance is shifted upfield by 1.8 ppm. The C-6 resonance shifted upfield by 17.5 ppm. The C-8 resonance shifted downfield by 1.0 ppm. All the $(AuStm)_n$ resonances appeared clearly and became more intense. At the higher concentrations of base (1.5 and 2.0 equivalents) all the peaks except at C-2 were broadened indicating an exchange between free and bound nucleoside. All the thiomalate resonances became sharp, indicating that thiomalate was replaced by the nucleoside from one side in the polymer forming [>C=S-Au-tm] species. At the ratio of 1.5:1 of base to $(AuStm)_n$ the C-6 resonance shifted a little downfield due to the equilibrium between free and bound ligand. The C-2 and C-8 resonances were almost unaffected. The other resonances were very much broadened. At the ratio of 2:1 of base to $(AuStm)_n$ the C-6 resonance shifted further downfield by 2 ppm, indicating an exchange between free and bound base. The b_1 resonance split into two resonances due to two isomeric forms of the complex 2-A-6-MPR-Au-Stm (see Figure 4.13).

Table 4.22 ^{1}H NMR chemical shifts of thiolated purine bases with and without addition of $(AuStm)_n$ in D_2O

RS:$(AuStm)_n$	pH	H-8	H-2	H-1′
RS = 6-MP				
1:0	9.96	8.07	8.17	
1:0	12.00	7.84	8.04	
1:2	9.95	8.11	8.30	
1:1	11.45	7.59	8.32	
1.5:1	11.15	7.94	8.12	
2:1	10.96	7.92	8.11	
RS = 6-MPR				
1:0	10.12	8.18	8.15	5.92, 5.90
1:2	7.40	8.29	8.19	5.95, 5.94
1:1	8.67	8.26	8.18	5.13, 5.91
1.5:1	10.75	8.21	8.15	5.90, 5.89
2:1	10.35	8.20	8.14	5.89, 5.88
RS = 2-A-6-MPR				
1:0	11.30	7.80	-	5.69, 5.71
1:2	8.20	7.88	-	5.71, 5.72
1:1	9.50	7.89	-	5.69, 5.71
1.5:1	10.55	7.85	-	5.73, 5.72
2:1	10.87	7.84	-	5.71, 5.72

Table 4.23 ^{13}C NMR chemical shifts of thiolated purine bases with and without addition of $(AuStm)_n$ in D_2O

RS:$(AuStm)_n$	pH	C-2	C-4	C-5	C-6	C-8	C-1′	C-2′	C-3′	C4′	C-5′
RS = 6-MP											
1:0	9.96	149.98	153.31	131.64	171.88	147.37	-	-	-	-	-
1:0	12.00	149.42	156.45	137.86	172.02	153.95	-	-	-	-	-
1:2	9.95	150.92	154.77	-	-	147.08	-	-	-	-	-
1:1	11.45	149.49	157.49	135.50	168.62	154.89	-	-	-	-	-
1.5:1	11.15	149.54	-	135.34	168.78	154.79	-	-	-	-	-
2:1	10.96	149.52	151.73	135.68	168.98	155.22	-	-	-	-	-
RS = 6-MPR											
1:0	10.12	151.53	146.21	136.85	178.94	141.64	89.16	74.33	71.50	86.57	62.37
1:2	7.40	-	-	-	171.80	142.77	89.47	74.85	71.04	85.97	62.08
1:1	8.67	151.38	147.22	134.85	161.28	142.56	89.33	74.581	71.28	86.29	62.23
1.5:1	10.75	147.05	151.56	135.74	166.21	142.29	89.92	74.48	71.38	86.41	62.29
2:1	10.35	146.76	151.52	135.92	163.46	142.15	89.27	74.45	71.41	86.45	62.32
RS = 2-A-6-MPR											
1:0	11.30	159.35	148.12	130.86	179.66	139.20	88.86	71.71	73.96	86.56	62.51
1:2	8.20	-	149.59	128.45	-	140.34	88.94	71.31	74.28	86.01	62.26
1:1	9.50	159.08	149.25	129.03	162.12	140.07	88.95	71.50	74.08	86.29	62.37
1.5:1	10.55	159.30	149.14	129.42	166.90	139.88	88.94	71.57	74.02	86.38	62.44
2:1	10.87	159.31	148.78	130.05	168.16	139.64	88.94	71.61	74.01	86.43	62.43

Refer Figure 2.1 for the numbering of the resonances

Table 4.24 ^{13}C chemical shifts of $(AuStm)_n$ with and without addition of bases in D_2O

$(AuStm)_n$: RS	pH[a]	b_1	b_2	b_3	b_4
1:0	6.93	47.66	48.01	181.70	179.24
RS = 6-MP					
2:1	9.95	43.73	48.02	184.88	181.34
1:1	11.45	43.74	48.14	185.05	181.22
1:1.5	11.15	43.91	48.14	185.28	181.26
		43.73	48.03	185.14	
1:2	10.96	43.89 (41.14)	48.04 (54.14)	185.31(180.26)	181.28
		43.74 (41.23)	48.14 (54.49)	185.18	(179.50)*
RS = 6-MPR					
2:1	7.40	-	47.82	-	179.85
1:1	8.67	43.77	48.08	185.17	180.95
1:1.5	10.75	43.76	48.08	185.08	181.09
1:2	10.35	43.78	48.10	184.99	181.19
		44.17			
RS = 2-A-6-MPR					
2:1	8.20	43.46	47.86	185.15	180.53
1:1	9.50	43.69	48.03	185.10	181.19
1:1.5	10.55	43.72	48.10	185.15	181.10
1:2	10.87	44.09	48.11	185.15	181.16
		43.74			

* values in parentheses are for $(Stm)_2$

[a]From pH 6 to 12 there is no change in chemical shift of $(AuStm)_n$ [122]

4.9 ^{13}C NMR Studies of the Redox and Exchange Reactions of Gold(I) Thiomalate with Diselenides

4.9.1 Reaction with Selenocystine

Figure 4.16a shows the ^{13}C NMR of 0.10 M $(AuStm)_n$ in D_2O at pH 7.0 (g_1 and g_2 are the CH and CH_2 resonances of glycerol [124,125]). The ^{13}C NMR spectrum of 0.05 M selenocystine in D_2O at pH 11.0 is shown in Figure 4.16b; it was insoluble below pH 10 and above pH 1.5. The resonances at 36 ppm and 57 ppm correspond to CH and CH_2 carbons of selenocystine while the resonance at 56 ppm is due to some impurity. When 0.50 equivalent selenocystine was added as a solid to 0.10 M $(AuStm)_n$ solution in D_2O, it was insoluble at pH 7.0; it dissolved at pH 10.8 and the color of solution changed from light to dark yellow. The $(AuStm)_n$ resonances are not affected by changing pH between 6 and 12 [122]. Figure 4.16c shows the ^{13}C NMR of the resulting solution after 2 hrs. The doublet at 36 ppm shifted to 38 ppm while the resonance at 57 ppm almost remained unshifted. The b_2 resonance of $(AuStm)_n$ appeared as a very weak and broad peak. Two new resonances, 42 ppm and 52 ppm were also observed in the spectrum. The DEPT experiment with 135° pulse sequence showed that the signal at 42 ppm is due to CH_2 while the one at 52 ppm is due to CH carbons of thiomalate group (Figure 4.17). This pattern could be only due to a selenyl sulfide species (RSe-Stm), since if it were a gold bound species, opposite trend should be observed; b_1 is shifted upfield upon interaction of $(AuStm)_n$ with other ligands [124,125,160]. The formation of selenyl sulfide species by the reaction of diselenides with thiols has been reported in the literature [161]. No

thiomalic disulfide $(Stm)_2$ resonances appeared until 5 hrs due to its low concentration. These observations can be explained by the following reaction;

$$(AuStm)_n + RSe\text{-}SeR \longrightarrow RSe\text{-}Stm + (AuSeR)_n \qquad (4.4)$$

Figure 4.16d shows the spectrum taken after 5 hrs; two new resonances around 41 ppm and 54 ppm appeared for thiomalic disulfide, $(Stm)_2$ [133]. These resonances were further confirmed by the reaction of thiomalic acid with *m*-chloroperbenzoic acid. Both are doublets, attributed to the diastereoscopic carbons of $(Stm)_2$. The CH and CH_2 resonances of $(Stm)_2$ were assigned by DEPT experiment using 135° pulse sequence. After 12 hours, b_2 resonance of $(AuStm)_n$ became prominent. The appearance of b_1 and b_3 resonances in the spectrum after 29 hrs (Figure 4.16e) indicated the formation of $[Au(Stm)_2]$ [133]. Some yellow ppts were also observed in the NMR tube, which were separated from the orange yellow solution. The spectrum after 65 hrs showed that the peaks due to RSe-Stm species (42 ppm and 52 ppm) became very weak (Figure 4.16f) while those due to $(Stm)_2$ and $[Au(Stm)_2]^-$ became intense. The formation of $(Stm)_2$ and $[Au(Stm)_2]^-$ is described by the reaction (4.5);

$$2RSe\text{-}Stm + 2(AuStm)_n \longrightarrow (Stm)_2 + [Au(Stm)_2]^- + [Au(SeR)_2]^- \qquad (4.5)$$

With time the color of the solution changed to red, becoming blood red after one week. After 10-12 days this resulted into dark brown ppts and slightly yellow color solution. The spectrum after 12 days showed the peaks only for $(Stm)_2$ (Figure 4.16g). This can be explained by the reaction (4.6);

$$[Au(Stm)_2]^- + [Au(SeR)_2]^- \longrightarrow (Stm)_2 + Au^o + 2Se^o + Au(R)_x \qquad (4.6)$$

The Stm^- resonances from RSe-Stm were observed as very intense at the start of the experiment but their intensity decreased with time, while the intensity of $(Stm)_2$ resonances increased with time. Figures 4.18 shows the approximate percentage intensity of CH resonance of Stm in $(Stm)_2$ and RSe-Stm with time relative to the g_2 resonance of glycerol.

When 0.25 equivalent selenocystine was reacted with 0.10 M $(AuStm)_n$ (1:4 of selenocystine:$(AuStm)_n$, the $(Stm)_2$ resonances were observed in ^{13}C NMR after 6 hrs showing that the reaction starts immediately with the formation of RSe-Stm species, which then gives $(Stm)_2$. The $(AuStm)_n$ resonances remained prominent in the spectrum showing that all $(AuStm)_n$ did not undergo exchange process. It was also observed that if successive additions of selenocystine were carried out simultaneously each after few hours, the solution remained transparent until the addition of 0.75 M selenocystine to 0.10 M $(AuStm)_n$. However the overall reaction was then completed within one week.

4.9.2 Reaction with Selenocystamine

To further characterize the exchange process of diselenides with $(AuStm)_n$, the interaction of $(AuStm)_n$ with selenocystamine was also studied. Figure 4.19b shows the ^{13}C NMR of 0.05 M selenocystamine in D_2O at pH 11.0. When 0.50 equivalent selenocystamine was added to 0.10 M $(AuStm)_n$ in D_2O, it was insoluble at pH 7.0 (selenocystamine itself is soluble at pH 7.0). It dissolved at pH 10.65 resulting in a pale

yellow solution. Figure 4.19c shows the ^{13}C NMR taken after 2 hrs of mixing. Two additional resonances, one at 42 ppm and the other at 52 ppm appeared in the spectrum showing that the reaction had taken place immediately. The appearance of these resonances at almost the same position as they were observed in the case of selenocystine proves that these are for the selenyl sulfide species (RSe-Stm). The $(Stm)_2$ resonances were also detected in the spectrum, which became more intense with time while the intensity of RSe-Stm resonances decreased with time. Figures 4.20 shows the approximate percentage intensity of CH resonance of Stm in $(Stm)_2$ and RSe-Stm with time relative to the g_2 resonance of glycerol. The resonances for $[Au(Stm)_2]^-$ were observed in the spectrum after 10 hrs as shown in the figure 4.19d. The solution started becoming thick after 6 hrs while after 15 hrs, it became gel type and after 24 hrs, yellow ppts were observed in the NMR tube. The spectrum after 30 hrs showed that the intensity of $[Au(Stm)_2]^-$ and selenocystamine carbons is significantly reduced showing their decomposition to $(Stm)_2$ (Figure 4.19e). After 100 hrs, the yellow ppts further degraded to brown ppts and metallic gold. In the spectrum taken after 110 hrs, all other resonances disappeared except the $(Stm)_2$ resonaces, indicating that the reaction had gone to completion (Figure 4.19f). Thus the overall reaction of selenocystamine, with $(AuStm)_n$ was completed in a period almost 3 times shorter than that required for the reaction of selenocystine.

The ^{13}C chemical shifts of various resonances are given in Table 4.25.

Table 4.25 ^{13}C NMR chemical shifts of various species in D_2O in the interaction of gold(I) thiomalate with diselenides

Species	Resonance assignment (δ in ppm)
$(AuStm)_n$	48.01 (b_1), 47.66 (b_2), 181.70 (b_3), 179.24 (b_4)
Selenocystine	
pH 11.0	56.92 and 56.98 (α-C), 36.04 and 36.16 (β-C), 181.7 (C=O)
pH 1.1	53.99 (α-C), 27.89 and 27.79 (β-C), 171.29 (C=O)
Selenocystamine	
pH 11.0	41.77 (α-C), 33.28 (β-C)
pH 7.0	40.71 (α-C), 24.70 (β-C)
RSe-Stm (only resonances from Stm)	52.46 and 52.64 (S_1), 42.42 (S_2), 180.30 (S_3), 179.90 (S_4)
$(Stm)_2$	54.26 and 54.60 (d_1), 41.22 and 41.32 (d_2), 180.16 and 180.22 (d_3), 179.47 and 179.49 (d_4)

Refer Figure 2.2 for the numbering of the resonances

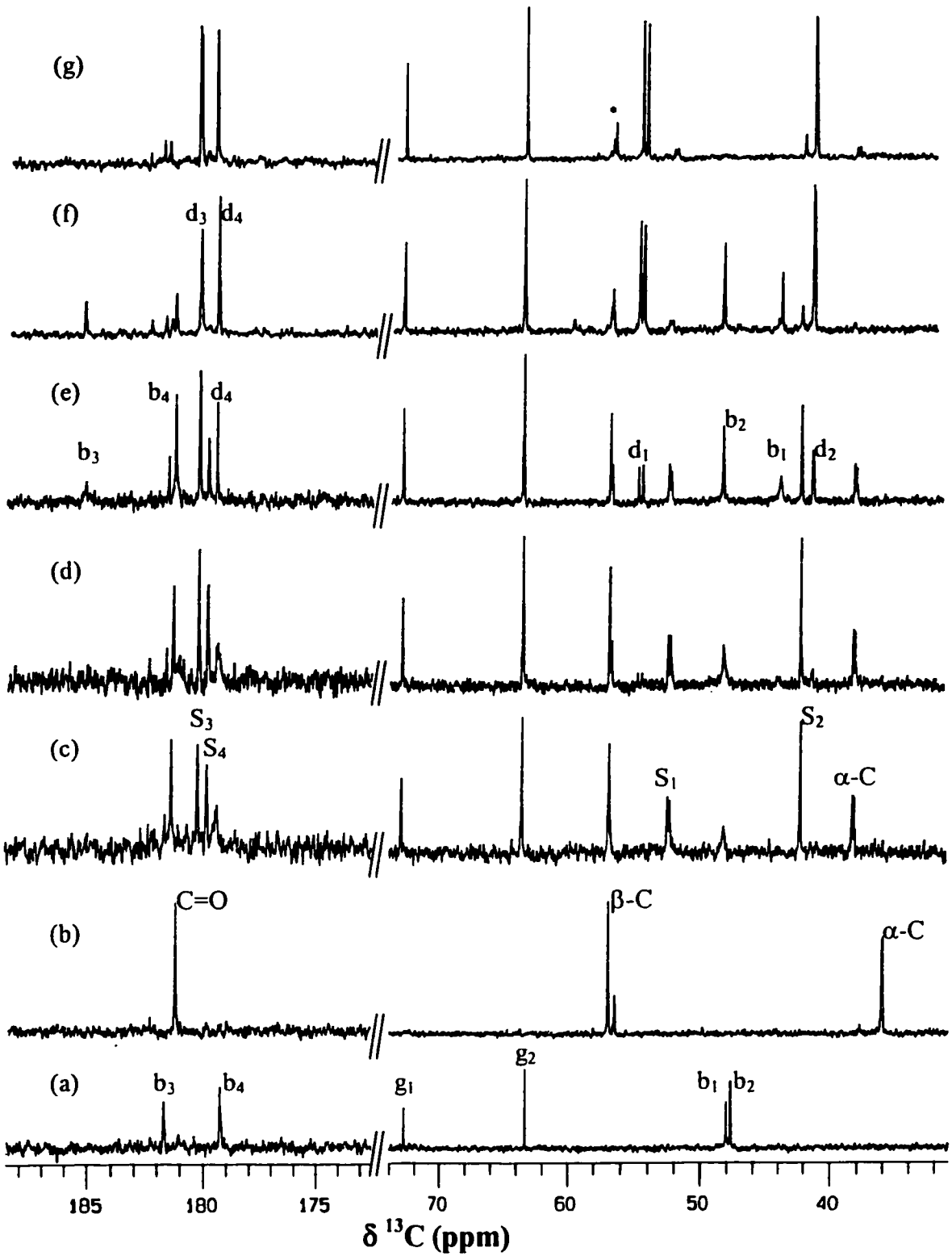

Figure 4.16 125.65 MHz $^{13}C\{^1H\}$ NMR spectra of 0.10 M $(AuStm)_n$:0.05 M selenocystine in D_2O, at various time intervals (a) 0.10 M $(AuStm)_n$ (b) 0.05 M selenocystine (c) after 2 hrs (d) after 5 hrs (e) after 29 hrs (f) after 65 hrs (g) After 12 days (For labeling refer Table 4.25 and Figure 2.2) *resonance due to some impurity

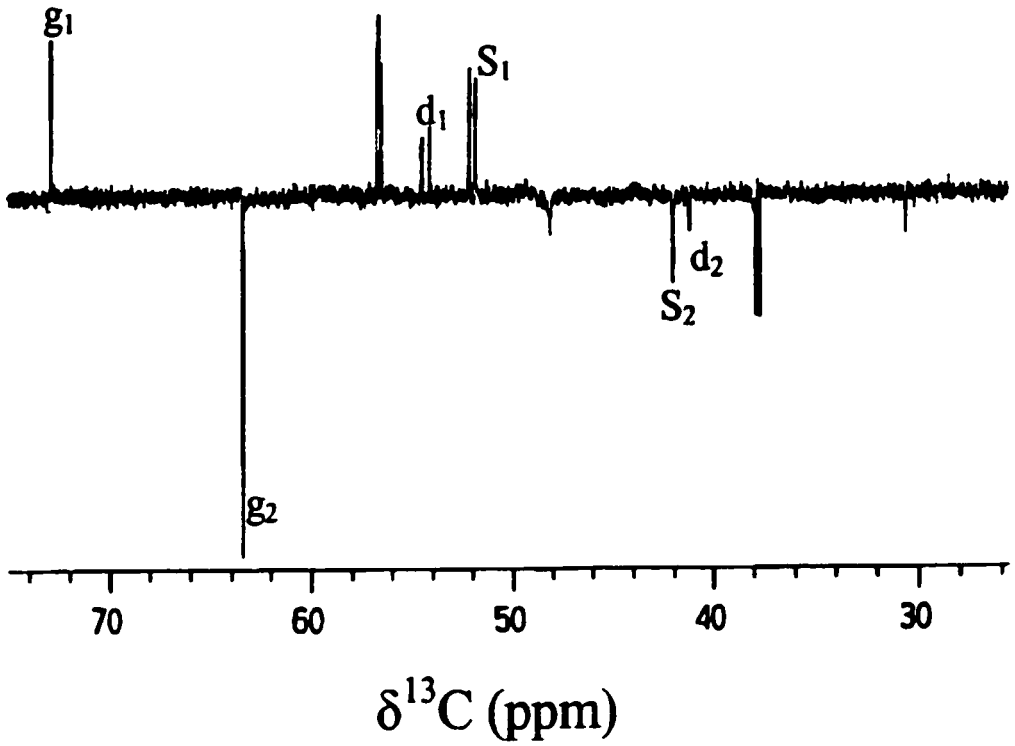

Figure 4.17 125.65 MHz $^{13}C\{^1H\}$ NMR spectrum of 0.10 M $(AuStm)_n$:0.05 M selenocystine in D_2O after 10 hrs using DEPT 135° pulse sequence.

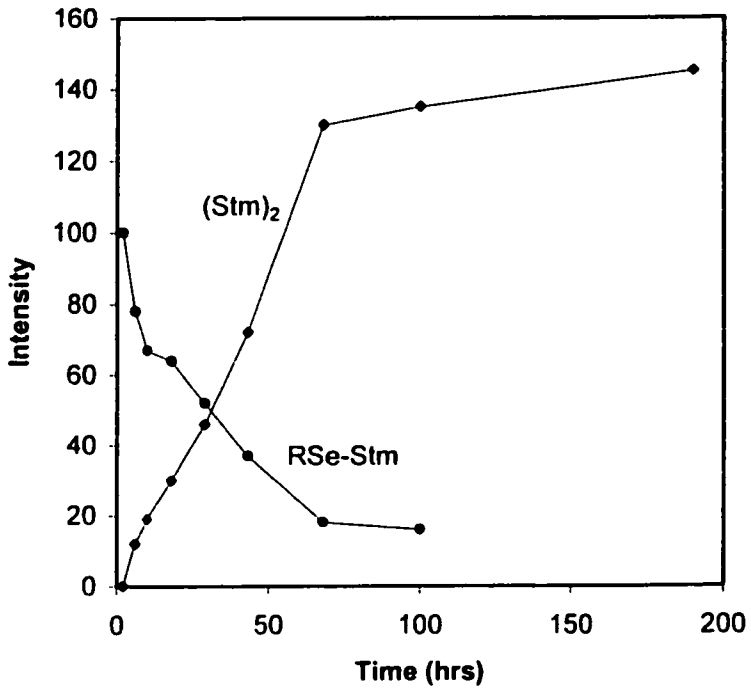

Figure 4.18 The percent intensity of $(Stm)_2$ and RSe-Stm resonances (from CH carbons of Stm) as a function of time in the interaction of $(AuStm)_n$ with selenocystine.

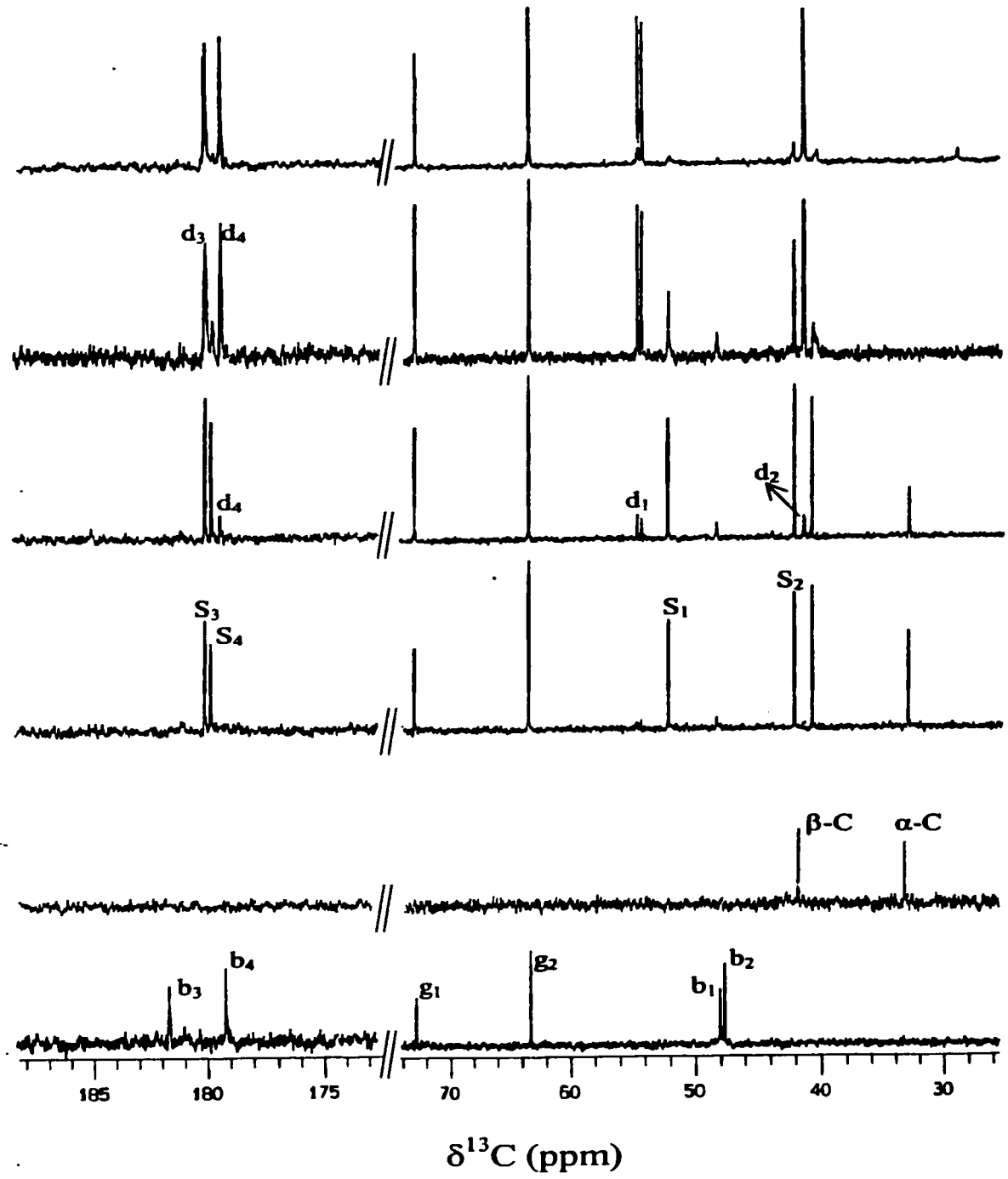

Figure 4.19 125.65 MHz $^{13}C\{^{1}H\}$ NMR spectra of 0.10 M $(AuStm)_n$:0.05 M selenocystamine in D_2O, at various time intervals (a) 0.10 M $(AuStm)_n$ (b) 0.05 M selenocystamine (c) after 2 hrs (d) after 10 hrs (e) after 30 hrs (f) after 110 hrs (a-e, from bottom to top)

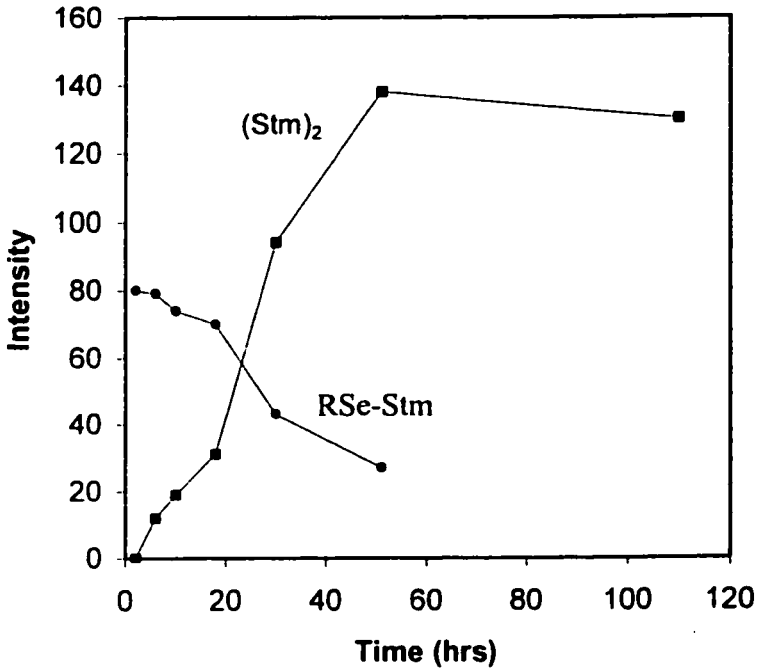

Figure 4.20 The percent intensity of $(Stm)_2$ and RSe-Stm resonances (from CH carbons of Stm) as a function of time in the interaction of $(AuStm)_n$ with selenocystamine.

4.10 ^{13}C, ^{31}P and ^{15}N NMR Studies of the Ligand Exchange Reactions of Gold(I) Thiomalate, Auranofin and Chloro(triethylphosphine) gold(I) with Thiourea

4.10.1 Interaction of Thiourea with $(AuStm)_n$

4.10.1.1 ^{13}C NMR Spectroscopy

Figure 4.21a shows the ^{13}C NMR of 0.05 M $(AuStm)_n$ and Figure 4.21b that of Tu in D_2O at pH 7.00. The >C=S resonance of Tu remained unshifted when its spectra were taken at pH of 3.5 and 11.0. In ^1H NMR, the resonance of NH_2 protons was not observed at any of above mentioned pH values, because of their exchange with D_2O. When 0.5 equivalent of Tu was added as solid to 0.20 M $(AuStm)_n$, the b_1 resonance of $(AuStm)_n$ shifted upfield and broadened, while b_3 and b_4 shifted downfield. The b_2 resonance remained almost unshifted throughout the titration. The solution of $(AuStm)_n$ was of pale yellow color and turned to colorless after addition of Tu. An upfield shift was observed in the >C=S resonance of Tu. A decrease in upfield shift in the >C=S resonance of Tu was observed on its further additions to $(AuStm)_n$ solution (Figures 4.21, b-e), showing an exchange between free and bound Tu. The observed chemical shifts of various resonances are summarized in Table 4.26. Because of the overlap of Tu resonance with b_4, the coupling constants could not be obtained by ^{13}C NMR. However, the $^1J(C\text{-}N)$ values were obtained by ^{15}N NMR.

4.10.1.2 ^{15}N NMR Spectroscopy

Figure 4.22a shows the ^{15}NMR spectrum of thiourea in normal H_2O at pH 7.40 (using D_2O of external standard, NH_4NO_3 as a source of deuterium lock). There is a doublet for Tu nitrogen around 108 ppm. When 0.5 equivalent of Tu was added to $(AuStm)_n$ solution, the above resonance shifted downfield by 1.2 ppm. On further additions of Tu this resonance became more sharp and shifted slightly upfield indicating a rapid exchange between free and bound Tu (Figures 4.22, b-e). The changes in the chemical shifts of Tu resonance and coupling constant are given in Table 4.27.

Table 4.26 ^{13}C NMR chemical shift changes (ppm) with and without addition of Tu to $(AuStm)_n$ solution in D_2O

$(AuStm)_n$:Tu	b_1	b_2	b_3	b_4	>C=S
1:0	47.66	48.01	181.70	179.24	-
0:1	-	-	-	-	182.75
1:0.5	46.77	47.80	182.71	179.89	179.19
1:1	46.61	47.80	183.08	180.11	180.11
1:1.5	46.37	47.80	183.30	180.21	180.86
1:2	46.24	47.81	183.40	180.26	181.28

Table 4.27 ^{15}N NMR chemical shift changes in Tu resonance on its addition to $(AuStm)_n$ solution in H_2O

$(AuStm)_n$:Tu	$\delta\ ^{15}N$	$^{1}J_{C\text{-}N}$ (Hz)
0:1	107.71	16.7
1:0.5	109.15	17.7
1:1	108.70	15.0
1:1.5	108.51	15.0
1:2	105.39	14.0

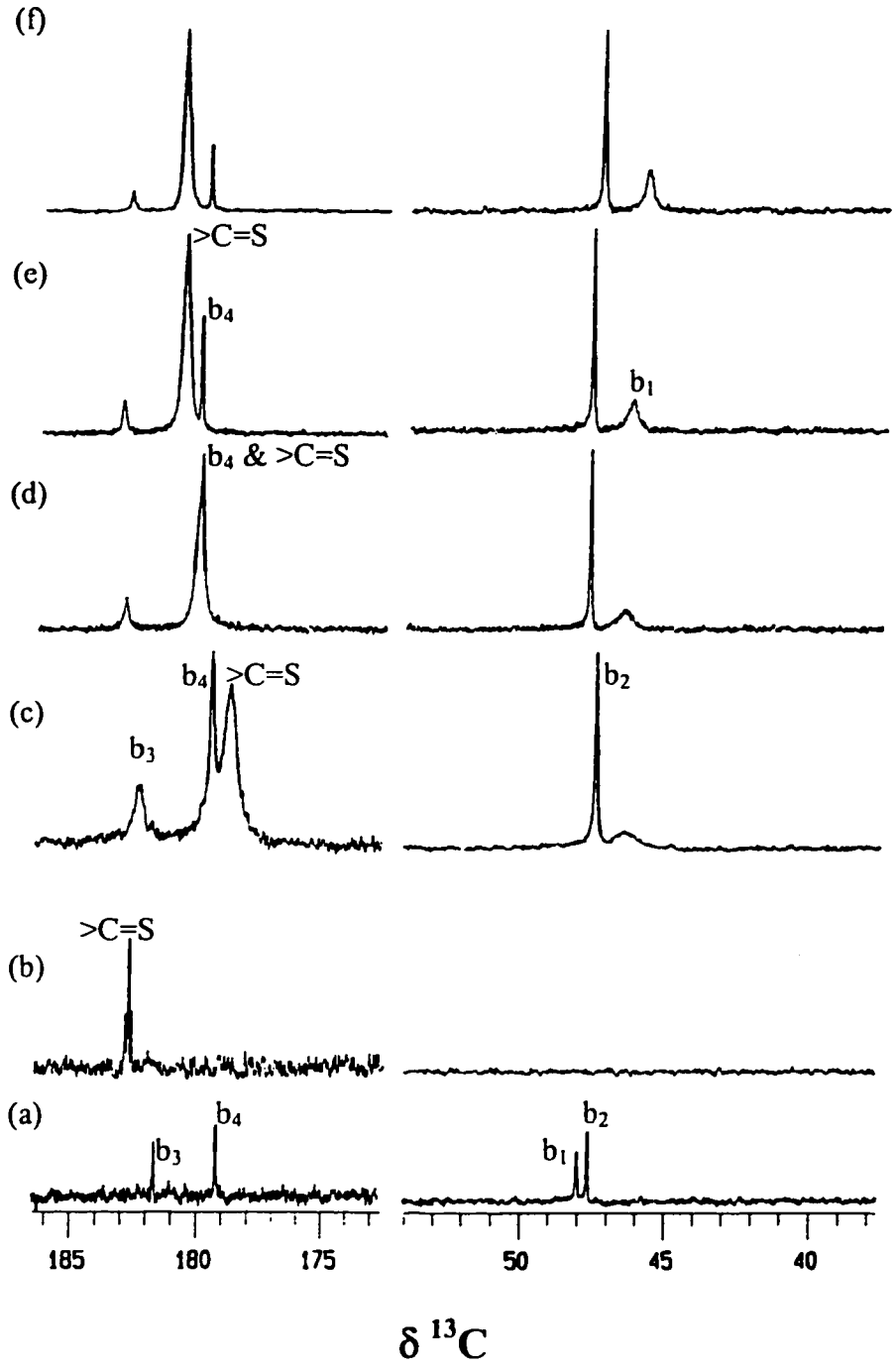

Figure 4.21 The 125.65 MHz $^{13}C\{^1H\}$ spectra of 0.20 M $(AuStm)_n$: Tu at various molar ratios in D_2O (a)1:0 (b) 0:1 (c) 1:0.5 (d) 1:1 (e) 1:1.5 (f) 1:2

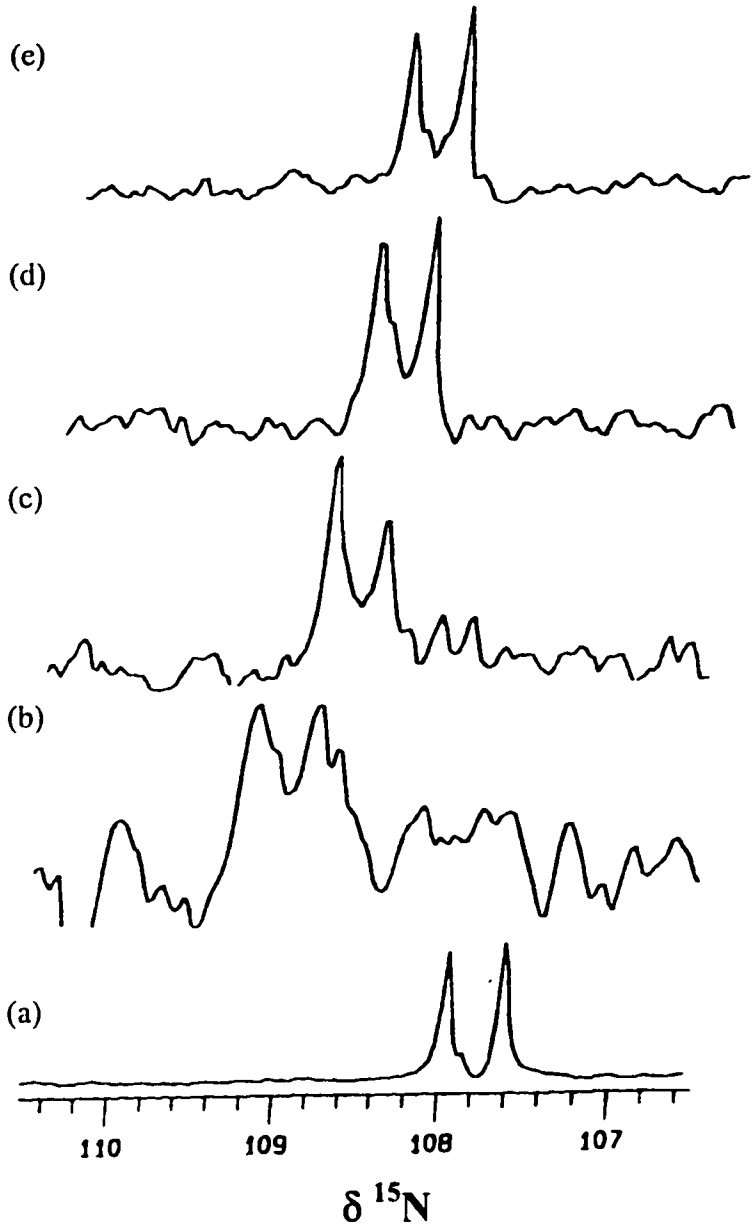

Figure 4.22 The 50.55 MHz $^{15}N\{^{1}H\}$ NMR spectra of 0.20 M $(AuStm)_n$:Tu at various molar ratios in H_2O (a) 0:1 (b) 1:0.5 (c) 1:1 (d) 1:1.5 (e) 1:2

4.10.2 Interaction of Thiourea with Auranofin

4.10.2.1 ^{31}P NMR Studies

Figure 4.23a shows the ^{31}P NMR spectrum of 0.20 M auranofin in methanol with a single resonance at 37.74 ppm [120]. When 0.50 equivalent of Tu was added to this solution, a slight upfield shift (0.40 ppm) in the auranofin resonance was observed and another resonance originated at 58.4 ppm due to Et_3PO [107,120]. When 1.0 and 2.0 equivalents of Tu were added, the auranofin resonance shifted further upfield and the resonance at 58.4 ppm became more prominent. At a 1:2 ratio of auranofin to Tu a new resonance appeared at 1.03 ppm (Figure 4.23c).

A time dependent experiment was carried out using 0.05 M auranofin at a 1:1 ratio of auranofin to Tu (Figure 4.24a). No change in the ^{31}P NMR spectrum was observed until 100 hours after mixing these solutions. After 110 hours two additional resonances appeared in the spectrum; one at 58.0 ppm, representing Et_3PO [107,120] and the other at 1.0 ppm, which is so far unassigned (Figure 4.24b). After one month these resonances were approximately 20 times more intense (Figure 4.24, c & d).

The ^{31}P NMR of auranofin:Tu (1:1) solution, after addition of CN^- is shown in Figure 4.24e. The auranofin resonance disappeared while the Et_3PO resonance and the resonance at 1.0 ppm became more intense. Another additional resonance was observed at 20.0 ppm due to free Et_3P. The Et_3PO resonance shifted slightly upfield. The ^{31}P chemical shifts of various resonances are described in Table 4.28.

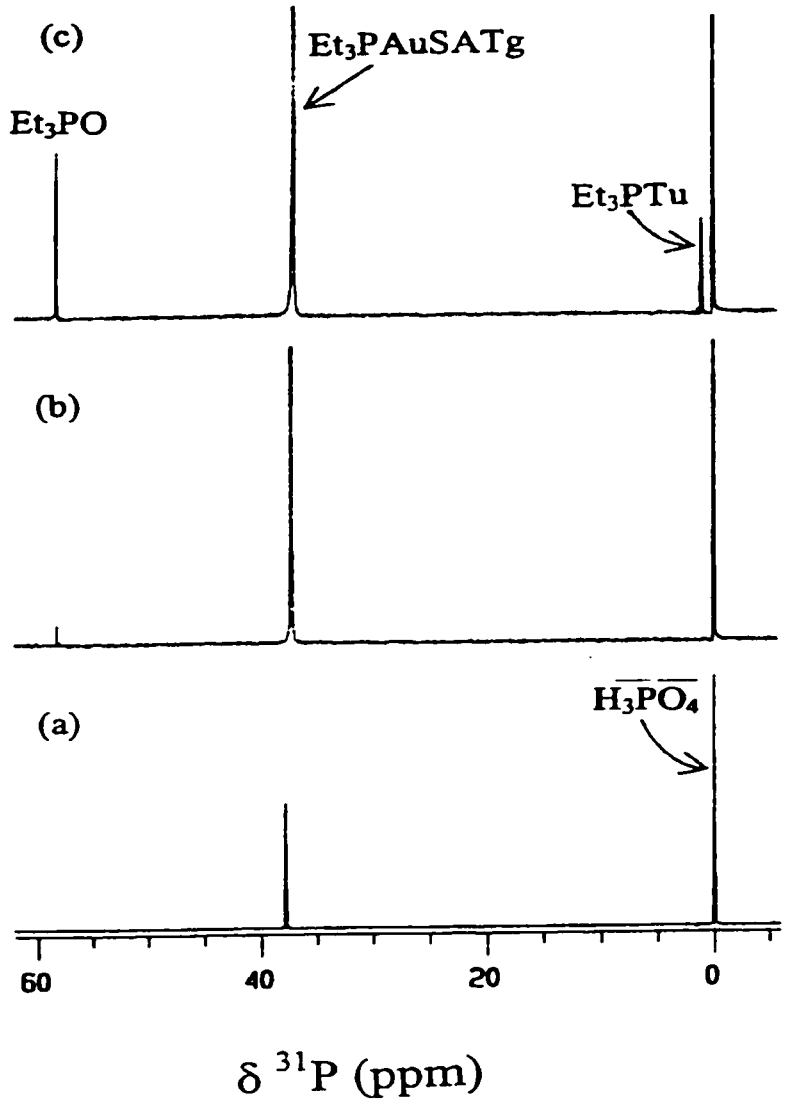

Figure 4.23 The 202.35 MHz $^{31}P\{^{1}H\}$ NMR spectrum of auranofin:thiourea at various molar ratios in methanol, (a) 1:0, (b) 1:1, (c) 1:2.

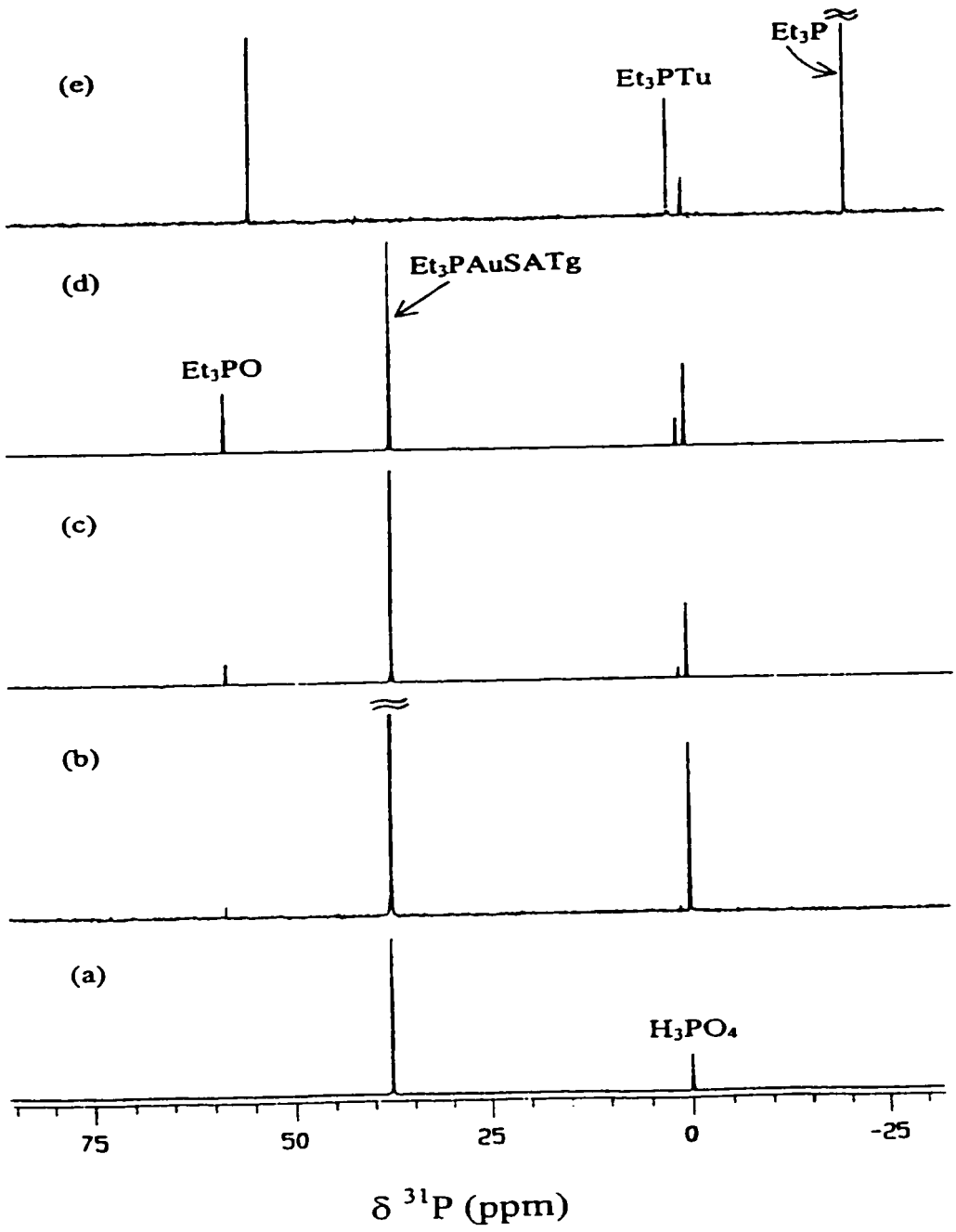

Figure 4.24 The 202.35 MHz $^{31}P\{^{1}H\}$ NMR spectrum of 0.05 M auranofin:0.05 M thiourea in methanol, at various time intervals (a) after 30 minutes, (b) after 110 hrs, (c) after 15 days, (d) after 1 month, (e) after addition of 0.10 M KCN.

4.10.2.2 ^{13}C NMR Studies

Figure 4.25 shows the ^{13}C NMR spectrum of 0.20 M Tu and Figure 4.26a that of 0.20 M auranofin in methanol. There are four sets of resonances in the auranofin spectrum. A very intense resonance at 9.50 ppm and a doublet around 19 ppm represent the PEt_3 carbons (due to CH_3 and CH_2 of PEt_3 respectively; CH_2 showing coupling with P). The next four downfield signals represent the methyl carbons of acetyl groups. The six clearly separated resonances of almost equal intensity in the region of 60-90 ppm are due to five pyranose ring carbons and one exocyclic methylene carbon. The most downfield three signals are due to carbonyl carbons of acetyl groups (Figure 4.26a). This assignment is consistent with the literature [162,163].

When 0.50 equivalent of Tu was added, the solution remained colorless and in ^{13}C NMR taken after 12 hours, no change in the auranofin or Tu resonances was observed (Figure 4.26b). The next addition of 0.50 equivalent of Tu (1:1 ratio) was carried out after 4 days. The ^{13}C NMR showed an upfield shift of 1.0 ppm in >C=S resonance of Tu. However, some extra peaks started appearing along the auranofin resonances (Figure 4.26c). These resonances were assigned to $(SATg)_2$, as a result of an independent reaction of $SATg^-$ with an oxidizing agent, *m*-chloroperbenzoic acid {$(SATg)_2$ is formed by the oxidation of $SATg^-$ after it is released [120,135]}. The ^{13}C NMR chemical shifts of auranofin resonances and of various other species are given in Table 4.29, while the changes in ^{13}C chemical shifts of Tu resonances are explained in Table 4.30.

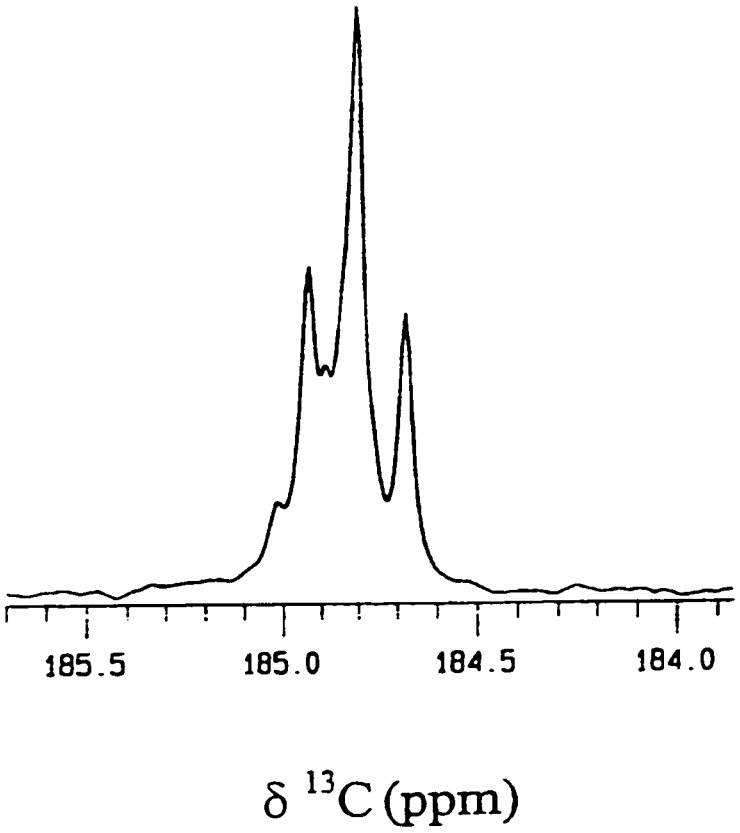

Figure 4.25 The 125.65 MHz $^{13}C\{^1H\}$ NMR spectrum of 0.20 M Thiourea (5 % ^{13}C and ^{15}N labeled) in methanol-d_4

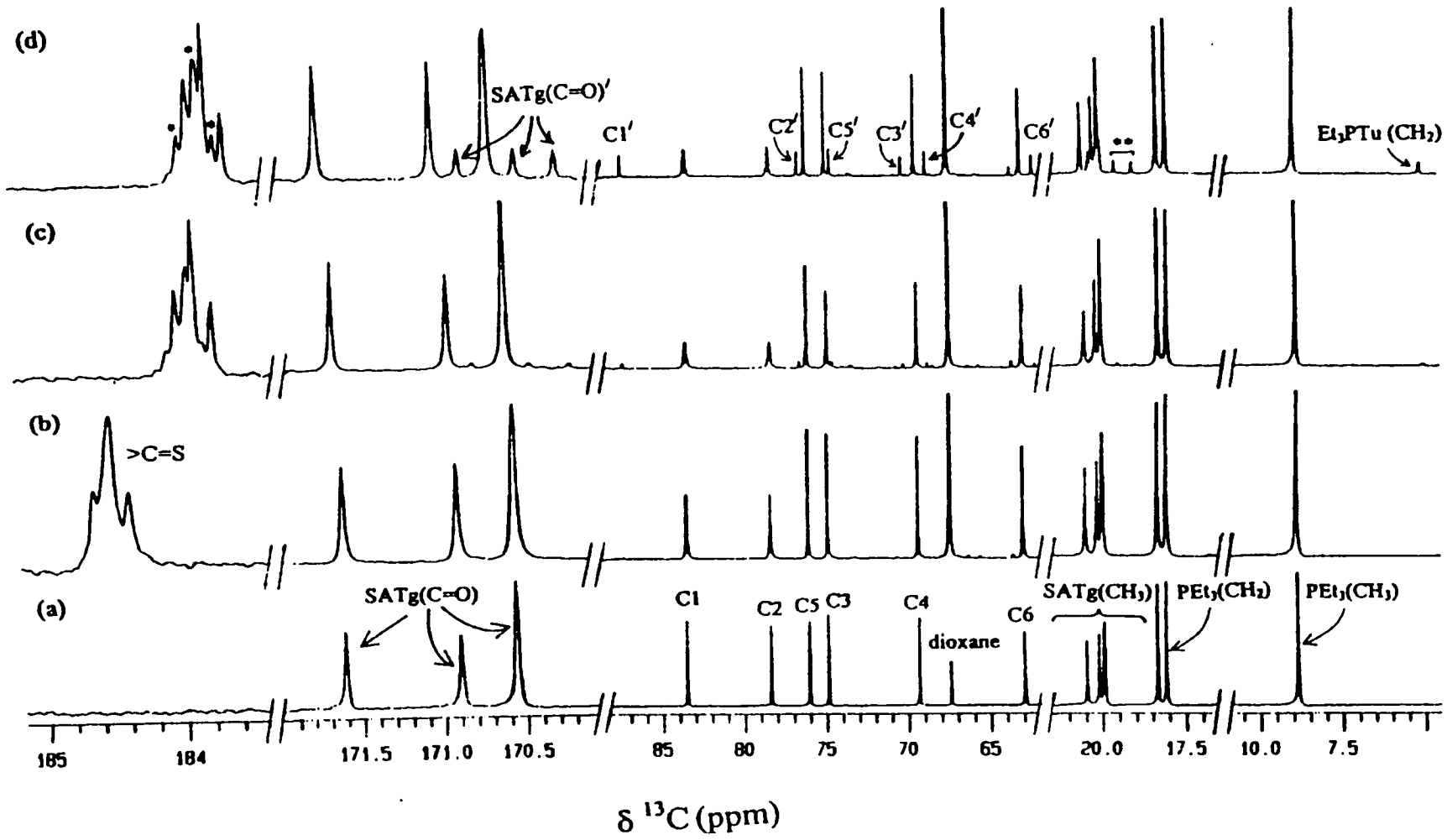

Figure 4.26 The 125.65 MHz $^{13}C\{^{1}H\}$ NMR spectrum of 0.20 M auranofin:thiourea at various molar ratios in methanol, (a) 1:0, (b) 1:0.5, (c) 1:1, (d) 1:2. Resonances with C′ are for $(SATg)_2$. *>C=S resonances of Tu due to isotopic shifts [157] **Resonances for CH_2 of $(CH_3CH_2)_3PO$.

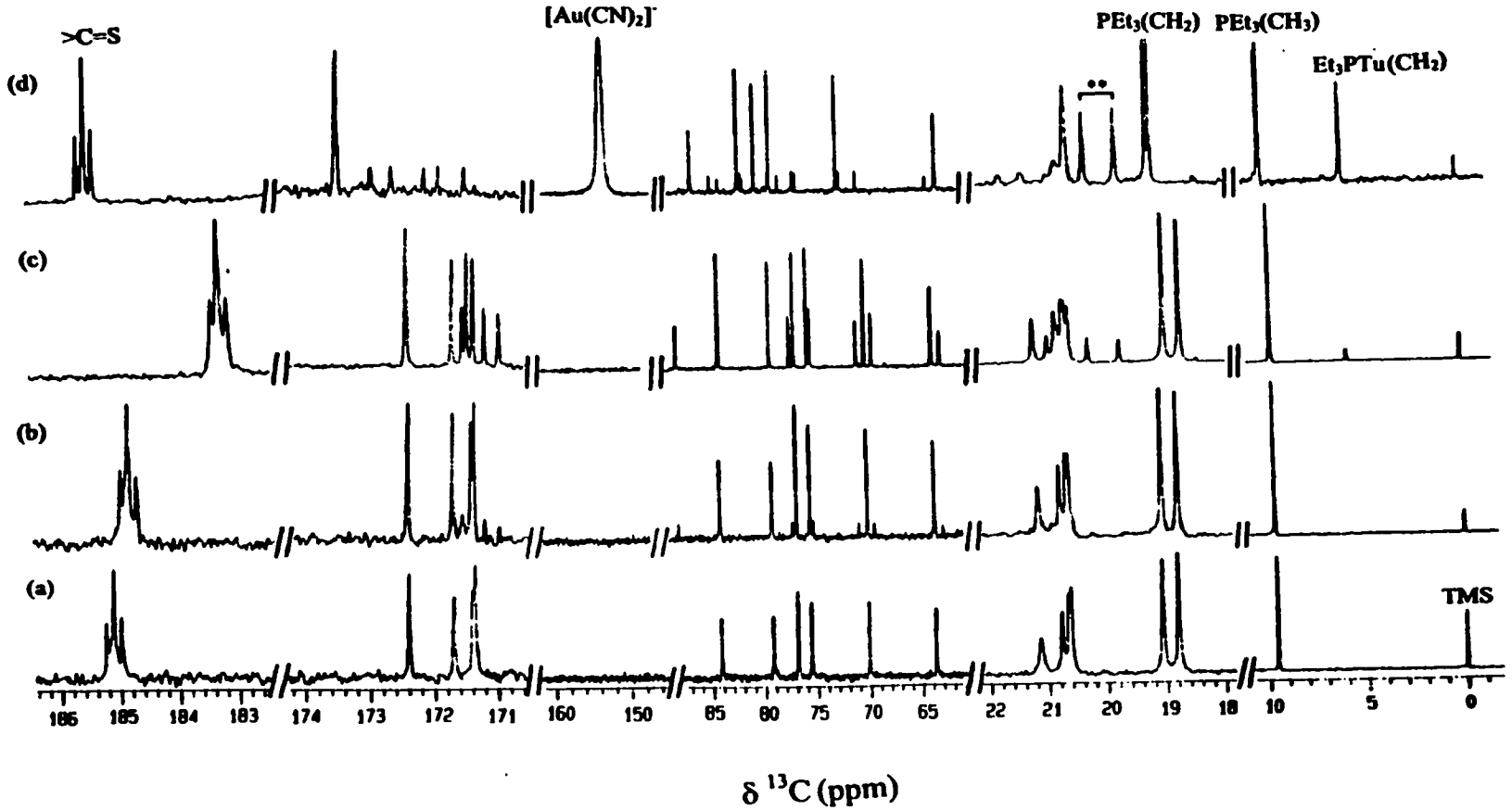

Figure 4.27 The 125.65 MHz $^{13}C\{^1H\}$ NMR spectrum of 0.05 M auranofin:0.05 M thiourea in methanol, at various time intervals (a) after 2 hrs, (b) after 115 hrs, (c) after 1 month, (d) after addition of 0.10 M KCN. The assignment in Figs. (a)-(c) is same as in Fig. 4.26. In Fig. d, the intense resonances represent the average resonances of $(SATg)_2$ and $SATg^-$, while the weaker ones are for $[Au(SATg)_2]^-$ and $[ATgS\text{-}AuCN]^-$ species. $PEt_3(CH_2)$ are resonances for free PEt_3. **Resonances for CH_2 of $(CH_3CH_2)_3PO$.

Upon further addition of 1.0 equivalent of Tu (1:2 ratio), $(SATg)_2$ resonances became more intense. The Tu resonance split into a multiplet instead of a triplet (Figure 4.26d) due to the isotopic effect (as it is observed in deuterated solvents) [164]. A doublet was observed at 20 ppm, which could be due to CH_2 of Et_3PO since it is becoming more intense with time as more Et_3PO is formed. Also, another doublet appeared at 5.7 ppm (Figure 4.26d).

In a separate experiment using 0.05 M auranofin and an equivalent amount of Tu, $(SATg)_2$ resonances appeared after 115 hours of mixing these solutions, and with the passage of time these resonances became more intense (Figure 4.27, a-c).

The addition of 2.0 equivalent of CN^- to auranofin:Tu (1:1) solution, caused several changes in the ^{13}C NMR. Figure 4.27d shows the ^{13}C NMR after addition of CN^-. The broad resonance at 152.58 is characteristic of $[Au(CN)_2]^-$ [35,165]. Some $SATg^-$ resonances became more intense. The CH_2 and CH_3 resonances of Et_3P of auranofin disappeared while those of free Et_3P appeared in the spectrum. Tu released from Au(I) and appeared as free Tu.

4.10.2.3 ^{15}N NMR Studies

In ^{15}N spectrum of Tu, a multiplet at 103.65 ppm was observed instead of a doublet probably due to isotopic effects [164], indicating the presence of various species (although it was a clear doublet in D_2O). When 0.50 equivalent of Tu was added to 0.20 M auranofin this resonance shifted downfield by 1.1 ppm. The next 0.50 equivalent addition of Tu caused a further downfield shift of 0.4 ppm. At a 1:2 ratio of thiourea to auranofin, the Tu resonance shifted upfield, indicating an exchange between free and

bound Tu. The changes in ^{15}N resonaces of Tu on its interaction with auranofin are explained in Table 4.30.

4.10.3 Interaction of Thiourea with Et_3P

The observation of an unusual resonance at 1.0 ppm in ^{31}P NMR spectrum of auranofin prompted us to examine the direct reaction of Et_3P with thiourea. The ^{31}P NMR spectrum of Et_3P solution in methanol was recorded and a free Et_3P resonance was observed at -18.60 ppm. Then thiourea (50 % ^{13}C and ^{15}N labeled) was added in excess to the Et_3P solution. The ^{31}P NMR spectrum of the resulting solution confirmed the resonance at 1.0 ppm. The ^{13}C NMR of this solution also confirmed that the doublet at 5.7 ppm was due to this reaction. The species formed by the reaction of Et_3P with thiourea could be only $Et_3P{=}SC(NH_2)_2$ since no splitting due to the coupling of 'P' with thiourea 'N' was observed in the ^{31}P NMR excluding the formation of $Et_3P(NH_2)_2CS$ species through the binding of Et_3P to NH_2 of thiourea.

4.10.4 Interaction of Thiourea with Et_3PAuCl

4.10.4.1 ^{31}P NMR Studies

Figure 4.28a shows the ^{31}P NMR spectrum of 0.20 M solution of Et_3PAuCl in methanol showing a single resonance at 32.81 ppm. When 0.25 equivalent of Tu was added as a solid, the above peak broadened and shifted downfield by 1.0 ppm. Also a resonance due to $(Et_3P)_2Au^+$ [32,166] was observed at 46.2 ppm (Figure 4.28b).

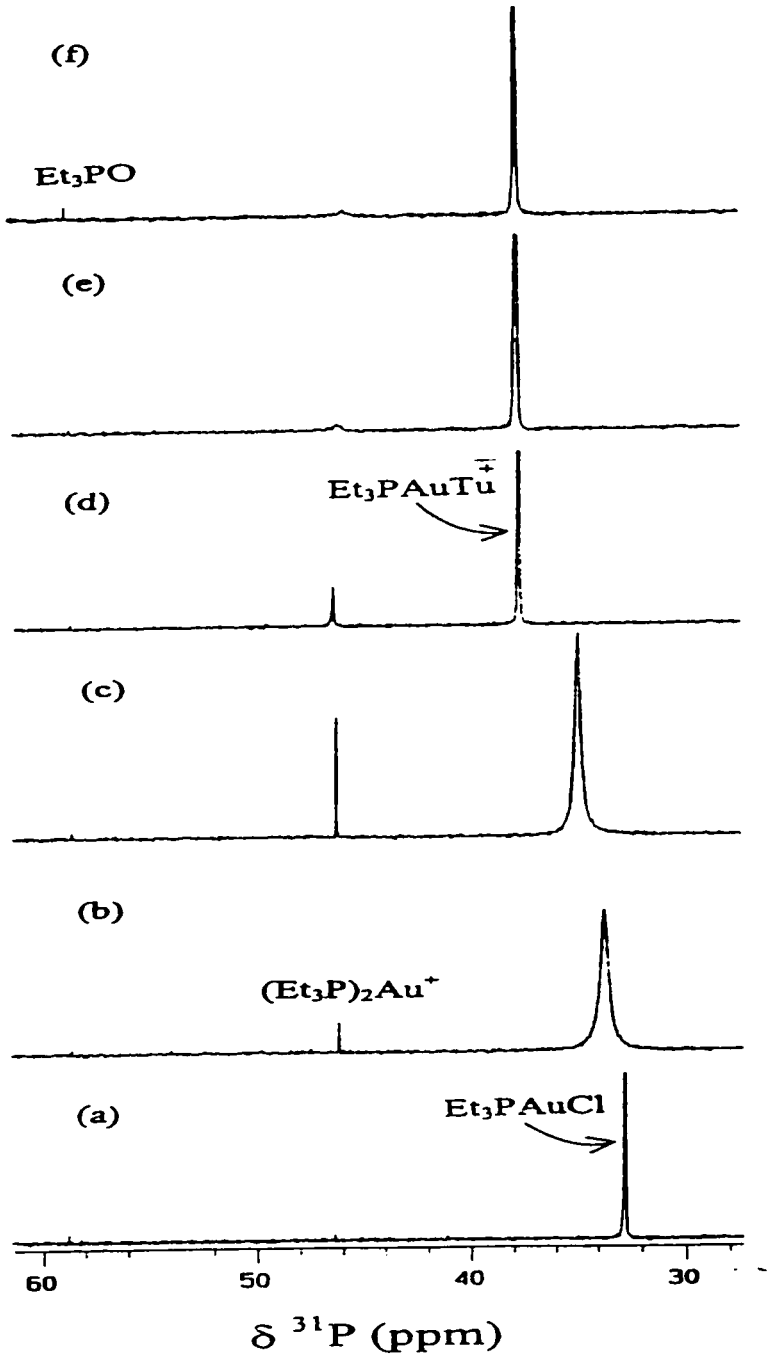

Figure 4.28 The 202.35 MHz $^{31}P\{^{1}H\}$ NMR spectrum of Et_3PAuCl:thiourea at various molar ratios in methanol, (a) 1:0, (b) 1:0.25, (c) 1:0.5, (d) 1:1, (e) 1:1.5 (f) 1:2

On addition of 0.50 equivalent of Tu, this peak became more intense while the one due to Et_3PAuCl became less intense and shifted further downfield by 1.0 ppm (Figure 4.28c). At a ratio of 1:1 the Et_3PAuCl resonance shifted further downfield by 2.7 ppm, indicating the formation of $[Et_3PAuTu]^+$, while the resonance at 46.2 ppm decreased in intensity (Figure 4.28d). Further two additions, each of 0.50 equivalent, caused the growth of the resonance around 37 ppm and the resonance at 46.2 ppm became very weak. The Et_3PO was only observed at a ratio of 2:1 of Tu to Et_3PAuCl [107,120] (Figure 4.28 e & f). The ^{31}P NMR chemical shifts of various species observed during the experiment are given in Table 4.28.

4.10.4.2 ^{13}C NMR Studies

Figure 4.29a shows the ^{13}C NMR spectrum of 0.20 M solution of Et_3PAuCl in methanol. Two prominent peaks due to CH_3 and CH_2 carbons of Et_3P were observed. Upon addition of 0.25 equivalent of Tu to 0.20 M Et_3PAuCl solution an upfield shift of 6.6 ppm was observed in >C=S resonance of Tu, while no shift in Et_3PAuCl resonances was observed (Figure 4.29b). When 0.50 equivalent of Tu was added, the solution remained colorless and almost all the resonances remained unshifted (Figure 4.29c). At a ratio of 1:1 the Et_3PAuCl resonance shifted slightly upfield (Figure 4.29d). Upon addition of 1.5 and 2.0 equivalents of Tu to Et_3PAuCl, the Tu resonance shifted downfield towards the free position due to an exchange between free and bound Tu (Figure 4.29, e & f). Observed ^{13}C chemical shifts of various resonances are given in Table 4.29.

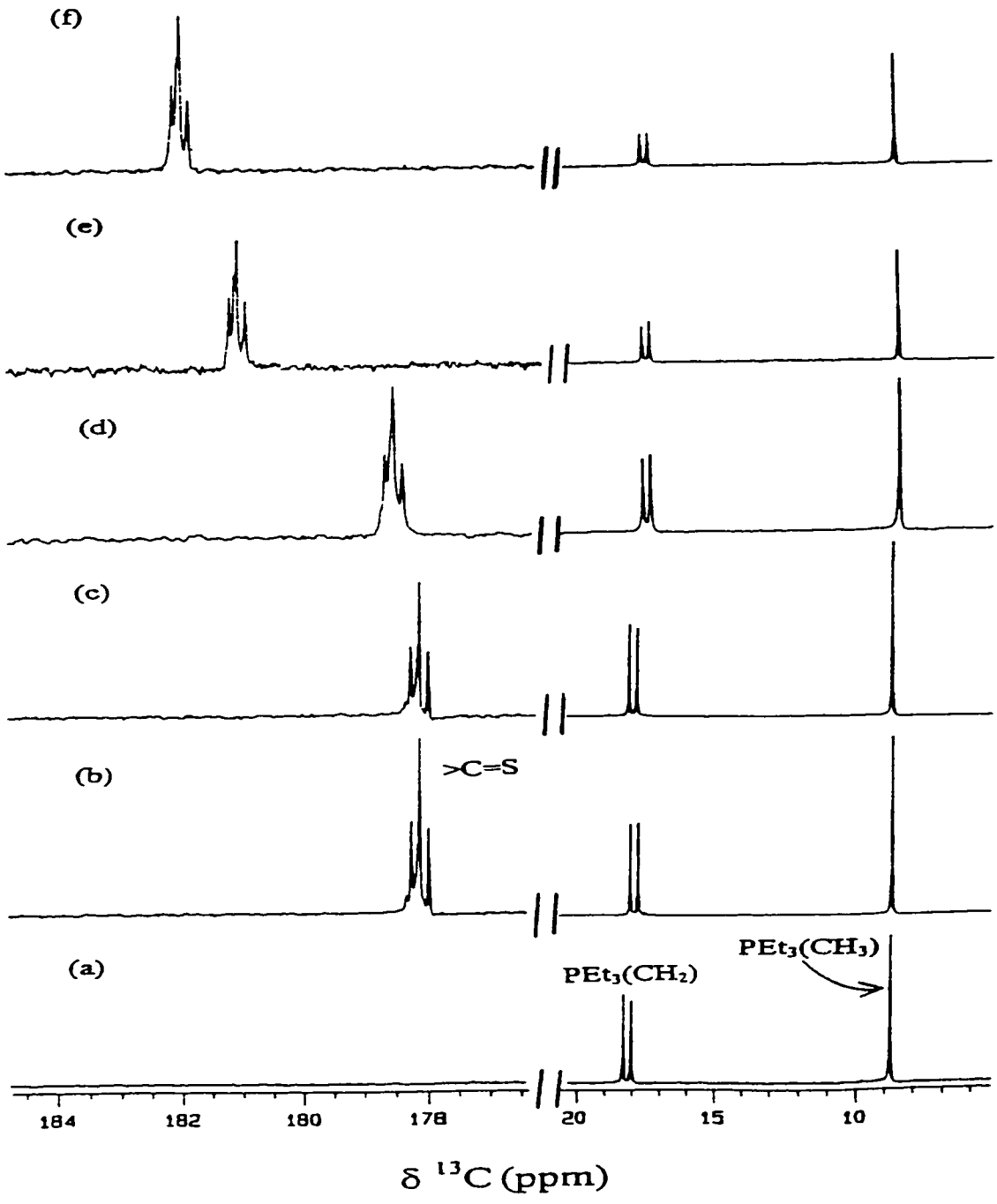

Figure 4.29 The 125.65 MHz $^{13}C\{^{1}H\}$ NMR spectrum of Et_3PAuCl:thiourea at various molar ratios in methanol, (a) 1:0, (b) 1:0.25, (c) 1:0.5, (d) 1:1, (e) 1:1.5, (f) 1:2.

4.10.4.3 ^{15}N NMR Studies

When 0.5 equivalent of Tu was added to Et_3PAuCl, a significant downfield shift of 6.0 ppm was observed in the ^{15}N resonance of Tu but the intensity of this resonance was very low. At 1:1 ratio of Et_3PAuCl and Tu, this resonance shifted a little upfield and became more prominent. On the next two additions of 0.50 equivalent of Tu, this resonance shifted further upfield by 2.0 ppm towards the free Tu position indicating an exchange between free and bound Tu. Changes in ^{15}N resonaces of Tu on its interaction with Et_3PAuCl are explained in Table 4.30.

Table 4.28 Observed ^{31}P NMR chemical shifts (in ppm) of various resonances in methanol

Species	$\delta\ ^{31}P$	Reference
Auranofin	37.74	120, This work
Et_3PAuCl	32.81	167, This work
$[Et_3PAuTu]^+$	37.75	This work
$(Et_3P)_2Au^+$	46.40	32,166
Et_3Ptu	1.03	This work
Et_3PO	58.40	107,120
Et_3P	-18.6	This work

Table 4.29 Observed ^{13}C NMR chemical shifts in ppm of various species in methanol

	Thioglucose								**PEt_3**	
	Ring carbons						*Acetate carbons*		*CH_3*	*CH_2*
	C_1	C_2	C_3	C_4	C_5	C_6	C=O	CH_3		
Auranofin	84.20	79.05	75.57	70.04	76.70	63.67	171.20, 171.23, 171.60, 172.32	20.63, 20.66, 20.80, 21.16	8.85	18.78, 19.04
$SATg^-$	79.30	77.10	75.03	69.70	75.12	63.32	171.22, 171.24, 171.56, 172.34	20.54, 20.61, 20.67		
$(SATg)_2$	88.00	77.22	70.87	69.41	75.25	62.88	170.95, 171.18, 171.54, 172.42	20.53, 20.61, 20.87		
$[AtgSAuCN]^-$	83.00	78.37	75.69	70.16	75.72	63.62	171.42, 171.65, 171.83, 172.68	20.60, 20.63, 20.79, 21.22		
Tu-Au-SATg	85.12	77.34	69.89	68.96	74.35	62.64	171.11, 171.14, 171.36, 172.10	20.42, 20.44, 20.47, 20.57		
Et_3PAuCl									9.53	18.75, 19.06
Et_3PAuTu	>C=S, 179.30								9.43	18.29, 18.57
Et_3PTu	>C=S, 162.77								9.56	5.67, 5.70
Et_3PO									9.87	19.70, 20.23
Et_3P									9.77	19.11, 19.17

Table 4.30 ^{13}C and ^{15}N NMR chemical shift changes (ppm) of Tu resonance on its addition to auranofin and Et_3PAuCl at various molar ratios

Molar Ratio	**Auranofin:Tu**			**Et_3PAuCl:Tu**		
	$\delta\ ^{13}C$	$\delta\ ^{15}N$	$^{1}J_{C\text{-}N\ (Hz)}$	$\delta\ ^{13}C$	$\delta\ ^{15}N$	$^{1}J_{C\text{-}N\ (Hz)}$
0:1	185.54	103.65	15.7	185.54	103.65	15.7
2:1	185.21	104.74	16.5	178.87	109.34	17.6
1:1	184.57	105.07	16.0	179.31	108.82	17.6
1:1.5	-	-	-	181.81	106.96	17.0
1:2	184.42	104.69	16.0	182.72	106.11	16.5

4.11 Comparative ^{13}C and ^{31}P NMR Studies of the Ligand Exchange Reactions of Auranofin with Ergothionine, Imidazolidine-2-thione and Diazinane-2-thione

4.11.1 ^{31}P NMR Studies

Figure 4.30a shows the ^{31}P NMR spectrum of 0.05 M auranofin in methanol-D_2O (75:25 v/v). One resonance at 38.34 ppm is for Et_3P of auranofin [107,120] and the other at 46.8 ppm is due to $(Et_3P)_2Au^+$ [32,164]. The $(Et_3P)_2Au^+$ resonance originated because of the facile transfer of Et_3P in hydrophobic environment [5] and with the passage of time this disappeared. When 1.0 equivalent of ergothionine (ErS) was added to auranofin solution, no change in the ^{31}P NMR spectrum was observed until 10 days. After 10 days an additional resonance appeared in the spectrum at 61.5 ppm due to Et_3PO [107,120] (Figure 4.30c). After 3 weeks, another resonance appeared at 1.3 ppm, which is assigned to Et_3P-ErS species, formed by the reaction of ErS with the liberated Et_3P (Figure 4.30e) as observed in the interaction of auranofin with thiourea. These resonances increased in intensity with time and after two months they were approximately 5 times more intense (Figure 4.30f). Such type of resonance was not observed in the interaction of auranofin with thiols [135].

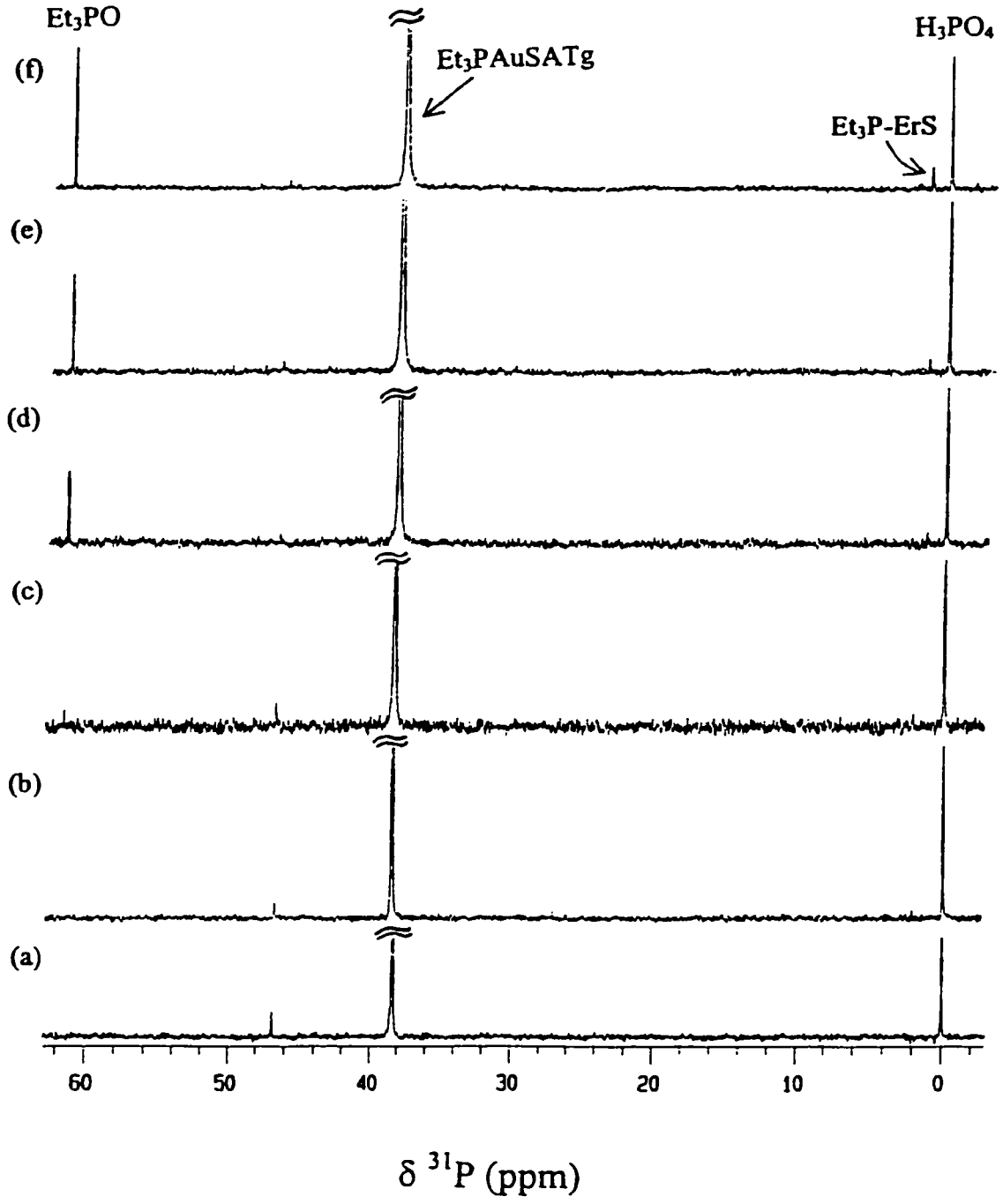

Figure 4.30 The 202.35 MHz $^{31}P\{^{1}H\}$ NMR spectrum of 0.05 M auranofin:0.05 M ergothionine in methanol-D_2O (75:25v/v) at various time intervals (a) 0.05 M auranofin (b) after 30 minutes of addition, (c) after 10 days, (d) after 3 weeks (e) after 1 month, (f) after 2 months.

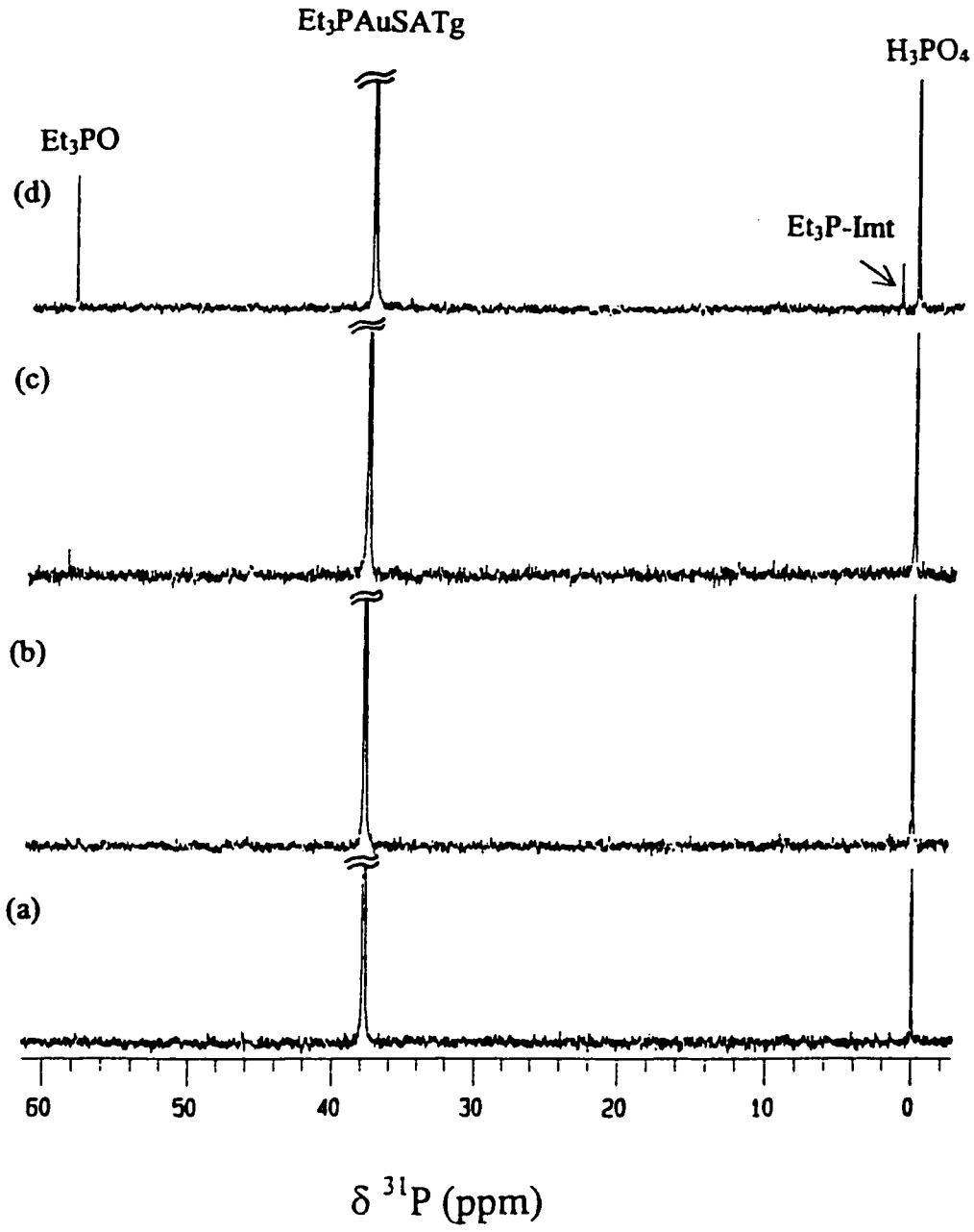

Figure 4.31 The 202.35 MHz $^{31}P\{^{1}H\}$ NMR spectrum of 0.05 M auranofin:0.05 M imidazolidine-2-thione in methanol at various time intervals (a) 0.05 M auranofin (b) after 30 minutes of addition, (c) after 19 days, (d) after 2 months.

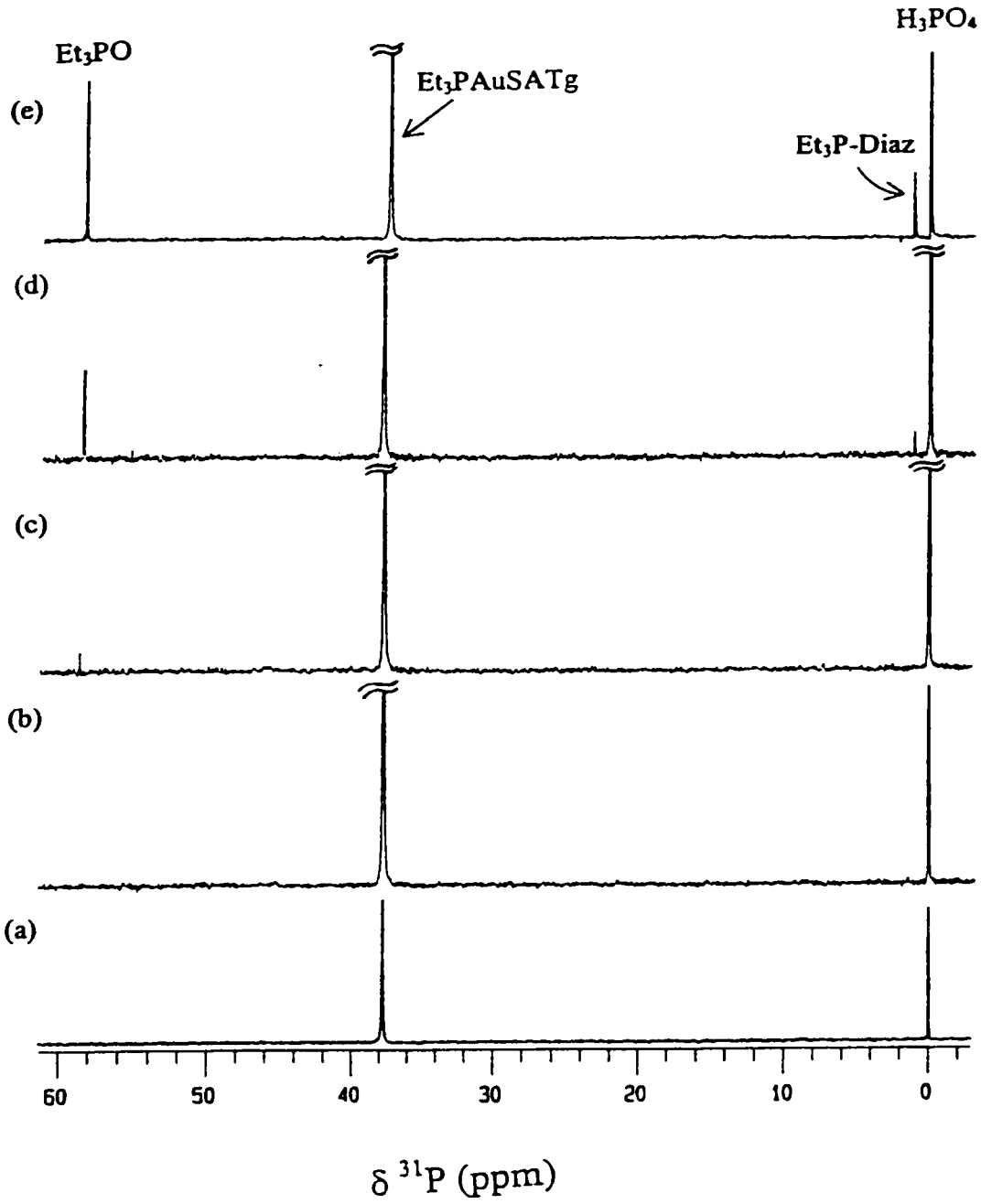

Figure 4.32 The 202.35 MHz $^{31}P\{^{1}H\}$ NMR spectrum of 0.05 M auranofin:0.05 M diazinane-2-thione in methanol at various time intervals (a) 0.05 M auranofin (b) after 30 minutes of addition, (c) after 6 days, (d) after 15 days (e) after 2 months.

In the interaction of Imt with auranofin the Et_3PO resonance appeared in ^{31}P NMR after about 19 days of mixing the two solutions (Figure 4.31 a-c). In the case of Diaz this was observed after 6 days (Figure 4.32a-c), while the resonance for >C=S-PEt_3 appeared after 2 weeks. After 2 months, the Et_3PO and Et_3P-Imt/Diaz resonances at 58.40 ppm [107] and 1.10 ppm respectively, became prominent (Figure 4.31d & 4.32d-e).

In all three cases the auranofin resonance in ^{31}P NMR shifted slightly upfield and broadened due to an exchange of Et_3P between auranofin and other species. The chemical shifts of various resonances are explained in Table 4.31.

4.11.2 ^{13}C NMR Studies

Figure 4.33a shows the ^{13}C NMR spectrum of 0.05 M auranofin and Figure 4.33b that of 0.05 M ErS in methanol-D_2O (75:25 v/v). The chemical shifts of all the resonances are consistent with those reported in the literature [143,162,163].

When 1.0 equivalent of ErS was added to 0.05 M auranofin, the solution remained colorless and in ^{13}C NMR recorded after 2.5 hours, no change in the auranofin spectrum was observed except the appearance of ErS resonances (Figure 4.33c). No change in the ^{13}C NMR spectrum was observed for 10 days. After that some resonances originated in the auranofin spectrum showing the start of reaction. After 3 weeks two sets of additional resonances were observed along with auranofin resonances. One set of resonances was assigned to $(SATg)_2$, which is formed by the oxidation of $SATg^-$ released [120,135]. $(SATg)_2$ resonances were assigned after reacting $SATg^-$ separately with an oxidizing agent, *m*-chloroperbenzoic acid. The other type of resonances were assigned to ErS-Au-SATg complex, since this could be the only possible species of $SATg^-$ when free $SATg^-$

resonances were not observed (Table 4.32). ErS resonances remained unshifted, except for the >C=S resonance which shifted upfield by 1.4 ppm. With the passage of time the ErS-Au-SATg and $(SATg)_2$ resonances became more intense (Figure 4.33 e & f).

Figure 4.34a shows the ^{13}C NMR spectrum of 0.05 M auranofin and Figure 4.34b that of 0.05 M Imt in methanol. Upon addition of 1.0 equivalent of Imt to auranofin solution no change in the spectrum was observed for 19 days. After 19 days some additional resonances appeared in the ^{13}C NMR (Figure 4.34c). After two months separate resonances for Imt-Au-SATg and $(SATg)_2$ were clearly observed in the ^{13}C NMR (Figure 4.34d). The >C=S resonance of Imt shifted upfield by 1.3 ppm.

Figure 4.35 shows the results of the interaction of auranofin with Diaz. The additional resonances for $(SATg)_2$ were observed after 6 days of addition of Diaz to auranofin, while Diaz-Au-SATg resonances started appearing after 15 days. After two months these resonances were more intense as compared to those observed in the other two cases.

A doublet around 5.7 ppm was observed in the ^{13}C NMR for all three cases due to CH_2 of Et_3P, which was assigned to a >C=S-PEt_3 species, formed by the reaction of Et_3P with thiones, ErS, Imt and Diaz. This resonance was detected for the first time in the interaction of auranofin with Tu and was assigned to $Et_3PS{=}C(NH_2)_2$ species after an independent reaction of Et_3P with Tu (Figure 4.33f, 4.34e & 4.35f).

Carbon-13 chemical shifts of various resonances observed in the interaction of auranofin with various thiones are explained in Table 4.32.

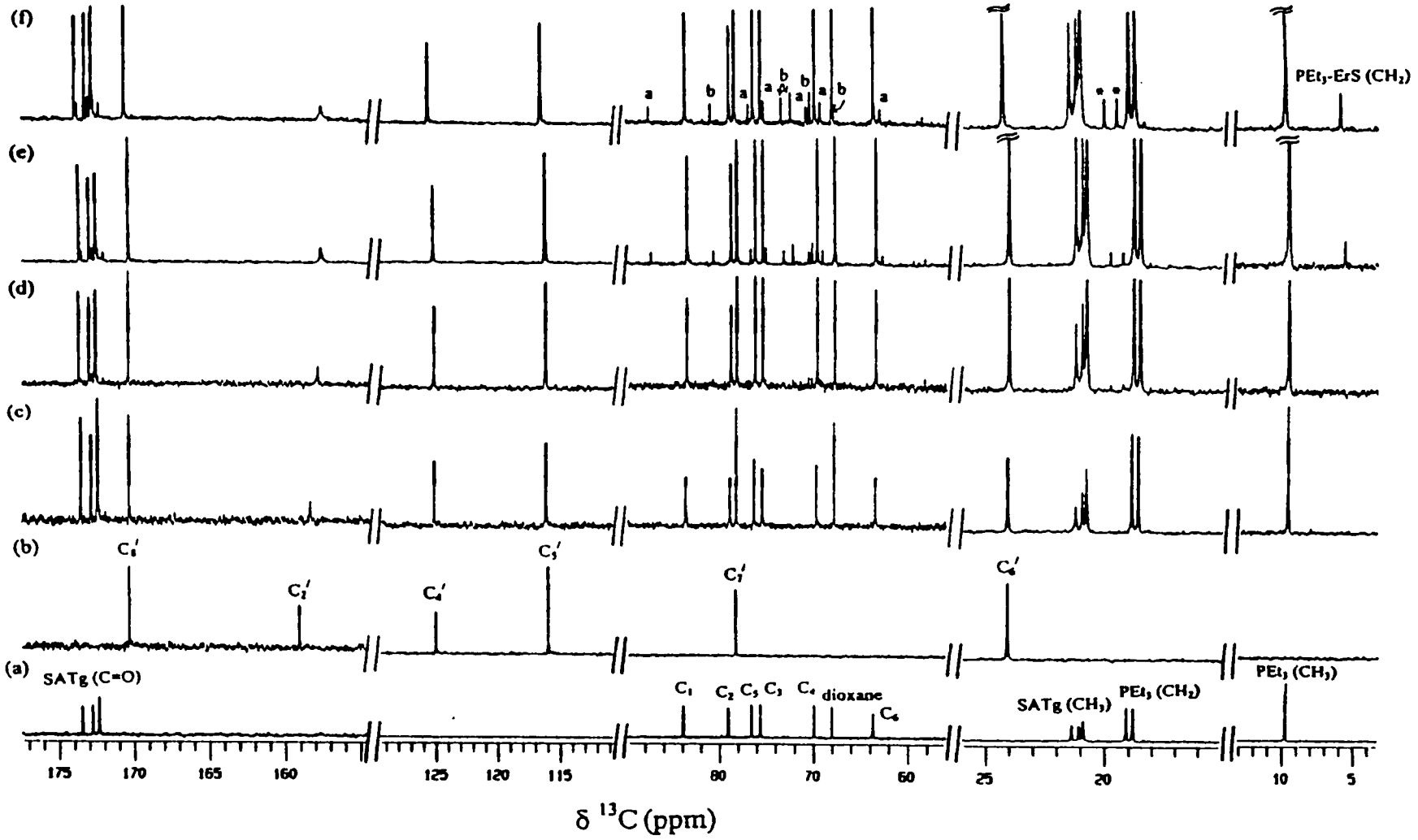

Figure 4.33 The 125.65 MHz $^{13}C\{^{1}H\}$ NMR spectrum of 0.05 M auranofin:0.05 M ergothionine in methanol-D_2O (75:25v/v) at various time intervals (a) 0.05 M auranofin (b) 0.05 M ergothionine (c) after 2.5 hrs, (d) after 10 days, (e) after 1 month, (f) after 2 months. [a]Resonances for $(SATg)_2$, [b]Resonances for ErS-Au-SATg complex. *Resonances for $(CH_3CH_2)_3PO$.

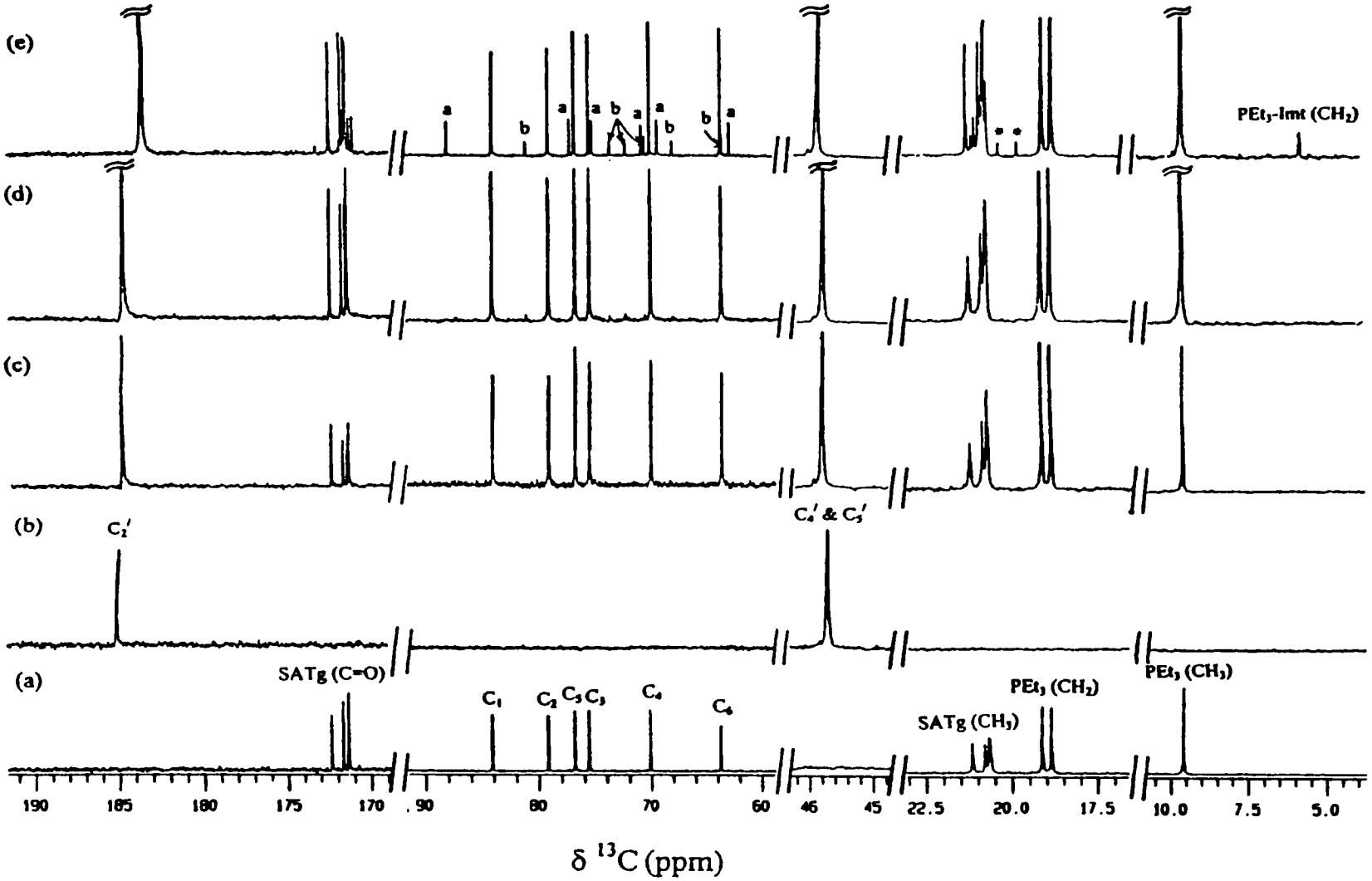

Figure 4.34 The 125.65 MHz $^{13}C\{^{1}H\}$ NMR spectrum of 0.05 M auranofin:0.05 M imidazolidine-2-thione in methanol at various time intervals (a) 0.05 M auranofin (b) 0.05 M imidazolidine-2-thione (c) after 2.5 hrs of addition, (d) after 19 days, (e) after 2 months. [a]Resonances for $(SATg)_2$, [b]Resonances for Imt-Au-SATg complex. *Resonances for $(CH_3CH_2)_3PO$.

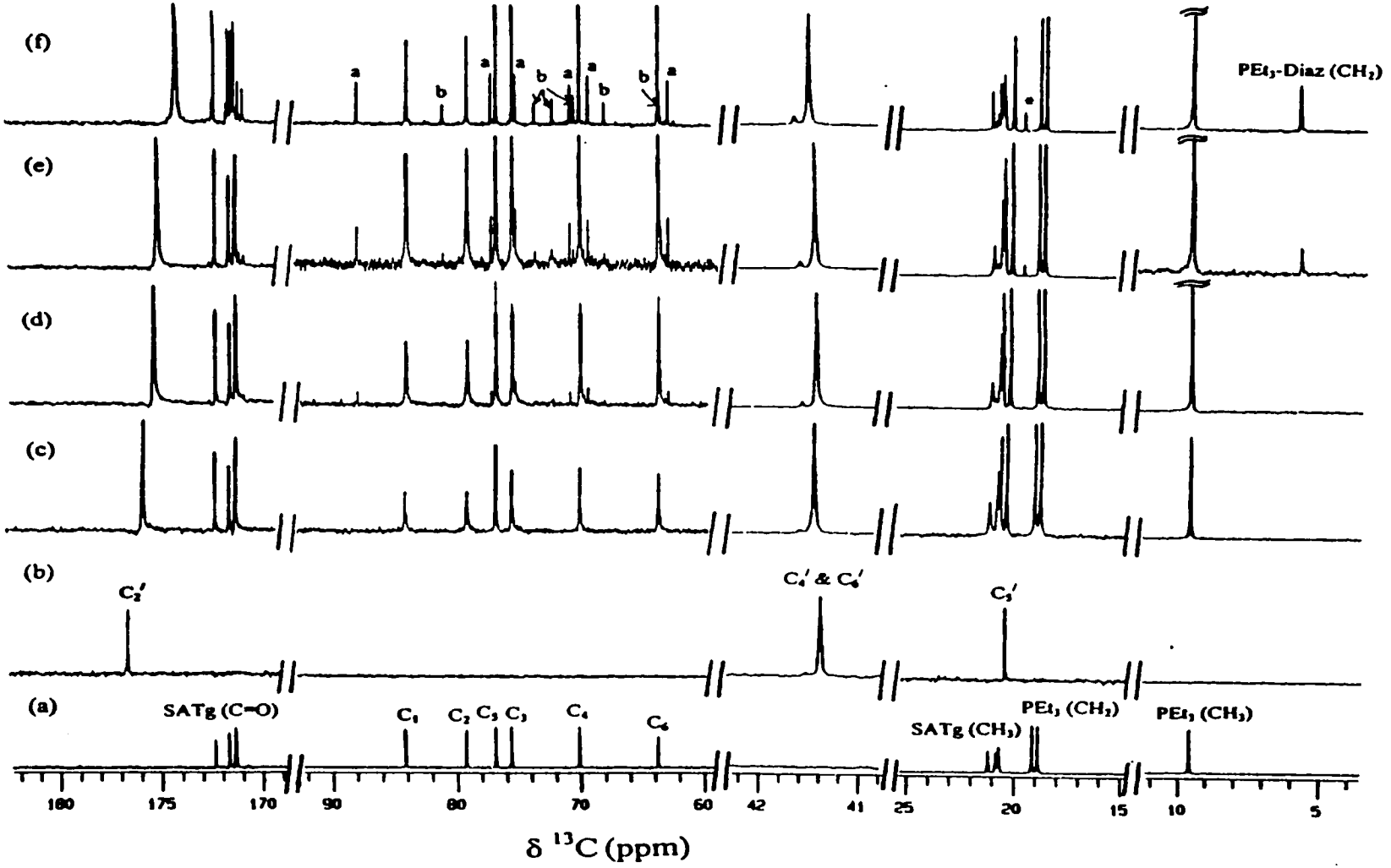

Figure 4.35 The 125.65 MHz $^{13}C\{^{1}H\}$ NMR spectrum of 0.05 M auranofin:0.05 M diazinane-2-thione in methanol at various time intervals (a) 0.05 M auranofin (b) 0.05 M diazinane-2-thione (c) after 2.5 hrs, (d) after 6 days, (e) after 15 days, (f) after 2 months. [a]Resonances for $(SATg)_2$, [b]Resonances for Diaz-Au-SATg complex. *Resonances for $(CH_3CH_2)_3PO$.

Table 4.31 ^{31}P NMR chemical shifts of various resonances observed in the interaction of auranofin with thiones in methanol

Species	$\delta\ ^{31}P$	Reference
Auranofin	37.74	107,120
	38.34*	This work
Et_3PO	58.35	107,120
	61.50*	This work
Et_3P-ErS	1.30*	This work
Et_3P-Imt	1.10	This work
Et_3P-Diaz	1.10	This work

*In methanol-water (75:25 v/v)

Table 4.32 ^{13}C NMR chemical shifts of various species in methanol

Species	Thioglucose								PEt$_3$	
	Ring carbons						*Acetate carbons*		*CH$_3$*	*CH$_2$*
	C_1	C_2	C_3	C_4	C_5	C_6	C=O	CH_3		
Auranofin	84.20	79.05	75.57	70.04	76.70	63.67	171.20, 171.23, 171.60, 172.32	20.63, 20.66, 20.80, 21.16	8.85	18.78, 19.04
	*83.81	78.98	75.53	69.82	76.46	63.55	172.20, 172.24, 172.65, 173.35	20.74, 20.76, 20.92, 21.22	9.61	18.66, 18.94
SATg$^-$	79.30	77.10	75.03	69.70	75.12	63.32	171.22, 171.24, 171.56, 172.34	20.54, 20.61, 20.67		
$(SATg)_2$	88.00	77.22	70.87	69.41	75.25	62.88	170.95, 171.18, 171.54, 172.42	20.53, 20.61, 20.87		
ErSAuSATg	81.09	73.51	70.48	68.17	72.53	63.72	173.04, 173.07, 173.26, 173.77	20.99, 21.10, 21.44		
ImtAuSATg	81.11	73.74	70.58	68.08	72.34	63.59	171.43, 171.70, 171.78, 172.39	20.56, 20.74, 21.00		
DiazAuSATg	81.09	73.77	70.59	68.08	72.31	63.61	171.45, 171.73, 171.81, 172.43	20.57, 20.71, 21.02		
ErS*	C_2 159.14, C_4 125.05, C_5 116.04, C_6 24.12, C_7 78.37, C_8 170.38, N-CH_3 53.11									
Imt	C_2 185.14, C_4 & C_5 45.71									
Diaz	C_2 176.69, C_4 & C_6 41.38, C_5 20.38									

*In methanol-water (75:25 v/v)

CHAPTER 5

DISCUSSION

5.1 Characterization of Gold(I) Complexes of Thiourea and Selenourea

The ambidentate ligand, thiourea $\{SC(NH_2)_2\}$ is potentially capable of bonding via the sulfur or the nitrogen atom. There are three major IR bands that are generally diagnostic of the particular binding mode of thiourea to metals. These include ν(C=S), ν(CN) and $\nu(NH_2)$. Upon coordination of thiourea to a metal via the sulfur atom, the carbon-sulfur double bond character is reduced and that of carbon-nitrogen single bond is increased. As a result, a decrease in ν(C=S) with a concomitant increase in ν(CN) and $\nu(NH_2)$ is expected. The opposite would be true if thiourea were coordinated via the nitrogen. A low frequency shift of the ν(C=S/Se) absorption and a high frequency shift of the band around 3200 cm^{-1} in the gold(I) complexes indicates the existence of thione/selenone forms of the lignads (Tu or Seu) in the solid state.

A downfield shift in ^{31}P resonance of the phosphines in $[R_3PAuTu/Seu]Cl$ complexes is related to π accepting ability of the phosphines from gold(I). The donation of electron density by Tu or Seu to gold(I) increases the back donation from gold(I) to phosphines, which would increase the double bond character of the Au-P bond resulting in a deshielding at phosphorus atom. This can also be explained by their comparison with R_3PAuCN complexes where, CN is a π acceptor with less donation of electron density to

gold(I). Therefore in the CN complexes, the ^{31}P resonance appears upfield compared to the Tu/Seu complexes [32]. The coupling constants $^{1}J(^{13}C\text{-}^{31}P)$ for $[R_3PAuSeu]Cl$ are found to be smaller than $[R_3PAuTu]Cl$ (Table 4.4). This shows that as the electron donation ability of the group trans to phosphine increases, the coupling constant is decreased.

A correlation between the basicity of phosphines and the ^{13}C chemical shift and the coupling constants (Table 4.3 & 4.4) is observed for $[R_3PAuTu]Cl$ complexes. The electronegativites of phosphines are measured in terms of the elctronic parameter, $\nu(CO)$ for the complex, $[R_3PNi(CO)_3]$ [150]. The $\nu(CO)$ values of the phosphines are compared in Table 4.3. A decrease in $\nu(CO)$ is associated with a decrease in electronegativity or an increase in basicity of the phosphine. With an increase in the electronegativity of the phosphine, the shift in δ ^{13}C also increases. A similar observation is made for the coupling constants, $^{1}J(^{13}C\text{-}^{31}P)$. This shows that Au-S bond becomes stronger as the electronegativity of the phosphine increases. Thus, Au-S bond would be strongest when R_3P is PPh_3 while, it would be weakest for Cy_3P complex. This observation can also be verified by ^{15}N NMR, where there is a greater shift for more electronegative PPh_3 ligand compared to less electronegative Cy_3P. A downfield shift in ^{15}N resonance in all complexes demonstrates that the nitrogen of Tu is not involved in bonding to gold(I) since metal binding through N should cause an upfield shift in ^{15}N resonance of Tu.

Crystal structure of one of these complexes, $[Ph_3P\text{-}Au\text{-}Seu]Cl$ has been reported in the literature [35], which shows that the compound is linear and two coordinate in the solid state. Therefore, it is expected that all these complexes would possess a linear geometry in the solid state.

In solution, whether these complexes remain as two coordinate or possess a trigonal structure can be established by their conductivity measurements. The molar conductance for two representative complexes ([Me_3PAuTu]Cl & [$Me_3PAuSeu$]Cl) was measured in methanol. A comparison with the conductance of the known coordination compounds [167] was made and it was proved that the solution consists of two ionic species. The molar conductances of the above mentioned complexes and some known coordination compounds are given in Table 5.1.

Table 5.1 Molar conductances and number of ions in solution for some complexes

Complex	Molar conductance[b]	No. of ions in solution
[Me_3PAuTu]Cl	95.7	2
[$Me_3PAuSeu$]Cl	85.1	2
[Me_3PAuCl]	1.8	0
NH_4NO_3	86.5	2
$[Pt(NH_3)Cl_3]Cl$[a]	96.8	2
$[Pt(NH_3)_2Cl_2]$[a]	4.96	0

[a] Values taken from reference 167, [b] For calculation procedure, refer section 3.2.8.

5.2 Characterization of Cyanogold(I) Complexes

Crystal structures of the two of the cyano(thione)gold(I) complexes (ImtAuCN and DmTuAuCN) being studied have already been reported in the literature [118]. The complex ImtAuCN exists as a linear two coordinate species but two ImtAuCN units form a dimer. The other complex, DmTuAuCN complex exists as an ionic complex $[Au(DmTu)_2]^+[Au(CN)_2]^-$ similar to a cyano(phosphine) complex, $[Au(CEP)_2]^+[Au(CN)_2]^-$ [116,118]. These observations can be obtained from the IR spectra of the complexes as well. The IR spectra of the above mentioned two ionic complexes showed two bands for ν(CN) characteristic of $[Au(CN)_2]^-$. In the present study, only one ν(CN) band was observed for all cyano(thione)gold(I) complexes except for DmTuAuCN. Thus it is established that the complexes, which show only one CN^- stretch in IR exist as nonionic complexes (i.e., as [L-Au-CN]), while those which possess two CN^- bands exist in the form (i.e., as $[AuL_2]^+[Au(CN)_2]^-$).

In the cyano(selenone)gold(I) complexes a low frequency shift in ν(C=Se) and the presence of a band around 3200 cm^{-1} in free ligands as well as in the complexes indicates the existence of the selenone form of the ligands in the solid state. One or two bands around 2100 cm^{-1} for CN stretch are observed in IR spectra of all the complexes. For the complexes of DmSeu, ImSe, DiazSe and MeDiazSe, only one ν(CN) mode was observed which appears at lower frequency compared to AuCN. A significant shift of approx. 150 cm^{-1} also indicates the selenone binding to gold(I) cyanide. The appearance of one peak for ν(CN) indicates that these four complexes exist in the nonionic form, i.e., as DmSeuAuCN, ImSeAuCN, DiazSeAuCN and MeDiazSeAuCN respectively.

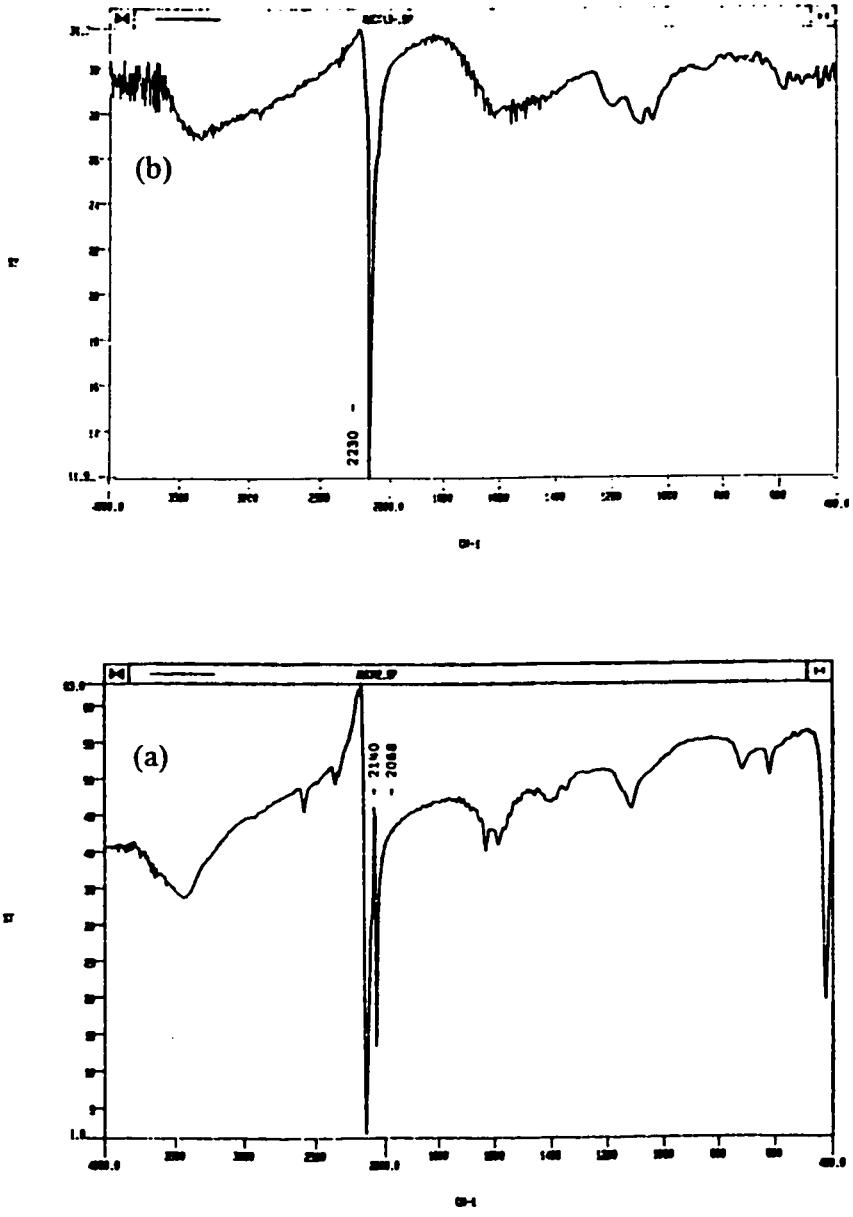

Figure 5.1 IR spectra of: (a) $K[Au(CN)_2]$ (b) AuCN

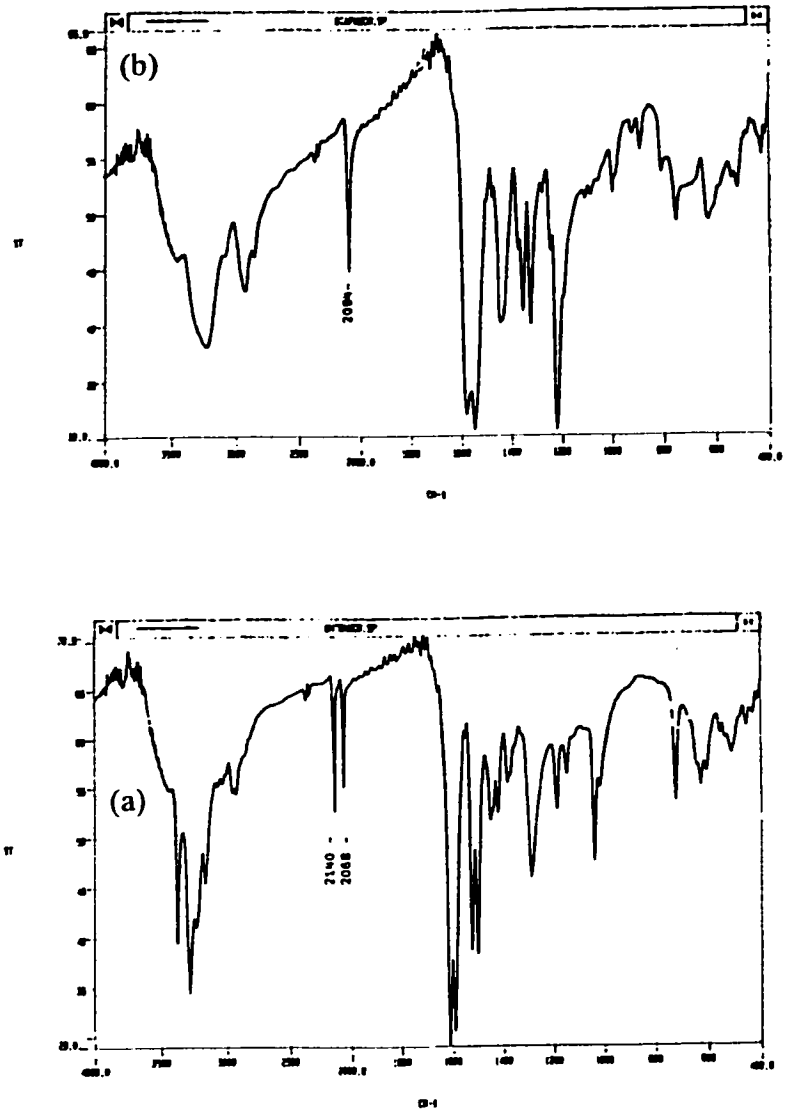

Figure 5.2 IR spectra of: (a) DmTuAuCN (existing as $[Au(DmTu)_2]^+[Au(CN)_2]^-$)

(b) DiapAuCN

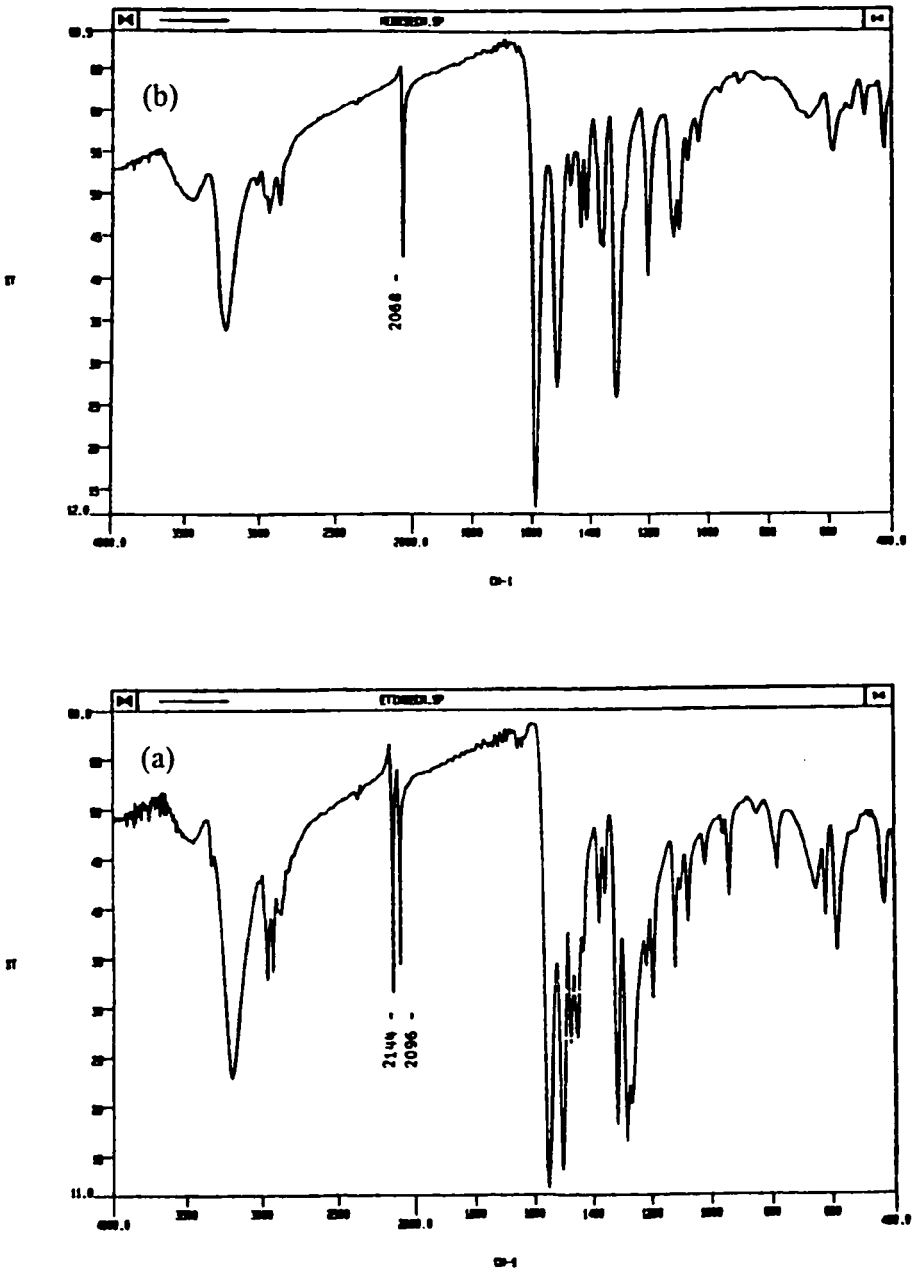

Figure 5.3 IR spectra of: (a) EtImSeAuCN (existing as $[Au(EtImSe)_2]^+[Au(CN)_2]^-$)
(b) MeDiazSeAuCN

For the rest of the complexes, two stretching bands are observed for CN (asymmetric & symmetric), which are the characteristic of $[Au(CN)_2]^-$ (NC-Au-CN bond angle in $[Au(CN)_2]^-$ is found to be less than 180°) [116,118]. Thus the appearance of two ν(CN) bands suggests that these complexes exist in the ionic form as, $[Au(>C=Se)_2]^+[Au(CN)_2]^-$ in the solid state similar to $[Au(CEP)_2]^+[Au(CN)_2]^-$ and $[Au(DmTu)_2]^+[Au(CN)_2]^-$ [116,118]. The IR spectra of [AuCN], $[Au(CN)_2]^-$ and some representative complexes are shown in Figures 5.1-5.3.

5.3 Spectroscopic Studies of the Silver(I) Complexes of (^{13}C, ^{15}N labeled) Thiourea and Selenourea

5.3.1 IR Studies

In IR spectra, a decrease in ν(C=S) is indicative of reduction in C=S bond order on sulfur coordination to silver(I) [65,154] as it is observed in other thione complexes of gold(I). The appearance of two bands for ν(C=S) clearly indicates that some Tu groups [bound to silver(I)] with the higher frequency (724 cm^{-1}) are terminal and some with the low frequency (698 cm^{-1}) are bridging. For $[TuAgNO_3]$, only the lower frequency band (698 cm^{-1}) was observed showing that complex contains all Tu groups in bridging mode. Thus the complex would have a polymeric structure through sulfur bridging. Further confirmation of its polymeric nature comes from its solubility; when dissolved in DMSO the complex gave black deposits indicating the breakage of the polymer. $[SeuAgNO_3]$ shows a similar behavior. Thus the most probable structures of the $[TuAgNO_3]$ and $[SeuAgNO_3]$ complexes would be as follows;

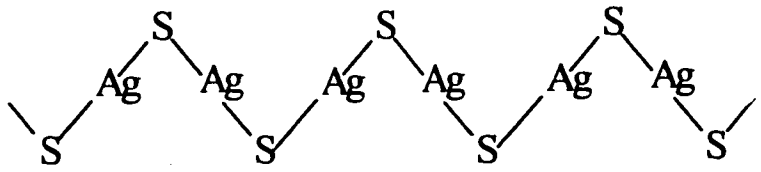

Where, S represents $S=C(NH_2)_2$

5.3.2 ^{1}H, ^{13}C, ^{15}N and ^{107}Ag NMR Studies

The upfield shift in ^{13}C NMR upon complexation of Tu to silver(I) is attributed to a lowering of the >C=S bond order upon coordination and a shift of N→C electron density producing partial double bond character in the C-N bond [85]. The upfield shift decreases as the number of Tu ligands attached to silver increases. The least upfield shift in the $[Ag(Tu)_4]NO_3$

to that in $[TuAgNO_3]$ where each Tu is sharing one Ag(I). The changes in ^{13}C NMR chemical shift are consistent with those reported for the solution studies [63]. The upfield shifts for $[TuAgNO_3]$ and $[Ag(Tu)_2]NO_3$ are of 7.0 and 4.5 ppm respectively while for analogous Seu complexes are of 12.0 and 7.0 ppm respectively. The greater shifts for Seu complexes suggests that Seu binds to silver(I) more strongly compared to Tu.

In the ^{1}H and ^{15}N NMR spectra, a downfield shift is observed on complexation. The downfield shift is consistent with an increase in double bond character of the C-N bond. There is a decrease in downfield shift as the number of Tu/Seu groups attached to silver is increasing. A smaller downfield shift, instead of a large upfield shift in ^{15}N NMR rules

out the Tu/Seu bonding to silver(I) via nitrogen. The metal binding through nitrogen should involve an upfield shift of at least 50 ppm as observed in some platinum(II) complexes [168,169]. The appearance of only one signal both in ^{13}C and ^{15}N NMR shows that all the Tu ligands in a complex are equivalent in solution and only average chemical shifts were observed. If they were nonequivalent, different chemical shifts should have been observed for the bridging and terminal Tu groups particularly for $[Ag(Tu)_2]NO_3$ and $[Ag(Tu)_3]NO_3$.

In ^{107}Ag NMR a downfield shift of 500-600 ppm indicates the complexation of Tu through sulfur. The silver chemical shifts for Seu complexes are found at approx. 100 ppm further downfield position than for Tu complexes. This may be because selenium is more polarizable compared to sulfur. This very large reduction in shielding appears to be a characteristic of silver(I) bonding to sulfur or selenium [156]. In the case bonding through nitrogen, the signal is shifted by approx. 100 ppm [156]. An increase in the downfield shift is observed as the number of ligands coordinating to silver(I) increases, however $[Ag(Tu)_2]NO_3$ shows deviation from this trend. The downfield shift is observed, because the number of electronegative groups attached to silver is increases.

The deviation shown by $[Ag(Tu)_2]NO_3$ can be explained by examining its structure. The crystal structures have been determined for 2:1 and 3:1 (Tu:Ag) complexes ($[(Ag(Tu)_2]Cl$ [170] and $[Ag(Tu)_3]ClO_4$ [171]). The 3:1 complex is dimeric with two bridging Tu groups, connecting 4-coordinate silver ions, while the 2:1 complex is polymeric with an equal number of bridging and terminal groups and the Cl^- fills the 4^{th} coordination site around silver(I). In the $[Ag(Tu)_2]NO_3$ complex, the fourth site is assumed to be filled by the NO_3^- ion. It is already known that C=S carbon is less shielded than are carbonyl carbons which are themselves less shielded than are carbons doubly

bonded to nitrogen [156]. Similarly silver will be more shielded if it is bonded to nitrogen or oxygen rather than to sulfur. Thus in $[Ag(Tu)_2]NO_3$ where one coordination is occupied by NO_3^- ion instead of sulfur of Tu, the Ag signal is shifted upfield instead of going downfield. The ^{107}Ag chemical shifts for $[Ag(Tu)_2]NO_3$ and $[Ag(Tu)_3]NO_3$ are comparable to the reported complexes of the thiones with the same stoichiometries [172].

When Ag:Tu were mixed in solution at the ratio of 1:5 the ^{107}Ag chemical shift was found at about the same position as for Ag:Tu of 1:4. Thus the maximum number of Tu's which can coordinate with each silver(I) ion is four.

5.4 Spectroscopic Characterization of the Silver(I) Complexes of Various Thiones

In the IR, a low frequency shift of the ν(C=S) band and the presence of a strong absorption band around 3200 cm^{-1} corresponding to N-H stretch in the free ligands as well as in the silver(I) complexes clearly indicates the existence of thione form for the lignads in the solid state.

5.4.1 ^{13}C, ^{15}N and ^{107}Ag NMR Studies

The ^{13}C NMR chemical shifts of 0.10 M solutions of the complexes in DMSO-d_6 are summarized in Table 4.11. In ^{13}C NMR, an upfield shift is associated with the lengthening of C-S bond and shortening of C-N bond upon complexation. The upfield shift decreases as the number of ligands attached to silver(I) increases from one in

[$LAgNO_3$] to two in [AgL_2]NO_3. This is because of the increased number of electronegative groups attached to silver(I). A small shift of 1-2 ppm is observed in other carbon atoms, which shows that nitrogen atoms are not involved in coordination. In the complexes of Imt and its derivatives a deshielding effect is observed at C-4/5 while in Diaz and EtDiaz complexes, a deshielding effect is observed at C-4 and C-6, but C-5 bears a shielding effect. The deshielding at C-4/6 is due to an increase in π character of the C-N bond.

The difference in shielding at C-2 is related to the strength of the metal-sulfur bond, which arises from the back donation of silver(I) to sulfur [155]. In mono complexes, the smallest C-2 shift, amounting to 5.18 ppm was detected in [*i*-PrImtAgNO_3], while the greatest one was found in [DiapAgNO_3]. Among the bis complexes, the DmTu complex with the most significant shift in C-2 (7.5) was found to be the most stable. From Table 4.11 it can be seen that as the size of the ring increases the shift difference at C-2 also increases. Thus Diap forms more stable complexes with $AgNO_3$ compared to Imt and Diaz. Also, for the complexes of N-ethyl derivatives (EtImt and EtDiaz), the shift is greater for EtDiaz complexes than for EtImt one. Changing the group at N-1 position has a little effect on C-2 shift.

A comparison of C-2 shifts of silver(I) and gold(I) complexes is given in Table 5.2. It is observed that the shift difference is more for gold(I) complexes than for silver(I) complexes. This suggests that thiones form more stable complexes with gold(I) than with silver(I), which is expected since thione is a softer ligand and would prefer to bind with a softer metal, gold(I).

A downfield shift in the ^{15}N NMR (Table 4.11) on coordination is consistent with an increase in double bond character of the C-N bond [155]. A similar observation was found in other silver(I) complexes of thiones [72]. As found in ^{13}C NMR, a greater shift in ^{15}N NMR is observed for Diaz complexes compared to those of Imt (Tables 4.11 and 4.12). The ^{15}N signal undergoes a slight shift (as discussed for Tu/Seu complexes) suggesting that the nitrogen of thiones is not involved in bonding with silver(I) [168,169].

In ^{107}Ag NMR, a very large reduction in shielding of 300-500 ppm indicates the silver(I) binding to sulfur of the thiones [156]. In the case bonding through nitrogen a smaller shift of around 100 ppm would have been observed in Ag NMR [156]. This provides a clear evidence that thiones bind to silver(I) through sulfur only. The ^{107}Ag chemical shifts of all the complexes are listed in Table 4.13. For $[LAgNO_3]$ type complexes, two categories of ^{107}Ag chemical shifts were found, one around 500 ppm and the other around 600 ppm or greater. The larger downfield shifts suggest that the compounds should be polymeric, since the electronegative ligands are coordinating from both sides of the metal ion in the polymer. The smaller shifts for MeImt, EtImt, PrImt and *i*-PrImt indicate that they are forming monomeric complexes. For Imt and its derivatives, ^{107}Ag chemical shifts are greater in bis complexes than for mono complexes, while for DmTu and Diaz, the trend is opposite. The opposite trend suggests that they exist in the form of polymers or involve some change in the geometry of the complex. The same trend was observed for $[Ag(Tu)_xNO_3]$ complexes (x = 1 to 4), which are also polymeric [63,170]. The crystal structure of $[Ag(DmTu)_2]ClO_4$ also shows that the compound is polymeric, having a tetrahedral geometry around silver(I) [64]. The greater downfield shifts for bis complexes than for mono complexes are because of the increase in number of electronegative groups attached to silver(I). The ^{107}Ag NMR chemical

shifts for the complexes are comparable to the reported complexes of other thiones with the same stoichiometries [172].

In this study we have shown that thiones react with silver nitrate to form the complexes of the type, $[LAgNO_3]$ and $[AgL_2]NO_3$. The study provides useful information about the nature of bonding in silver(I) complexes. The chemical shifts for different complexes presented here are useful, especially if the ^{107}Ag NMR is used to study silver(I) complexes with sulfur containing biological ligands.

Table 5.2 Comparison of C-2 shift difference of thiones in silver(I) and gold(I) complexes

Species	$\Delta\delta$ (C-2)	Reference
$[Ag(Imt)_2]NO_3$	5.63	This work
$[Au(Imt)_2]Cl$	6.76	26
$[Ag(MeImt)_2]NO_3$	4.63	This work
$[Au(MeImt)_2]Cl$	7.64	26
$[Ag(Diaz)_2]NO_3$	6.71	This work
$[Au(Diaz)_2]Cl$	9.45	25

5.5 Spectroscopic Characterization of the Silver(I) Complexes of Various Selenones

A low frequency shift in the ν(C=Se) vibration and the presence of a band around 3200 cm^{-1} in free ligands as well as in the complexes indicates the existence of the selenone form of the ligands in the solid state.

The upfield shift in ^{13}C NMR for C-2 resonance of the complexes may be explained on the basis of back donation of electrons from the filled metal d-orbitals to the anti-bonding π orbitals of C=Se group which will reduce the C=Se double bond character, resulting in the shielding at C-2 carbon. The upfield shift decreases as the number of ligands attached to silver(I) increases from one in $[LAgNO_3]$ to two in $[AgL_2]NO_3$. This is because of the increase in number of electronegative groups attached to silver(I). The difference in shielding may be related to the strength of Ag-Se bond. The smallest complexation shifts are observed for PhImSe complexes, while the most significant shifts are observed for DmSeu complexes (Table 4.16). This shows that the DmSeu complexes are the most stable, while the PhImSe complexes are the least stable.

A comparison of the shift differences in C-2 resonance of thiones and selenones is given in Table 5.3. It can be seen that the shifts are greater for selenone complexes than for thione ones, showing that the selenones form more stable complexes with silver(I) than do the thiones. This trend is expected because selenium being softer compared to sulfur would prefer to bind strongly to a softer metal.

In ^{107}Ag NMR, a large downfield shifts of 500-600 ppm clearly indicate the selenium binding to silver(I). As it is observed in ^{13}C NMR data, the shift is the largest

for DmSeu complexes and is the smallest for PhImSe complexes (Table 4.17). Thus ^{107}Ag NMR also suggests that DmSeu forms stable complexes with silver(I), while the PhImSe forms the least stable among the selenones. The more downfield shifts for bis complexes compared to mono complexes are because of the increase in number of electronegative groups attached to silver(I). For $[Ag(ImSe)_2]NO_3$, the silver resonance appears upfield compared to its mono complex suggesting that the compound may be polymeric, since a similar trend is observed for polymeric silver-thiourea complexes.

A comparison of silver chemical shifts of the silver(I) complexes of the selenones and thiones (Tables 5.3) shows that the shifts for the selenone complexes are 30-200 ppm more downfield than for the thione complexes which may be because selenium is more polarizable.

Table 5.3 Comparison of the shift difference in ^{13}C (C-2 resonanace) and ^{107}Ag NMR for silver(I) complexes of thiones and selenones

Thione complexes	$\Delta\delta$ (^{13}C)	$\Delta\delta$ (^{107}Ag)	Selenone Complexes	$\Delta\delta$ (^{13}C)	$\Delta\delta$ (^{107}Ag)
[ImtAgNO$_3$]	6.48	405.0	[ImSeAgNO$_3$]	10.97	549.9
[Ag(Imt)$_2$]NO$_3$	5.63	442.3	[Ag(ImSe)$_2$]NO$_3$	6.61	473.1
MeImtAgNO$_3$	5.87	327.7	[MeImSeAgNO$_3$]	11.38	526.3
[Ag(MeImt)$_2$]NO$_3$	4.63	479.4	[Ag(MeImSe)$_2$]NO$_3$	7.22	559.7
[EtImtAgNO$_3$]	5.22	314.2	[EtImSeAgNO$_3$]	9.93	500.1
[Ag(EtImt)$_2$]NO$_3$	4.79	479.2	[Ag(EtImSe)$_2$]NO$_3$	6.69	510.9
[*i*-PrImtAgNO$_3$]	5.18	323.6	[*i*-PrImSeAgNO$_3$]	10.96	495.9
[Ag(*i*-PrImt)$_2$]NO$_3$	4.97	484.3	[Ag(*i*-PrImSe)$_2$]NO$_3$	6.79	511.7
[DiazAgNO$_3$]	6.48	-	[DiazSeAgNO$_3$]	11.92	-
[Ag(Diaz)$_2$]NO$_3$	6.71	-	[Ag(DiazSe)$_2$]NO$_3$	5.90	-
[EtDiazAgNO$_3$]	7.98	446.0	[MeDiazSeAgNO$_3$]	12.04	446.0

5.6 Ligand Scrambling Reactions of Cyanogold(I) Complexes

It has been observed that cyano(thione/selenone)gold(I) undergo ligand scrambling reactions to form the symmetrically substituted complexes according to the eq (5.1);

$$2\,[>C=S/Se\text{-}Au\text{-}CN] \Leftrightarrow [Au(>C=S/Se)_2]^+ + [Au(CN)_2]^- \quad (5.1)$$

It is observed that K_{eq} for this reaction is affected by several external parameters, which are; initial concentration, ionic strength, temperature and polarity of the solvent. Except temperature, an increase in all other factors leads to an increase in K_{eq}. An increase in $[Imt\text{-}Au\text{-}CN]_o$ generates more $[Au(Imt)_2]^+$ and $[Au(CN)_2]^-$ resulting in the larger K_{eq} values [114]. Since ionic complexes are generated from the scrambling process, therefore an increase in ionic strength leads to an increase in the activity coefficients for $[Au(Imt)_2]^+$ and $[Au(CN)_2]^-$ with a subsequent increase in K_{eq}. A decrease in K_{eq} at $[NH_4NO_3]$ greater than 1.0 M is perhaps due to ion pairing. This result is consistent with that reported for Et_3PAuCN [114]. The increase in K_{eq} observed by increasing ionic strength is more than that observed by changing concentration. The K_{eq} values are consistently increasing with the polarity of the solvent except in methanol. Methanol being a protic solvent solvates the anion, $[Au(CN)_2]^-$ (which is more stable) strongly and thus would result in larger K_{eq}.

The K_{eq} value decreased with increasing temperature indicating that the scrambling reaction is exothermic in forward direction [eq. (5.1)]

$\ln K = -\Delta H^o/RT + C$. The >C=S and C-4/5 resonances of Imt-Au-CN and $[Au(>C=S)_2]^+$

which are observed as average resonances at 298 K, are clearly separated into two peaks at 240 K (Figure 4.4c). Thus, we were able to detect both species, $[Au(>C=S)_2]^+$ and $[Au(CN)_2]^-$ formed as a result of the scrambling of Imt-Au-CN. The analogous species in the scrambling of some R_3P-Au-CN complexes, $[Au(R_3P)_2]^+$ was detected at room temperature by ^{31}P NMR. The ΔH^o value for this reaction can be obtained if ln*K* is plotted against 1/T in the van't Hoff equation, $\ln K = -\Delta H^o/RT + C$. Such a plot is shown in Figure 5.4 and the ΔH^o value obtained from this plot is –1.81 kJ/mole.

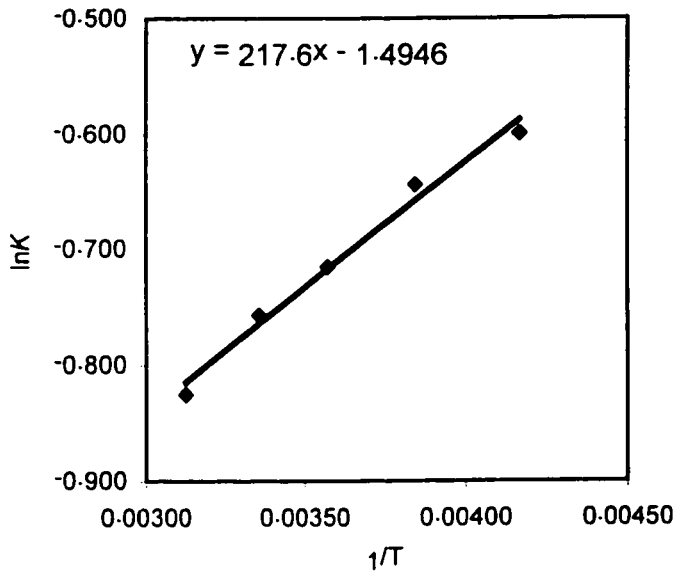

Figure 5.4 A plot of ln*K* Vs 1/T for Imt-Au-CN in methanol

Besides external factors, it was observed that K_{eq} for the scrambling reactions of cyanogold(I) complexes of phosphines, was also affected by the intrinsic factors which are electronic and steric [114]. Among the intrinsic factors, the basicity of the phosphine is the most important factor, which affects K_{eq}. An increase in K_{eq} was observed with an increase in basicity of the phosphine [114]. R_3PAuCN complexes, in which phosphine ligands have ν(CO) values equal or less than 2066.7 cm^{-1} exhibited the equilibrium at room temperature and separated resonances were also detected for the equilibrium components. For the complexes with ν(CO) values greater than 2066.7 cm^{-1}, the equilibrium species were found to be in fast exchange with each other at room temperature. However, separate resonances were detected at lower temperature [32]. In the present study, the scrambling reactions for all [>C=S/Se-Au-CN] complexes could be observed at room temperature. However, separate resonances for [>C=S/Se-Au-CN] and $[Au(>C=S/Se)]^+$ could only be separated when the spectrum was recorded at lower temperature. The intrinsic factors were also known to influence the kinetics of the scrambling reaction. For example, for Cy_3PAuCN due to its larger size the equilibrium was established after several weeks [32,114]. For complexes with even bulkier phosphines $(o\text{-Tol})_3P$ and $(Naphthyl)_3P$, no scrambling was observed. In the present case, a rapid scrambling process was observed for [>C=S/Se-Au-CN] complexes, which could be due to smaller sizes of the ligands [32].

As shown in Tables 4.18, 4.19 and 4.20, the K_{eq} values for the cyanogold(I) complexes of selenones are found much larger than for the complexes of other ligands. The larger K_{eq} values indicate that the selenones are more basic towards Au(I) compared to phosphines and thiones. A shift of 9 to 13 ppm in C-2 resonance also indicates that

they are very strong σ donors (for thiones 8-10 ppm). In the case of phosphines, π accepting ability of phosphines stabilizes the Au-P bond [42] and thus would result in the lower value of K_{eq}. This shows that the selenones are much weaker π acceptors compared to phosphines and thiones. A comparison of the K_{eq} value for scrambling of $Cy_3PSeAuCN$ with its sulfur analogue, $Cy_3PSAuCN$ (Table 4.20) further suggests that the K_{eq} values for the selenones complexes should be greater than for the complexes of their sulfur analogues (thiones). Moreover, since five of the nine selenone complexes, being reported exist in the solid state as ionic complexes, therefore in solution the ionic form will also be more populated resulting in a larger value of K_{eq}. Thus the order of ability of different L-Au-CN complexes undergoing dispropotionation is, [>C=SeAuCN] > [$R_3PSeAuCN$] > [>C=SAuCN] > [R_3PAuCN] ≥ [$R_3PSAuCN$].

In the scrambling reactions of cyano(phosphine)gold(I) complexes, it was observed that with increasing basicity of phosphines, δ ^{13}C for CN in R_3PAuCN also increased due the increased π bond character in Au-C bond, while there was a decrease in δ ^{15}N [32,114]. However in the present study, δ ^{13}C and δ ^{15}N for CN and the coupling constants, $^1J_{C\text{-}N}$ in all the complexes are very close showing that the difference in their basicity is small. For thione complexes, as shown in Table 4.18, the highest value of $\delta^{13}C$ for CN resonance of Diaz-AuCN indicates that it is the most basic, while the PrImt-AuCN with the lowest $\delta^{13}C$ is the least basic among the thiones. Table 4.19 shows the highest value of δ ^{13}C for CN resonance of DiazSe-AuCN indicating that it is the most basic, while the Et_2ImSe-AuCN with the lowest $\delta^{13}C$ is the least basic among the selenones. In both cases, the six membered ring ligand is forming the most stable complexes. The least basicity of Et_2ImSe-AuCN is due to its inability to exhibit selenol-

selenone equilibrium. However, the greater δ ^{13}C and smaller δ ^{15}N of selenone complexes compared to that of thione ones indicate that the selenones are comparatively more basic than thiones.

5.7 ^{13}C NMR Studies of the Interaction of Gold(I) Thiomalate with 6-Mercaptopurine and Its Derivatives

Gold(I) is found in AuS_2 coordination environments for the various types of gold(I) thiolate complexes [69-71]. When excess thiols such as cysteine and glutathione are added to $[Au(SR)]_n$ polymers, they usually eject thiomalate by forming $[Au(thiolate)_2]^-$ species [70,173,174]. However, when thiones such as ergothionine [143], Imt (imidazolidine-2-thione) and Diaz (1,3-diazinane-2-thione) are added to $(AuStm)_n$ solution, usually a ternary complex of the type [>C=S-Au-Stm] is formed without ejecting thiomalate [124,125]. In the present study, when mercaptopurines (which are soluble only at high pH) were added to the $(AuStm)_n$ solution, no free thiomalate was released from $(AuStm)_n$ at the ratio of 1:1 suggesting that they are not binding as strongly as thiolates and they coordinate in the form of thiones. However, in the case of 6-MP, at the ratios 1.5:1 and 2:1 of 6-MP to $(AuStm)_n$, less intense thiomalic disulfide, $(Stm)_2$ resonances are observed (Figure 4.13). This indicates that some of the thiomalate is released from $(AuStm)_n$ as a free ligand and is consequently oxidized to thiomalic disulfide, $(Stm)_2$ [133]. Since the free thiomalate [131] or $(Stm)_2$ resonances are observed [123,173] on interaction of $(AuStm)_n$ with thiols, therefore, there is a possibility that 6-MP could bind to gold(I) as a thiolate ligand or in thione form. Cookson et al [20]

reported several gold(I) complexes showing that 6-MP coordinates as a thiolate ligand. For 6-MPR and 2-A-6-MPR it is suggested that they bind to AuStm only in thione form, since no $(Stm)_2$ resonances are observed upon their addition to $(AuStm)_n$.

For 6-MP at the ratio 2:1 of 6-MP: $(AuStm)_n$, the $(AuStm)_n$ resonances, b_1, b_2 and b_3 split into two resonances (Figure 4.13) showing that 6-MP forms two geometrical isomers when binds to $(AuStm)_n$. The structures of these two isomers are shown below;

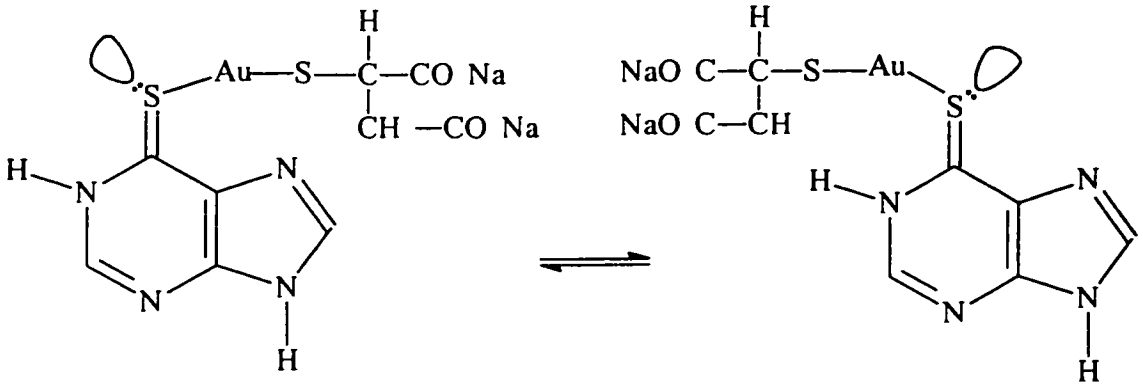

I II

The sulfur atom of 6-MP with its two lone pairs, is sp^2 hybridized. In one isomer of 6-MP-Au-Stm, the AuStm moiety could be oriented towards the imidazole ring while in the other, it could be towards the lone pair. The isomer in which the AuStm moiety is oriented towards imidazole ring, I, b_2 should appear downfield because the b_2 carbon atom of thiomalate is near to more electronegative nitrogen atom of aromatic ring. The peak intensities of ^{13}C NMR show that form I is less populated than II (Figure 4.13). For 6-MPR and 2-A-6-MPR only b_2 is separated into two resonances while for b_2 and b_3 this

splitting is not observed. This is the first example in which two isomers are observed in the ^{13}C spectrum of $(AuStm)_n$ on its interaction with thiones. However, such kinds of isomers have already been reported for several platinum complexes [175,176].

The thiolated purines are all ambidentate ligands, since they offer a multiplicity of potential binding sites, such as nitrogen and sulfur. In metal complexes they could act as a monodentate ligand through sulfur or as an S-6/N-7 chelating ligand [177]. Gold(I) and mercury(II) coordinate through sulfur [91,94] while, the chelating mode is observed in Ru(II) [178,179], Co(II) [90], Cd (II) [177] and Au(III) [180] complexes. In the case of Hg(II) interaction with 2-A-6-MPR, it was observed that >C=S carbon underwent a shift of 15.1 ppm indicating the binding of only sulfur atom to Hg(II) [91]. In the present study, the largest chemical changes in ^{13}C NMR of all the bases occur at C-6 position providing clear evidence for selective binding via the sulfur atom. This is consistent with the stronger binding expected between a class b (soft metal) such as gold(I) and a softer sulfur ligand. The carbon atom of >C=S group undergoes a shift of up to 17 ppm upon formation of Au-S bond in 6-MPR and 2-A-6-MPR, while in 6-MP the shift is of 3.40 ppm (Table 4.23). There was no significant shift for the C-8 position during the reaction, indicating that N-7 position is not involved in coordination to $(AuStm)_n$. Also the ribose hydroxyl groups do not participate in binding since their resonance remained unshifted.

The present study describes that in the ^{1}H NMR spectra of all the complexes, the H-2 protons became less intense and shifted a little downfield with respect to the free ligands but shifted again upfield upon addition of excess ligand. This has been attributed to the π electron redistribution on protonation or complex formation [181,182]. For complexes of thiolated bases where coordination occurs through N-7 site, the proton at C-

8 position shifts more downfield than the others and becomes less intense [89]. The intensity of H-8 was not affected by addition to $(AuStm)_n$. Since the shift in H-8 is very small, so it can be concluded that N-7 is not involved in the binding.

In case of 6-MP, it was observed that at more basic pH, the C-8 is significantly shifted downfield indicating that deprotonation occurs at the N-9 position. Such a downfield shift upon deprotonation was also observed in 6-MP complexes of Mo(II) [95]. It has also been observed that upon addition of base to the solution of $[Ru(6\text{-}MP)_2\{P(C_6H_5)_3\}_2]Cl_2$ H-8 signal in ^1H NMR is most affected, consistent with the N-9 deprotonation [183]. The pK_a value for N-9 deprotonation is reported to be 9.1, while for N-1, it is 2.2 [183]. Since C-8 resonance is not significantly shifted when 6-MP is added to $(AuStm)_n$ at higher pH therefore, it is suggested that N-9 is not involved in coordination and gold(I) binds only through sulfur.

In the previous studies of interaction of $(AuStm)_n$ with thiones by ^{13}C NMR, it has been observed that 2-thiouracil, Imt (imidazolidine-2-thione) and Diaz (1,3-diazinane-2-thione) form a ternary complex of the type [>C=S-Au-Stm] without ejection of Stm^- as a free ligand [124,125,184]. In these cases the chemical shift differences between free thione and the complex at the 1:1 ratio of RS:$(AuStm)_n$ are 3.64, 2.55 and 2.05 ppm respectively. Whereas in the present case it was found to be around 17 ppm for 6-MPR and 2-A-6-MPR, while 3.40 ppm for 6-MP. A comparison of the ^{13}C chemical shifts of the carbon atom attached to the coordinating sulfur atom of various thione ligands at the 1:1 ratio of thione:$(AuStm)_n$ is given in Table 5.4. It is observed that the thiolated bases binds more strongly than the simple thiones with gold(I). From this interaction it is clear

that thiolated bases only form [RS-Au-Stm]$^-$ complex and excess base is in continuous exchange with bound ligand.

Table 5.4 Difference in the ^{13}C NMR chemical shifts ($\Delta\delta$) in ppm of the >C=S resonance of thione at a 1:1 ratio of RS:$(AuStm)_n$

RS	pH	$\Delta\delta$	Reference
6-MP	11.45	3.40	This work
6-MPR	8.67	17.66	This work
2-A-6-MPR	9.50	17.54	This work
2-Thiouracil	10.50	3.63	184
Ergothionine	7.40	2.99	143
Imt	7.40	2.55	124
Diaz	7.40	2.05	125

5.8 Exchange Reactions of Gold(I) Thiomalate with Diselenides

The reaction of gold(I) thiomalate [$(AuStm)_n$] with diselenides (RSe-RSe) most probably starts with the formation of selenyl sulfide species, RSe-Stm, as explained by eq. 4.4. Since the resonances from $(AuStm)_n$ became broad, suggesting that some Stm^- is replaced in the polymer structure leading to the formation of $(AuRSe)_n$. It seems that the gold nuclei are transferred to the incoming ligand with the result that the diselenide linkage is opened. The resonances for free thiomalate were not observed as they were observed in the exchange reactions of $(AuStm)_n$ with selenolates [131,132]. Thiomalate is subsequently oxidized to RSe-Stm and $(Stm)_2$ as it is released. The formation of $(Stm)_2$ indicates the occurrence of a redox reaction along with the exchange process. There is no evidence in the spectrum to support the formation of $[RSe\text{-}Au\text{-}Stm]^-$ complex during the initial reactive step since the thiomalate resonances corresponding to this ternary complex were not observed in the beginning.

The rate constant, k was determined for the decomposition of RSe-Stm species, in the reaction of selenocystine with $(AuStm)_n$ using the second order rate equation ($1/a = kt + 1/a_o$) for reaction (4.5). The reaction (4.4) was assumed quantitative and therefore the initial concentration of RSe-Stm was taken as 0.05 M. A plot of 1/a Vs t is shown in figure 5.5 (a = [RSe-Stm]). The rate constant found for this reaction is 3.21×10^{-4} L. $mol^{-1}.sec^{-1}$. The accurate rate constant value for the reaction of selenocystamine could not be obtained, since Figure 4.20 is not showing a proper exponential decrease in intensity of RSe-Stm.

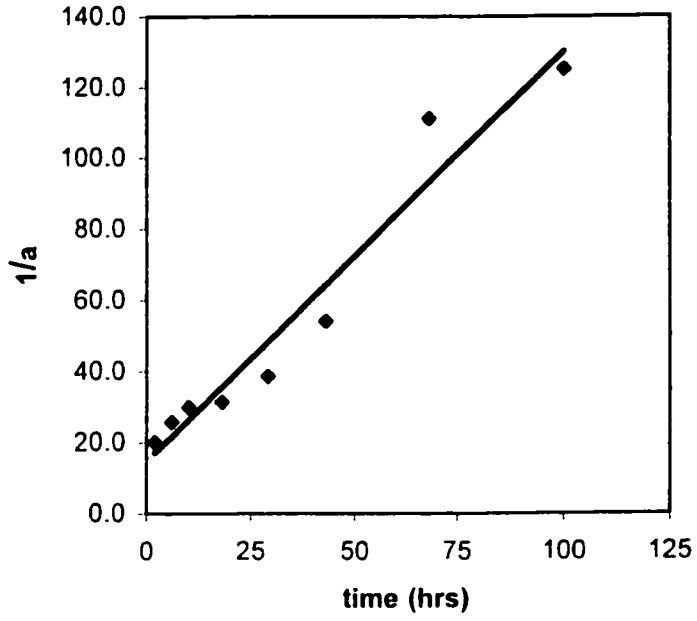

Figure 5.5 A plot of 1/[RSe-Stm] Vs time from the 2nd order rate equation, $1/a = kt + 1/a_o$ (a = [RSe-Stm]) in the interaction of $(AuStm)_n$ with selenocystine (the values are taken from Figure 4.18).

The diselenides are found to undergo very fast exchange reactions with $(AuStm)_n$ as indicated by the appearance of peaks at 42 ppm and 52 ppm in ^{13}C NMR immediately after mixing the two species. It is observed that they initially form a selenyl sulfide (RSe-Stm) species which further undergoes exchange reactions with $(AuStm)_n$ producing thiomalic disulfide, $(Stm)_2$. The reactions of RSe-Stm with $(AuStm)_n$ are found to be slow and are completed within one to two weeks. The rates of disappearance of (RSe-Stm) and formation of $(Stm)_2$ species are shown in Figures 4.18 and 4.20. In the exchange reactions of $(AuStm)_n$ with disulfides, different kind of exchange processes were observed for the two disulfides [134]. In the case of Ellmans reagent, the overall degradation process of $(AuStm)_n$ was slow compared to the terminal group exchange, which resulted in a polymeric species and mixed disulfide (RS-Stm). In the case of lipoic acid, a slow direct reaction was observed, producing only $(Stm)_2$ and no mixed disulfide was detected. The $(Stm)_2$ resonances were observed after one week in ^1H NMR showing that the exchange process was very slow.

The study provides a model for the exchange reactions of RSe-SeR and RSe-SR with $(AuStm)_n$. Although RSe-SR bond does not exist *in vivo*, it is known that Se-glutathione peroxidase exists in the selenolate form in red blood cells; therefore it is possible that glutathione (which occurs at 2.5 mM level concentration [135]) or some other thiol may form RSe-SR bond. It is shown in the present study that this bond (RSe-SR) is unstable in the presence of gold(I) thiomalate and undergoes decomposition. The formation of $(Stm)_2$ indicates the occurrence of a redox reaction along with the exchange process.

5.9 ^{13}C, ^{31}P and ^{15}N NMR Studies of the Ligand Exchange Reactions of Gold(I) Thiomalate, Auranofin and Chloro (triethylphosphine) gold(I) with Thiourea

Gold(I) is found in AuS_2 coordination environments for the various types of gold(I) thiolate complexes [69-71]. When thiols, such as cysteine and glutathione are added to $(AuSR)_n$ polymers, they usually eject thiomalate by forming $[Au(thiolate)_2]^-$ species [70, 173,174]. However, when thiones, such as ergothionine [143], Imt (imidazolidine-2-thione) and Diaz (1,3-diazinane-2-thione) are added to $(AuStm)_n$ solution, usually a ternary complex of the type [>C=S-Au-tm] is formed without ejecting thiomalate [124,125]. In the present study, upon addition of Tu to $(AuStm)_n$, no free thiomalate resonances are observed in the ^{13}C NMR (even at the ratio of 1:2 of $\{(AuStm)_n$:Tu$\}$, suggesting that Tu binds to gold(I) only as a thione ligand.

Several studies have shown that during the exchange reactions of auranofin with various biological sulfur containing ligands, *e.g.*, bovine serum albumin and red blood cells, the $SATg^-$ ligand of auranofin is readily displaced while the gold-bound phosphine is displaced slowly [119-121,135,136]. The presence of Et_3P bound to Au(I) appears to enhance the thiol exchange rates because of the high trans influence of phosphines [5]. Ligands with moderate to high affinities for gold, *e.g.*, ATgSH, 1-thioglucose, glutathione or cyanide displace the phosphine from auranofin, which is then oxidized to Et_3PO [135,166]. Recently, the interaction of auranofin with $SeCN^-$ in methanol-water (95:5 v/v) has been studied using ^{13}C and ^{31}P NMR spectroscopy, and a simultaneous replacement of both the thiol and phosphine ligands was observed [165]. This interaction

resulted in the generation of [ATgS-Au-CN]$^-$ and [Et_3P-Au-SeCN] complexes which further underwent dissociation releasing [$Au(Et_3P)_2]^+$, [$Au(CN)_2]^-$, [$Au(SATg)_2]^-$, elemental selenium and Et_3PO species.

The results obtained in the present study through ^{13}C and ^{31}P NMR, indicate that the reaction of auranofin with Tu results in the formation of several species. The appearance of several resonances in ^{13}C NMR upon addition of Tu to auranofin solution indicates the replacement of both ligands, SATg$^-$ and Et_3P by Tu. These are consequently oxidized to $(SATg)_2$ and Et_3PO respectively. Dissolved oxygen is probably the source of oxygen [5,135]. Although the equilibrium for thiol displacement should be favored over Et_3P displacement, the irreversible oxidation of Et_3P would shift the equilibrium to Tu-Au-SATg and Et_3PO. Resonances for Tu-Au-SATg and [Et_3P-Au-Tu]$^+$ are not observed in ^{13}C NMR, which indicates that they are in rapid exchange with auranofin. Resonances for Tu-Au-SATg complex are assigned separately, by reacting $AuBr.2H_2O$ with Tu and SATg$^-$ at 1:1:1 ratio in methanol (Table 4.29).

The appearance of $(SATg)_2$ resonances in ^{13}C NMR after 115 hours of the addition of Tu to auranofin solution shows that the reaction is very slow.

In ^{31}P NMR, the auranofin resonance shifted upfield upon addition of Tu, and broadened due to an exchange of Et_3P between auranofin and other species. At 2:1, Tu:auranofin, along with Et_3PO resonance another resonance appeared at 1.03 ppm (Figure 4.23), which was not observed in any of the previous studies of auranofin reactions [119-121,135]. This resonance could be either due to some Et_3P-Au complex or because of the reaction of Et_3P with thiourea. If it were a gold bound species it should be replaced by the addition of cyanide, but when cyanide was added it did not disappear, disproving this possibility. It was therefore assumed that it must be due to the reaction of

Et_3P with thiourea. So it was assigned to the $Et_3PSC(NH_2)_2$ species as a result of an independent reaction between Et_3P and thiourea. The reaction of the phosphine released from an auranofin analogue, *i*-Pr_3P-Au-SATg with serum albumin in water has already been reported [185].

The overall interaction of Tu with auranofin may be explained by the scheme 5.1.

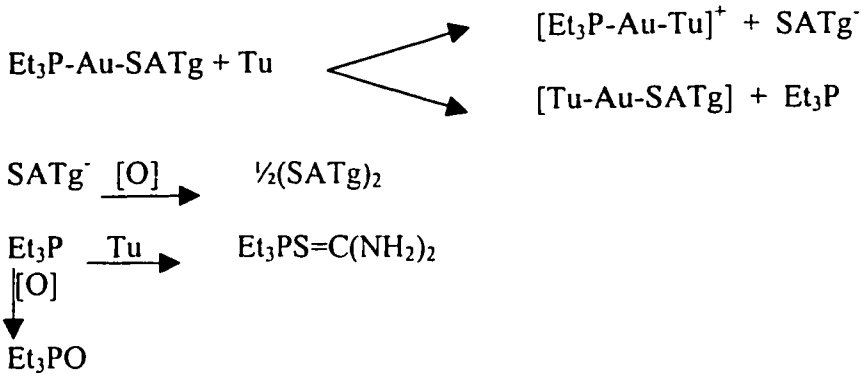

Scheme 5.1

With a 0.05 M auranofin solution at a 1:1 ratio of auranofin and Tu, the Et_3PO resonance in ^{31}P NMR was observed after 110 hours of addition of Tu (Figure 4.24). With thiols this resonance appeared in the period of 24 to 72 hours [135], and with CN^- it appeared immediately after the reaction [107]. This observation shows that thiones react slowly with auranofin compared to thiols and CN^-. The integration of the ^{31}P NMR (after one month) demonstrates that about 18 % of phosphine is released as Et_3PO and about 12 % as Et_3P-Tu species. The rest of the phosphine is in the form of unreacted auranofin and Et_3PAuTu, which are not resolved due to their rapid exchange.

The appearance of free Tu and absence of auranofin resonaces in ^{13}C NMR upon addition of CN^-, shows that CN^- has displaced all the ligands from gold(I) (Figure 4.27). The broadness of $[Au(CN)_2]^-$ peak indicates that other cyano-gold species, *e.g.*, [ATgS-Au-CN]$^-$ [165], are formed, which are in exchange with $[Au(CN)_2]^-$. Since 2 equivalents of CN^- was added therefore most of the Au^+ is in the form of $[Au(CN)_2]^-$ as indicated by the intense resonance of $[Au(CN)_2]^-$. The weaker resonances represent the [ATgS-Au-CN]$^-$ and $[Au(SATg)_2]^-$ species (Figure 4.27). [ATgSAuCN]$^-$ resonances are assigned as a result of the reaction of $[Au(CN)_2]^-$ with $SATg^-$ (Table 4.29). The intense resonances could only be the average resonances for the exchange of $(SATg)_2$ and $SATg^-$, since CN^- has replaced all the $SATg^-$ from gold(I) and thus no other gold(I)-SATg species is present in excess.

The absence of auranofin resonance in ^{31}P NMR upon addition of CN^- confirms that the reaction has gone to completion (Figure 4.24). The ^{31}P NMR spectrum demonstrates that all Et_3P is released from auranofin and some is oxidized. Thus CN^- generates Et_3PO from auranofin much more rapidly than do thiones. The free Et_3P has not previously been observed in auranofin spectrum; previous studies [119-121,135,136] report that Et_3P is immediately oxidized after it is released formig Et_3PO. The integration of peaks shows that the intensity of the Et_3P resonance is almost double than that of the Et_3PO resonance.

When Tu was added to Et_3PAuCl, the >C=S resonance of Tu shifted upfield by 6.2 ppm in the ^{13}C NMR, indicating the replacement of Cl^- by Tu and the formation of Et_3PAuTu complex. The upfield shift of 6.2 ppm indicates the very strong binding of Tu to gold(I).

In the ^{31}P NMR spectrum of Et_3PAuCl, the broadening and downfield shift in the Et_3PAuCl resonance is indicative of an exchange of Et_3PAu^+ between Cl^- and Tu. The $(Et_3P)_2Au^+$ resonance appears when Et_3P is displaced from the gold and then extracts a second Et_3PAu^+ moiety from another site [186]:

$$Et_3P + Et_3PAu^+ \rightarrow [Au(Et_3P)_2]^+ \qquad (5.2)$$

The resonance at 46 ppm increased in intensity when a further 0.25 equivalent of Tu was added because of the further loss of Et_3P from Et_3PAuCl, but upon further additions this signal became less intense since Et_3PAuCl was not available for this reaction. The resonance due to Et_3PO did not appear until after the addition of the two equivalentss of Tu, showing that at lower concentrations Et_3P is involved in several exchange reactions. At a 1:1 ratio of Et_3PAuCl to Tu, the complex $[Et_3PAuTu]^+$ is stabilized and appears at 37.75 ppm (which is close to the auranofin resonance) and this resonance is not affected by further additions of Tu. Since the stability of complexes is related to δ ^{31}P value [135] it is assumed that the complex $[Et_3PAuTu]^+$ has almost the same stability as auranofin.

A downfield shift in Tu resonance in the ^{15}N NMR in all three cases, $(AuStm)_n$, auranofin and Et_3PAuCl, indicates the binding of Tu to gold(I). It does not give information about the nature of different species observed in the cases of $(AuStm)_n$ and auranofin. However, a shift of 6.0 ppm in ^{15}N NMR of Tu on its interaction with Et_3PAuCl provides a clear evidence of the formation of $[Et_3PAuTu]^+$ complex. The downfield shift is indicative of Tu coordination to gold(I) via sulfur only. The downfield shift is because of an increase in the double bond character of the C-N bond of Tu. The

metal binding through nitrogen should involve an upfield shift of at least 50 ppm in the NH_2 resonance of Tu as it is observed in some Pt(II) complexes [168,169].

In the present study we have shown that a thione (being a weaker ligand than thiols and CN^-) can also replace both ligands (Et_3P and $SATg^-$) from auranofin. Therefore, ergothionine, which is present in the blood and possesses a thione group can not be ignored and it can compete with thiols for gold(I) during chrysotherapy. Since ergothionine can replace both strongly bound ligands from auranofin, there is a possibility that it can also undergo exchange reactions with the adducts (*e.g.*, Et_3P-Au-SR or $Au(SR)_2^-$) formed between gold(I) and other thiols like glutathione. The reaction of Tu with $(AuStm)_n$ is found to be faster compared to its reaction with auranofin; since in auranofin both ligands are strongly bound, while $(AuStm)_n$ has a chain structure.

The results of the study also establish that Et_3P released from auranofin, in addition to its oxidation, can react with the cellular species as indicated by the formation of Et_3P-Tu species.

5.10 Comparative ^{13}C and ^{31}P NMR Studies of the Ligand Exchange Reactions of Auranofin with Ergothionine, Imidazolidine-2-thione and Diazinane-2-thione

The results obtained in the present study through ^{13}C and ^{31}P NMR indicate that the reaction of auranofin with a thione results in the formation of several species. On addition of thiones to auranofin solution, a number of resonances appear in ^{13}C NMR along with auranofin resonances (Figure 4.33 c-f) which indicates the replacement of both

ligands, Et_3P and $SATg^-$ by thiones. These ligands are consequently oxidized to Et_3PO and $(SATg)_2$ respectively. Dissolved oxygen is probably the source for oxidation [5,135]. The irreversible oxidation of Et_3P would shift the equilibrium to >C=S-Au-SATg and Et_3PO. In the exchange reactions of auranofin with Tu, only the weighted average resonances for Tu-Au-SATg and auranofin were observed showing a rapid exchange between the two species. However, separate resonances for >C=S-Au-SATg are observed in ^{13}C NMR showing that the >C=S-Au-SATg complexes are in slow exchange with auranofin. The appearance of >C=S-Au-SATg and $(SATg)_2$ resonances in ^{13}C NMR after several days of addition of thiones to auranofin shows that these exchange reactions are very slow.

The overall interaction of the thiones with auranofin may be explained by the scheme 5.2.

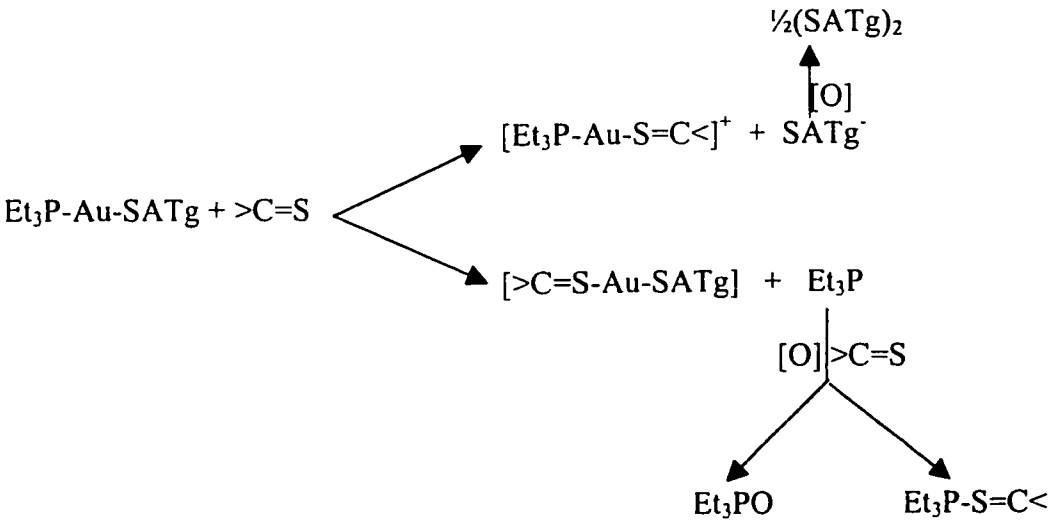

Scheme 5.2

The Et_3PO resonance is observed in the interaction of these thiones after several days of their addition to auranofin. We observed the Et_3PO resonance in ^{31}P NMR in the interaction of auranofin and Tu (1:1), after 115 hours of addition of Tu. With thiols this resonance appeared in the period of 24 to 72 hours [135] and with CN^- it appeared immediately after the reaction [135]. These observations show that these thiones react slowly with auranofin compared to thiourea, thiols and CN^-. A comparison of the rate of formation of Et_3PO from auranofin with various thiones is shown in Figure 5.6.

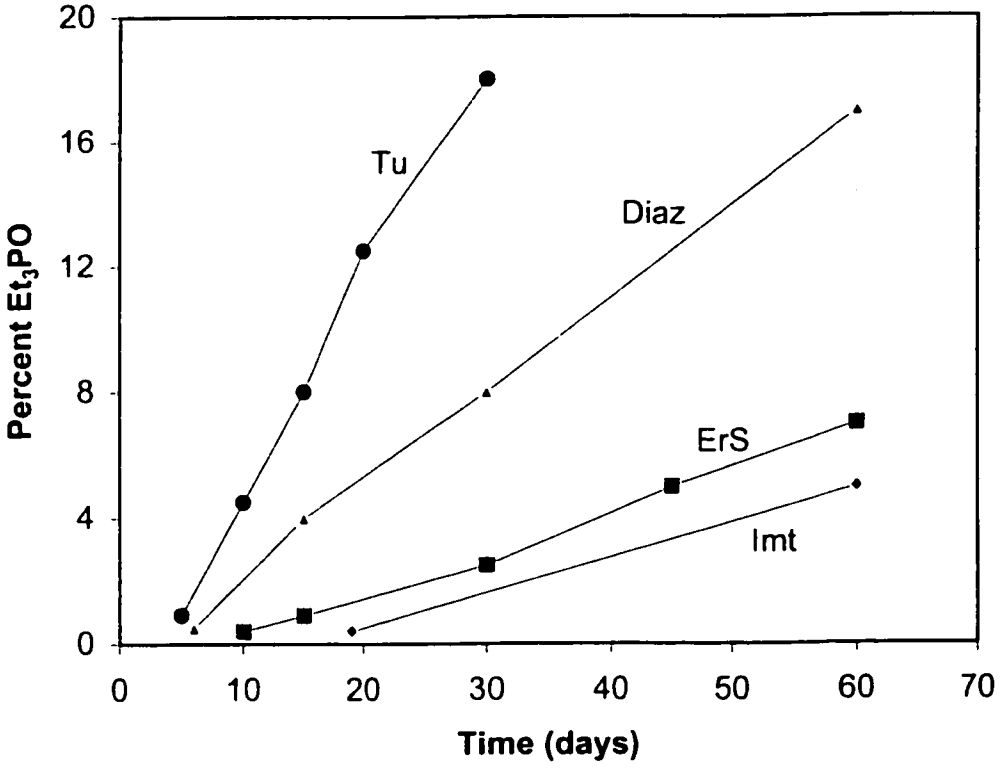

Figure 5.6 Rate of formation of Et_3PO from auranofin with various thiones (The percentage of Et_3PO was determined by integration of ^{31}P NMR spectra; For structures of thiones, refer Figure 2.3)

The integration of the ^{31}P NMR in the interaction of ergothionine (ErS) demonstrates that about 4 % of auranofin is converted to Et_3PO and Et_3P-ErS species after one month and it was about 10 % after 2 months. In the case of Imt only about 7 %, while in the case of Diaz about 23 % of auranofin generated Et_3PO and Et_3P-S=C< species. We observed in the interaction of Tu that about 30 % of auranofin was converted to other species after one month. Thus among thiones the order of reactivity towards auranofin is Tu > Diaz > ErS > Imt.

The present study demonstrates a pathway for the ligand exchange reactions of auranofin by which both the ligands from auranofin are replaced by thiones and the Et_3P released from auranofin reacts with thiones to form Et_3P-thione species. The slow reaction of ergothionine with auranofin shows that it has a greater affinity for gold(I) thiomalate [143] compared to that for auranofin. This gold binding with cellular species could also be a cause of several toxic reactions. Among cellular species, glutathione, GSH (a thiol containing molecule) is in excess compared to ErS in RBCs and gold has a stronger affinity for GSH than for ErS, so the most probable species formed in RBCs is the GS-gold(I) complex. When gold concentration is limiting during chrysotherapy, this would be the most probable reaction, but when gold is in excess there is possibility that ErS can bind to gold(I) in RBCs. However, the reaction of ErS is slow enough to allow any ErS-gold(I) adduct formed to diffuse away from its site of biogenesis.

Conclusions

Following conclusions are drawn from the present research work:

(1) Gold(I) and Silver(I) form stable complexes with thiones and selenones; the selenone complexes are found to be more stable.

(2) Some cyanogold(I) complexes of thiones and selenones exist as nonionic complexes, [LAuCN] and some exist as ionic complexes, $[Au(L)_2]^+[Au(CN)_2]^-$ in the solid state. However, in solution all undergo ligand scrambling reactions possessing the equilibrium, 2 [L-Au-CN] $\rightleftharpoons$ $[Au(L)_2]^+ + [Au(CN)_2]^-$.

(3) The order of ability of different L-Au-CN complexes to undergo dispropotionation is, [>C=SeAuCN] > $[R_3PSeAuCN]$ > [>C=SAuCN] > $[R_3PAuCN]$ ≥ $[R_3PSAuCN]$.

(4) Gold(I) thiomalate undergoes exchange reactions with thiones forming the complexes of the type, [>C=S-Au-Stm].

(5) The reaction of diselenides with gold(I) thiomalate is an exchange as well as a redox reaction. The reaction results in the formation of thiomalic disulfide along with the deposition of metallic gold and elemental selenium.

(6) Auranofin undergoes ligand exchange reactions with thiones forming the complexes of the type, $[Et_3P\text{-}At\text{-}S{=}C{<}]^+$ and [>C=S-Au-SATg]. However, the reactions are slower compared to thiols. The results of the study also establish that Et_3P released from auranofin, in addition to its oxidation, reacts with thiones forming $Et_3P\text{-}S{=}C{<}$ species.

References

1. B. E. Douglas, D. H. McDaniel and J. J. Alexander, *Concepts and Models of Inorganic Chemistry, 3rd edition*, John Wiley and Sons, Inc., 1994, p 725.
2. F. A. Cotton, G. Wilkinson, C. A. Murillo and M. Bochmann, *Advanced Inorganic Chemistry, 6th edition*, John Wiley and Sons, Inc., 1999, p 1084.
3. R. J. Puddephat, "The Chemistry of Gold", Elsevier Scientific Publishing Co., Amsterdam, 1978, p 5.
4. T. L. Brown, H. E. LeMay and B. E. Bursten, *Chemistry, the Central Science, 6th edition*, Prentice-Hall International, Inc., 1994, p 129.
5. S. J. Lippard, *Platinum, Gold and Other Metal Chemotherapeutic Agents, ACS Symposium Series*, **209**, 1983, p 356.
6. P. J. Sadler, *Struct. Bonding* (Berlin), **29**, 1976, 175.
7. C. F. Shaw, *Inorg.Perspect. Biol. Med.*, **2**, 1979, 287.
8. G. B. Kaufman, *Gold Bull*, **18**, 1985, 31.
9. W. E. Smith, *Coord. Chem. Rev.*, **45**, 1982, 307.
10. R. M. E. Richards, R. B. Taylor and D. K. L. Xing, *J. Pharm. Sci.*, **80**, 1991, 861.
11. K. Nomiya, K. Onoue, Y. Kondoh, N. Kasuga, H. Nagano, M. Oda and S. sakuma, *Polyhedron*, **14**, 1995, 1359.
12. D. F. Shriever, P. W. Atkins and C. H. Longford, "Inorganic Chemistry" 2nd edition, ELBS, Oxford, 1994, p 283 & 345.
13. M. C. Gimeno and A. Laguna, *Chem. Rev.*, **97**, 1997, 511.

14. J. E. Huheey, *Inorganic Chemistry, Principles of Structure and Reactivity*, Harper and Row Publishers, 1983, p 465.

15. Y. Ishikawa, K. Saiti, K. Kikuchi and H. Anzai, *Acta Crystallogr.*, **C46**, 1990, 1652.

16. A. Terzis, A. Hountas and J. Pfeiffer, *Acta Crystallogr.*, **C46**, 1990, 224.

17. A. Hountas, A. Terzis and J. Zambounis, *Acta Crystallogr.*, **C46**, 1990, 228.

18. G. A. Bowmaker, B. J. Kennedy and J. C. Reid, *Inorg. Chem.*, **37**, 1998, 3968.

19. K. Kikuchi, Y. Ishikawa, K. Saito and I. Kemoto, *Acta Crystallogr.*, **C44**, 1988, 466.

20. P. D. Cookson, E. R. Tiekink and M. W. Whitehouse, *Aust. J. Chem.*, **47**, 1994, 57.

21. E. Delgado and E. Hernandez, *polyhedron*, **11**, 1992, 3135.

22. G. Lewis and C. F. Shaw III, *Inorg. Chem.*, **25**, 1986, 58.

23. L. C. Porter, J. P. Fackler, J. Costamagna and R. Schmidt, *Acta Crystallogr.*, **C48**, 1992, 1751.

24. V. I. Belevantsev, B. I. Peshchevitskii and L. D. Tsvelondub, *Russ. J. Inorg. Chem.*, **31**, 1986, 1762.

25. A. A. Isab, *Polyhedron*, **8**, 1989, 2823.

26. A. A. Isab and M. S. Hussain, *Polyhedron*, **4**, 1985, 1683.

27. A. A. Isab and M. S. Hussain, *J. Coord. Chem.*, **15**, 1986, 125.

28. M. S. Hussain and E. O. Schlemper, *Acta Cryst.*, **C43**, 1987, 450.

29. P. G. Jones and E. Bembenek, *J. Cryst. Spect. Res.*, **22**, 1992, 397.

30. S. Ahmad, A. A. Isab, H. P. Perzanowski, M. S. Hussain and M. N. Akhtar, *Transition Met. Chem.*, **27**, 2002, 177.

31. P. G. Jones and J. Launter, *Acta Cryst.*, **C44**, 1988, 2091.

32. A. A. Isab, M. S. Hussain, M. N. Akhtar, M. I. M. Wazeer and A. R. Al-Arfaj, *Polyhedron*, **18**, 1999, 1401.

33. M. N. Akhtar, A. A. Isab, A. R. Al-Arfaj, and M. S. Hussain, *Polyhedron*, **16**, 1997, 125.

34. C. S. W. Harker, E. R. T. Tiekink and M. W. Whitehouse, *Inorg. Chim. Acta*, **181**, 1991, 23.

35. P. G. Jones and G. Thone, *Chem. Ber.*, **124**, 1991, 2725.

36. M. Sakhawat Hussain, *J. Cryst. Spect. Res.*, **16**, 1986, 91.

37. S. Ahmad, A. A. Isab, M. N. Akhtar, M. S. Hussain and A. R. Al-Arfaj, *J. Coord. Chem.*, **51**, 2000, 225.

38. J. D. E. T. Wilton-Ely, A. Schier and H. Schmidbaur, *Inorg. Chem.*, **40**, 2001, 4656.

39. W. Eikens, C. Kienitz, P. G. Jones and C. Thone, *J. Chem. Soc. Dalton Trans.*, 1994, 83.

40. R. G. Pearson, *Hard and Soft Acids and Bases*, Dowden, Hutchinson & Ross, 1973.

41. Ali K. H. Alsa'ady, K. Moss, C. A. McAuliffe and R. V. (Dick) Parish, *J. Chem. Soc. Dalton Trans.*, 1984, 1609.

42. C. M. Leukhart, *Fundamentals of Transition Metal Organometallic Chemistry,* Brooks/Cole Publishers, 1985.

43. P. G. Jones, *Acta Crystallogr.*, **B36**, 1980, 3105.

44. R. C. Elder, E. H. K. Zeiher, M. Onady and R. R. Whittle, *J. Chem. Soc. Chem. Commun.*, 1981, 900.

45. P. G. Jones, J. J. Guy and G. M. Sheldrick, *Acta. Crystallogr.*, **B31**, 1975, 2687.

46. M. R. Caira, L. R. Nassimbeni and A. L. Rodgers, *Acta. Crystallogr.*, **B31**, 1975, 112.

47. C. D. Garner and S. C. Wallwok, *J. Chem. Soc.* **A**, 1970, 3093.

48. G. Bandolini, D. A. Cemente and G. Marangoni, *J. Chem. Soc. Dalton Trans.*, 1973, 886.

49. S. Komiya, J. C. Huffman, and J. K. Kochi, *Inorg. Chem.*, **16**, 1977, 1253.

50. E. S. Clark, D. H. Templeton and C. M. McGillarvy, *Acta Crystallogr.*, **11**, 1958, 284.

51. S. A. Cotton and F. A Hart, *The Heavy Transition Elements*, The MacMillan Press Ltd, U.K., 1975, pp 137-153.

52. V. F. Duckworth and N. C. Stephenson, *Inorg. Chem.*, **8**, 1969, 1661.

53. R. Timkovich and A. Tulinsky, *Inorg. Chem.*, **16**, 1977, 962.

54. W. T. Robinson and E. Sinn, *J. Chem. Soc. Dalton. Trans.*, 1975, 726.

55. W. E. Spiar, A. H. Sommer and J. G. White, *Phys. Rev.*, **57**, 1959, 115.

56. J. Knecht, P. Fischer, H. Overhoff and F. Hensel, *J. Chem. Soc. Chem. Commun*; 1978, 905.

57. H. Schmidbaur, J. R. Mnall, A. Frank and G. Huttner, *Chem. Ber.*, **109**, 1976, 466.

58. S. M. Cortez and R. G. Raptis, *Coord. Chem. Rev.*, **162**, 1997, 495.

59. C. E. Housecroft, *Coord. Chem. Rev.*, **115**, 1992, 141.

60. C. E. Housecroft, *Coord. Chem. Rev.*, **131**, 1994, 1.

61. K. I. Tudoryanu, P. K. Migal and L. F. Konishesku, *Zh. Neorg. Khim.*, **35**, 1990, 129.

62. M. R. Udupa, G. Henke and B. Krebs, *Inorg. Chim. Acta*, **18**, 1976, 173.

63. P. M. Henrichs, J. J. H. Jackerman and G. E. Maciel, *Inorg. Chem.*, **16**, 1977, 2544.

64. C. Pakawatchai, K. Sivakumar and H. K. Fun, *Acta Crystallogr.*, **C52**, 1996, 1954.

65. M. M. El-Etri and W. M. Scovell, *Inorg. Chim. Acta*, **187**, 1991, 201.

66. A. J. Blake, R. O. Gould, G. Reid and M. Schroder, *J. Chem. Soc. Chem. Commun.*, 1990, 974.

67. S. M. Socol and J. G. Verkade, *Inorg. Chem.*, **23**, 1984, 3487.

68. R. D. Willett *et al.*, *Inorg. Chem.*, **29**, 1990, 4805.

69. C. F. Shaw III, *Chem Rev.*, **99**, 1999, 2589.

70. S. L. Best and P. J. Sadler, *Gold Bulletin*, **29**, 1996, 87.

71. D. H. Brown and W. E. Smith, *Chem. Soc. Rev.*, **9**, 1980, 217.

72. D. T. Hill and B. M. Sutton, *Cryst. Stuct. Commun.*, **9**, 1980, 679.

73. R. Bau, *J. Am. Chem. Soc.*, **120**, 1998, 9380.

74. R. C. Elder, K. Ludwig, J. N. Cooper and M. K. Eidness, *J. Am. Chem. Soc.*, **107**, 1985, 5024.

75. A. Lorber, C. M. Pearson, W. L. Meredith and L. E. Gantz Mandell, *Ann. Intern. Med.*, **61**, 1964, 423.

76. D. A. Garber, *Proc. Soc. Exp. Biol. Med.*, **119**, 1965, 100.

77. R. C. Elder, *Chem. Rev.*, **87**, 1987, 1027.

78. *AMA Drug Evaluations*, 4th Edition, American Medical Association, Chicago, illionis, **105**, 1980, p 87.

79. R. V. Parish, J. Mack, L. Hargreaves and J. P. Wright, *J. Chem. Soc. Dalton. Trans.*, 1996, 69.

80. C. F. Blank, J. C. Dabrowiak, *J. Inorg. Biochem.*, **21**, 1984, 21.

81. S. P. Frickler, *Gold Bull.*, **29**, 1996, 53.

82. B. Ward and J. C. Dabrowiak, *J. Am. Chem. Soc.*, **109**, 1987, 3810.

83. K. Nomiya, R. Noguchi, K. Ohsawa, K. Tsuda and M. Oda, *J. Inorg. Biochem.*, **78**, 2000, 363.

84. W. A. Spofford and E. L. Amma, *Acta Crystallgr.*, **B26**, 1474 (1970).

85. U. Bierbach, T. W. Hambly and N. Farrell, *Inorg. Chem.*, **37**, 1998, 708.

86. S. Patai and Z. Rappoport, *The Chemistry of Organic Selenium and Tellurium Compounds*, Wiley, Chichester, 1986, vol. 1, p 679.

87. S. Hauge and M. Tysseland, *Acta Chem. Scand.*, **25**, 1971, 3072.

88. O. Vikane, *Acta Chem. Scand.*, **A29**, 1975, p 152, 763, 787.

89. N. Hadjiliadis, T. Theophanides, *Inorg. Chim. Acta*, **15**, 1975, 167.

90. K. Yamanari, M. Kida, M. Yamamoto, T. Fujihara, A. Fuyuhiro and s. Kaizaki, *J. Chem. Soc., Dalton Trans.*, 1996, 305.

91. K. W. Jennette, S. J. Lippard and D. A. Ucko, *Biochimica et Biophysica Acta*, **402**, 1975, 403.

92. U. Kela and R. Vijayavargiya, *Biochem. J.*, **193**, 1981, 799.

93. P. D. Cookson, E. R. Tiekink and M. W. Whitehouse, *Aust. J. Chem.*, **47**, 1994, 57.

94. G. Stocco, F. Gattuso, A. A. Isab and C. F. Shaw III, *Inorg. Chim. Acta*, **209**, 1993, 129.

95. B. Fischer, E. Dubler, M. Meienberger and K. Hegetschweiler, *Inorg. Chim. Acta*, **279**, 1998, 136.

96. N. Katsaros and A. Grigoratou, *J. Inorg. Biochem.*, **25**, 1985, 131.

97. A. A. Isab and M. S. Hussain, *Transition Met. Chem.*, **11**, 1986, 298.

98. A. A. Isab, *Transition Met. Chem.*, **17**, 1992, 374.

99. A. A. Isab and H. P. Perzanowski, *Polyhedron*, **15**, 1996, 2397.

100. U. Rajalingam, P. W. A. Dean and H. A. Jenkis, *Can. J. Chem.*, **78**, 2000, 590.

101. S. J. Berners Price, C. Brevard, A. Pagelot and P. J. Sadler, *Inorg. Chem.*, **24**, 1985, 4279.

102. C. Sasakura and K. T. Suzuki, *J. Inorg. Biochem.*, **71**, 1998, 159.

103. C. J. Dollard and A. L. Tappel, *J. Inorg. Biochem.*, **28**, 1986, 13.

104. G. G. Graham and M. M. Dale, *Biochem. Pharm.*, **39**, 1990, 1697.

105. G. G. Graham and A. J. Kettle, *Biochem. Pharm.*, **56**, 1998, 307.

106. G. G. Graham, J. R. Bales, M. C. Gtootveld and P. J. Sadler, *J. Inorg. Biochem.*, **25**, 1985, 163.

107. A. A. Isab, A. L. Hormann, M. T. Coffer and C. F. Shaw III, *J. Am. Chem. Soc.*, **110**, 1988, 3278 and references therein.

108. A. J. Canunumalla, S. Schraa, A. A. Isab, C. F. Shaw III, E. Gleichman, L. Dunemann and M. Turfeld, *J. Biol. Inorg. Chem.*, **3**, 1998, 9.

109. A. J. Canumalla, N. Al-Zamil, M. Philips, A. A. Isab and C. F. Shaw III, *J. Inorg. Biochem.*, **85**, 2001, 67.

110. Y. Zhang, E. V. Hess, K. G. Pyrhuber, J. G. Dorsey, K. Tepperman and R. C. Elder, *Inorg. Chim. Acta*, **229**, 1995, 271.

111. R. D. Hancock, N. P. Finnkelstein and A. Avers, *J. Inorg. Nucl. Chem.*, **34**, 1972, 3747.

112. D. Lewis, H. A. apell, C. J. McNeil, M. S. Iqbal, D. H. Brown and W. E. Smith, *Ann. Rheum. Dis.*, **42**, 1983, 566.

113. A. L. Hormann, C. F. Shaw III, D. W. Bennett and W. M. Reiff, *Inorg. Chem.*, **25**, 1986, 3953.

114. A. L. Hormann and C. F. Shaw III, *Inorg. Chem.*, **29**, 1990, 4683.

115. A. R. Al-Arfaj, J. H. Reibenspies, M. S. Hussain, M. Y. Darensbourg, M. N. Akhtar and A. A. Isab, *Acta Crystallogr.*, **C53**, 1997, 1553.

116. M. S. Hussain, A. R. Al-Arfaj, M. N. Akhtar and A. A. Isab, *Polyhedron*, 16, 1996, 2781.

117. G. Lewis and C. F. Shaw III, *Inorg. Chem.*, **25**, 1986, 58.

118. F. B. Stocker and D. Britton, *Acta Crystallogr.*, **C56**, 2000, 798.

119. N. A. Malik, G. Otiko and P. J. Sadler, *Biochem. Soc. Trans.*, **8**, 1980, 635.

120. M. T. Coffer, C. F. Shaw III, M. K. Eidsness, J. W. Watkins and R. C. Elder, *Inorg. Chem.*, **25**, 1986, 333.

121. D. J. Ecker, J. C. Hemple, B. M. Sutton, R. Krisch and S. T. Crook, *Inorg. Chem.*, **25**, 1986, 3139.

122. A. A. Isab and P. J. Sdaler, *J. Chem. Soc., Dalton Trans.*, 1981, 1657.

123. A. A. Isab and P. J. Sadler, *J. Chem. Soc., Chem. Comm.*, 1976, 1051.

124. A. A. Isab, *J. Chem. Soc., Dalton Trans.*, 1986, 1049.

125. A. A. Isab, *Inorg. Chim. Acta*, **135**, 1987, 19.

126. P. Roy-Burman, "*Anologues of Nucleic Acid Compounds*", Springer-Verlag, New York, Heidelberg, Berlin, 1970, p 16, 24.

127. S. Krischner, Y. K. Wei, D. Francis and J. G. Bergman, *J. Med. Chem.*, **9**, 1969, 369.

128. J. Chaudiere and A. L. Tappel, *J. Inorg. Biochem.*, **20**, 1984, 313.

129. W. C. Hawakws, E. C. Wilhelmsen and A. L. Tappel, *J. Inorg. Biochem.*, **23**, 1985, 77.

130. C. J. Dillard and A. L. Tappel, *J. Inorg. Biochem.*, **28**, 1986, 13.

131. A. A. Isab and A. P. Arnold, *J. Coord. Chem.*, **20**, 1989, 95.

132. A. A. Isab, *Transition Met. Chem.*, **19**, 1994, 595.

133. A. A. Isab, M. N. Akhtar and A. R. Al-Arfaj, *J. Chem. Soc, Dalton Trans.*, 1995, 1483.

134. J. Reglinski, S. Hoey and W. E. Smith, *Inorg. Chim. Acta*, **152**, 1988, 261.

135. M. T. Coffer, C. F. ShawIII, A. L. Horman, C. K. Mirabelli and S. T. Crooke, *J. Inorg. Biochem.*, **30**, 1987, 177.

136. C. F. Shaw III, A. A. Isab, M. T. Coffer and C. K. Mirabelli, *Biochem. Pharmacol.*, **40**, 1990, 1227.

137. M. P. Hacker, E. B. Douple and I. H. Karkloff, *Platinum Coordination Complexes in Cancer Chemotherapy*, Martinus Nijoff Publishers, Boston, 1984, p 290.

138. D. H. Brown, G. McKlinlay and W. E. Smith, *J. Chem. Soc. Dalton Trans.*, 1977, 1874.

139. A. A. Isab and P. J. Sadler, *J. Chem. Soc. Dalton Trans.*, 1981, 1657.

140. A. P. Intoccia, T. L. Flanagan, D. T. Walz, L. Gutzait, J. E. Swagzdis, J. Flagillano Jr, B. Y. Hwang, R. H. Dewey and H. Noguchi, in: B. M. Sutton (Ed.), *Bioinorg. Chem. of Gold Coord. Comp.*, Smith Kline and French Laboratories, Philadelphia, 1983, p 21.

141. C. F. Shaw III, M. T. Coffer, J. Klingbeil and C. K. Mirabelli, *J. Am. Chem. Soc.*, **110**, 1988, 729.

142. D. L. Rabenstein and A. A. Isab, *FEBS letters*, **121**, 1980, 61 and references therein.

143. A. A. Isab, *J. Inorg. Biochem.*, **45**, 1992, 261.

144. J. Xu and J. C. Yadan, *J. Org. Chem.*, **60**, 1995, 6296.

145. P. W. Atkins, *Physical Chemistry*, 5th edition, Oxford University Press, Oxford, 1994, 834.

146. G. D. Thorn, *Can. J. Chem.*, **33**, 1955, 1278.

147. L. Maier, *Helv. Chim. Acta*, **53**, 1970, 1417.

148. F. Cristiani, F. A. Devillanova and G. Verani, *J. Chem. Soc. Perkin II Trans.*, 1977, 324.

149. F. A. Devillanova and G. Verani, *Aust. J. Chem.*, **31**, 1978, 2609.

150. C. A. Tolman, *Chem. Rev.*, **77**, 1977, 313.

151. K. L. Brown and S. Satyanarayana, *Inorg. Chem.*, **31**, 1992, 1366.

152. F. A. Devillanova, A. Diaz, F. Isaia and G. Verani, *Transition Met. Chem.*, **14**, 1989, 153.

153. J. Milne, *Mag. Res. Chem.*, **31**, 1993, 652.

154. M. M. El-Etri and W. M. Scovell, *Inorg. Chem.*, **29**, 1990, 480.

155. Z. Popovic, G. Pavlovic, D. Matkovic-Calogovic, Z. Soldin, M. Rajic, D. Vikic-Topic and D. Kovacek, *Inorg. Chim. Acta.*, **306**, 2000, 142.

156. P. M. Henrichs, S. Sheard, J. J. H. Jackerman and G. E. Maciel, *J. Am. Chem. Soc.*, **101**, 1979, 3222.

157. T. H. Lowry and K. S. Richardson, *Mechanism and Theory in Organic Chemistry*, Harper and Row Publishers, New York, 1981, p 162.

158. A. D. Broom, M. P. Schweizer and P. O. P. Ts'o, *J. Am. Chem. Soc.*, **89**, 1967, 3612.

159. A. J. Jones, D. M. Grant, M. W. Winkkley and R. K. Robins, *J. Am. Chem. Soc.*, **92**, 1970, 4079.

160. A. A. Isab, A. R. Al-Arfaj and M. N. Akhtar, *J. Coord. Chem.*, **33**, 1994, 287.

161. K. S. Tan. A. P. Arnold and D. L. Rabenstein, *Can. J. Chem.*, **66**, 1988, 54.

162. M. T. Razi, P. J. Sadler, D. T. Hill and B. M. Sutton, *J. Chem. Soc., Dalton Trans.*, 1983, 1331.

163. C. F. Shaw III, in: B. M. Sutton (Ed.), *Bioinorg. Chem. of Gold Coord. Comp.*, Smith Kline and French Laboratories, Philadelphia 1983, p 98.

164. H. Friebolin, *Basic One- and Two- dimensional NMR Spectroscopy*, VCH Publishers, Germany, 1991, p 45.

165. A. R. Al-Arfaj, A. A. Saeed, M. N. Akhtar and A. A. Isab, *J. Coord. Chem.*, **43**, 1998, 257.

166. C. F. Shaw III, M. T. Coffer, J. Klingbeil and C. K. Mirabelli, *J. Am. Chem. Soc.*, **110**, 1988, 729.

167. F. Basolo and R. Johnson, *Coordination Chemistry*, W. A. Benjamin, Inc. USA, 1964 (Reproduced by National Book Foundation, Pakistan, 1988), p 7.

168. T. G. Appletone, J. R. Hall and S. T. Ralph, *Inorg. Chem.*, **24**, 1985, 637.

169. F. M. Macdonald and P. J. Sadler, *Magn. Res. Chem.*, **29**, 1991, S52.

170. E. A. Vizzini, I. F. Taylor and E. L. Amma, *Inorg. Chem.*, **7**, 1968, 1351.

171. M. R. Udupa and B. Krebs, *Inorg. Chim. Acta*, **7**, 1973, 271.

172. J. S. Casas, E. G. Martinez, A. Sanchez, A. S. Gonzalez, J. Sordo, U. Casellato and R. Graziani., *Inorg. Chim. Acta*, **241**, 1996, 117.

173. A. A. Isab and P. J. Sadler, *J. Chem. Soc. Dalton Trans.*, 1982, 135.

174. A. P. Arnold, K. S. Tan and D. L. Rabenstein, *Inorg. Chem.*, **25**, 1986, 2433.

175. T. G. Appleton, J. W. Connor and J. R. Hall, *Inorg. Chem.*, **27**, 1988, 130.

176. R. E. Norman, J. D. Ranford and P. J. Sadler, *Inorg. Chem.*, **31**, 1992, 877.

177. E. Dubler and E. Gyr, *Inorg. Chem.*, **27**, 1988, 1466.

178. R. Cini, A. Cinquantini, M. Sabat and L. G. Marzilli, *Inorg. Chem.*, **24**, 1985, 3903.

179. R. Cini, R. Bozzi, A. Karaulov, M. B. Hursthouse, A. M. Calafat and L. G. Marzilli, *J. Chem. Soc. Chem. Commun.*, 1993, 899.

180. U. Abram, J. Mack, K. Ortner and M. Muller, *J. Chem. Soc., Dalton Trans.*, 1998, 1011.

181. N. A. Berger and G. L. Eichorn, *Biochemistry*, **10**, 1971, 1847.

182. S. M. Wang and N. C. Li, *J. Am. Chem. Soc.*, **90**, 1968, 5069.

183. M. M. Taqui Khan and C. R. Krishnamoorthy, *J. Inorg. Nul. Chem.*, **33**, 1971, 1417.

184. A. A. Isab, *Inorg. Chim. Acta*, **207**, 1993, 73.

185. C. F. Shaw III, A. A. Isab, J. D. Hoeschele, M. Starich, J. Locke, P. Schulties and J. Xiao, *J. Am. Chem. Soc.*, **116**, 1994, 2254.

186. J. Xiao and C. F. Shaw III, *Inorg. Chem.*, **31**, 1992, 3706.

List of Publications

1) **Saeed Ahmad**, A. A. Isab, *Synthesis of cyano(ergothionine) gold(I) complex and its disproportionation in solution*, **Inorg. Chem. Comm.**, 4, 2001, 362-364.

2) **Saeed Ahmad**, A. A. Isab, *^{13}C, ^{31}P and ^{15}N NMR Studies of the ligand exchange reactions of auranofin and chloro(triehylphosphine)gold(I) with thiourea*, **J. Inorg. Biochem.**, 88, 2002, 44-52.

3) A. A. Isab, **Saeed Ahmad**, *Comparative ^{13}C, and ^{31}P NMR Studies of the ligand exchange reactions of auranofin with ergothionine, imidazolidine-2-thione and diazinane-2-thione*, **J. Inorg. Biochem.**, 88, 2002, 53-60.

4) **Saeed Ahmad**, A. A. Isab, *^{13}C NMR studies the interaction of gold(I) thiomalate with 6-mercaptopurine and its derivatives*, **J. Coord. Chem.**, 55, 2002, 189-203.

5) **Saeed Ahmad**, A. A. Isab and H. P. Perzanowski, *Silver(I) complexes of thiourea*, **Transition Met. Chem.**, (accepted for publication) 2002.

6) **Saeed Ahmad**, A. A. Isab, *Silver(I) complexes of selenourea (^{13}C and ^{15}N labeled); characterization by ^{13}C, ^{15}N and ^{107}Ag NMR*, **Inorg. Chem. Comm.**, (accepted for publication) 2002.

7) A. A. Isab, **Saeed Ahmad,** M. Arab, *Synthesis of silver(I) complexes of thiones and their characterization by ^{13}C, ^{15}N and ^{107}Ag NMR*, **Polyhedron,** (accepted for publication) 2002.

8) **Saeed Ahmad**, A. A. Isab and H. P. Perzanowski, *Ligand scrambling reactions of cyano(thione)gold(I) complexes and determination of their equilibrium constants* (submitted for publication) 2002.

9) **Saeed Ahmad**, A. A. Isab, A. R. Al-Arfaj and A. P. Arnold, *Synthesis of cyano(selenone)gold(I) complexes and investigation of their scrambling reactions using ^{13}C and ^{15}N NMR spectroscopy*, (submitted for publication), 2002.

10) **Saeed Ahmad**, A. A. Isab and M. I. M. Wazeer, *^{13}C NMR studies of the redox and exchange reactions of gold(I) thiomalate with diselenides*, (submitted for publication) 2002.

11) A. A. Isab, **Saeed Ahmad,** *^{13}C and ^{15}N NMR studies of the ligand scrambling reactions of some cyano(selenone)gold(I) complexes in dimethyl sulfoxide*, (submitted for publication) 2002.

12) **Saeed Ahmad**, A. A. Isab, A. P. Arnold, *Synthesis and spectroscopic characterization of silver(I) complexes of selenones*, (submitted for publication) 2002.

Under preparation

13) Synthesis and characterization of mixed ligand gold(I) complexes of thiourea.

14) Mixed ligand gold(I) complexes with phosphines and selenourea

15) ^{13}C and ^{15}N NMR studies of the interaction of gold(I) thiolates with thiourea.